The involvement of central and peripheral mechanisms in the control of octopus arm movement

Thesis submitted for the degree of
"Doctor of Philosophy"

by

Germán Sumbre

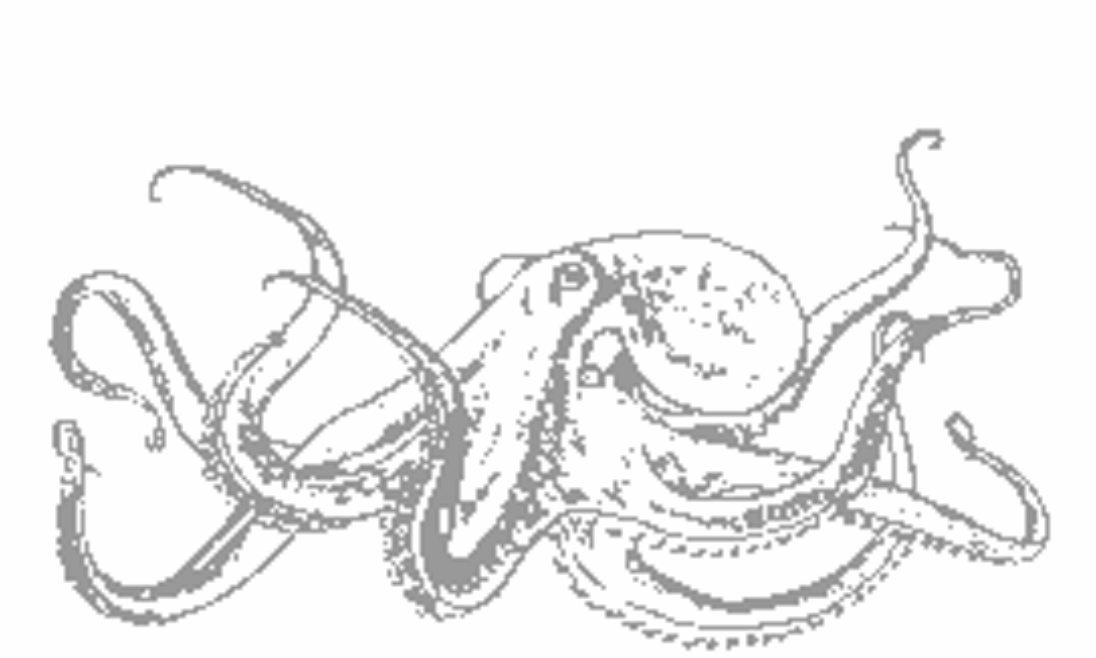

Submitted to the Senate of the Hebrew University of Jerusalem

2004

This work was carried out under the supervision of

Dr. Binyamin Hochner

Prof. Yosef Yarom

Abstract

The' extremely flexible arms and the ~300 suckers along the length of the arm provide octopuses with extraordinary manipulative skills. They can move their arms with a virtually infinite number of degrees of freedom (DOFs) and grasp objects with an exceptionally strong grip. Octopuses are thus ideal for studying motion control in hyper-redundant appendages, to gain important insights for the construction and control of continuum flexible robotic devices.

Continuing on from previous studies (Gutfreund et al., 1996, 1998), I have investigated the motor control principles underlying the octopus arm extension movement, a movement octopuses produce when reaching towards an object, swimming or crawling. The movement is executed by propagating a bend along the arm, a strategy which reduces the number of controlled DOFs to only three (yaw, pitch and propagation velocity of the bend). This strategy thus greatly simplifies motor control of the flexible arms, because the entire movement characteristics can be described by these 3 variables.

I have shown that further simplification is achieved by the use of peripheral rather than centralized control. The existence of a feed-forward motor program embedded within the neuromuscular system of the arm was demonstrated by electrically or mechanically evoking movements in 'denervated' arms, where the connection with the central brain had been severed. The evoked movements were qualitatively, kinematically and dynamically similar to arm extensions in freely behaving octopuses. The movement direction (pitch and yaw) could be modulated by modifying the initial posture of the arm (yaw and pitch) and bend propagation velocity could be set by adjusting the frequency and duration of the triggering stimulus. I was not able to modulate the propagation distance of the bend along the arm, which suggests that the arm extension motor program propagates the bend right to the tip of the arm, as generally observed in freely behaving octopuses. This motor program is feed-forward, i.e. the movement cannot be re-planned or corrected after it has already started. However, in some trials during which the target was displaced, octopuses were able to actively stop the propagation of the bend.

Since the octopus arms have suckers distributed through their entire length, a target can be grasped at any location along the arm. In contrast, when bringing the grasped target to the mouth, a point-to-point task has to be executed, where the

end-effector (the site on the arm grasping the object) has to reach a specific and precise target (the mouth). I show here that octopuses accomplish this task by generating a stereotypical fetching movement

Fetching movements are performed by creating three bends in the arm that act like joints (distal, medial and proximal), forming a *qua*si-articulated structure. By rotating these joints in a single plane, the end-effector is accurately brought to the target. The joint positions follow a stereotypical spatial pattern, in which the distal one is formed proximally to the grasped object, while the proximal joint occurs at the base of the arm, and the medial one roughly midway between the distal and proximal joints. Joint locations are positively correlated with the object's position along the arm; objects grasped more distally generate a *quasi*-articulated structure with longer segments. Hence, this dynamic *quasi*-articulated structure enables the octopus to accurately bring an object to the mouth, regardless of its position along the arm. This strategy immensely reduces the controlled variables to 3 DOFs only (one for each joint), therefore greatly simplifying motor control while still ensuring high accuracy. This strategy also allows the octopus to bring an object to its mouth, without requiring any information about the arm's position in space.

The formation of the distal joint before the medial one, the necessity of higher motor centers for movement execution, and muscle activity recordings (EMG) showing that two waves of muscle activation propagate in opposite directions towards each other along the proximal and medial segments; lead me to suggest an hypothesis for the generation of fetching movements where the combination of stimulation produced by the grasped object with a central command may trigger the two opposing waves of muscle activity that create or initiate the formation of the medial joint at their collision point. This scheme would be an efficient mechanism for forming an object-dependent articulated structure without requiring central representation of the arm, and thus further simplifying the computational needs for this complex movement task.

Interestingly, from all possible types of movement that a flexible arm can generate to bring an object to the mouth, the octopus produces a *quasi*-articulated structure that both morphologically and kinematically resembles the multi-joint articulated limbs of vertebrates (e.g. human arms). This functional evolutionary convergence suggests that a kinematically constrained articulated limb could be nature's optimal solution for achieving accurate point-to-point movements. Fetching is thus a unique

example where evolution has selected similar solutions through two totally different mechanisms, through morphology as in arthropod and vertebrate limbs, and through a stereotypical motor control program in the octopus.

I conclude that, to efficiently control its hyper-redundant arms during goal directed movements, the octopus uses stereotypical motor control programs which drastically reduce the number of DOFs of the arms (to only 3). This enables the nervous system to solve the problems associated with controlling truly flexible arms, simply and adequately according to the task requirements.

Despite the redundancy limitations during goal directed movements, flexible octopus arms still have some advantages relative to rigid skeletal arms, since they can generate movements with particular arm geometries that articulated limbs cannot produce (e.g. bend propagation during reaching movement and dynamic articulation during fetching). This ability allows octopuses to generate movements which minimize the drag forces to achieve fast movements (e.g. in fast reaching) or create highly stiffened dynamic arm geometries to bring an object to the mouth from any location along the arm (e.g. in fetching). Besides goal directed movements that involve the entire arm, octopuses make non-goal directed movements, such as arm foraging and cleaning maneuvers, where it is evident that a large number of DOFs are exploited. These are apparently controlled locally by the arm's nervous system.

The results obtained here provide further insight on how biological systems have evolved to overcome the complex problem of controlling a highly redundant motor system. This knowledge will be of great relevance to the ongoing multi-disciplinary effort of developing and controlling truly flexible robotic manipulators.

Contents

Chapter 1

General Introduction……1

1.1 Movement generation……1

1.2 Movement planning……2

1.3 Movement coordination……..4

1.4 Neural correlates of motion (central pattern generators)……..8

1.5 Hyper-redundancy……10

1.5.1 Robotic manipulators……..10

1.5.2 Hyper-redundancy in nature……..…12

1.6 Octopus *vulgaris*……14

1.6.1 Nervous system morphology……16

1.6.2 Neurophysiology……..18

1.6.3 Motor control of the arm ……19

1.7 Research objectives……21

Chapter 2

Materials and Methods……...22

Chapter 3

Results

3.1 Control of octopus arm extension by a peripheral motor program……35

3.2 Insights on the motor control mechanism of the octopus reaching……..39

3.3 Vertebrate-like strategy in octopus point-to-point arm movements suggests convergence toward an optimal control solution……58

Chapter 4

General Discussion……82

3.1 Motor control of reaching movements ……..…82

3.2 Fetching movements: kinematics and motor control……..83

3.3 Final conclusions……..85

References……87

Chapter 1

General Introduction

Throughout the animal kingdom, skeletons have evolved to provide protection and body support. In addition, they allow generation of movement, serving as anchor points for the muscles, whose contractions allow motion specifically at the joints. In contrast to such multi-jointed structures, the octopus arm belongs to a group of organs named muscular hydrostats (e.g. elephant trunks, tongues and tentacles), which are composed almost entirely of incompressible muscle tissue. In such muscular hydrostats, the lack of rigid structure allows motion with an almost infinite number of degrees of freedom (DOF), while the muscles are arranged so as to create both force generation and the skeletal support necessary for movement generation (Kier and Smith, 1985).

These features together with the sucker rings that provide a powerful grip and a highly elaborated peripheral nervous system endow the octopus arm with outstanding manipulative abilities unmatched by kinematically constrained articulated limbs (arthropods and vertebrates). Octopuses uses their arms to swim, crawl, dig and build shelters, providing substantial advantage when foraging or escaping from predators in the highly restricted environments like the rocky and coral reefs where they usually live.

Using behavioral and electrophysiological methods to obtain new insights on the organizational principles and neuronal circuitry of the motor control system of the octopus arm may shed light on how biological systems have evolved to overcome the complex problem of controlling a highly redundant motor system. The insights gained on Nature's solutions to this problem may be of great relevance to robotics, aiding development and control of truly flexible robotic manipulators.

I shall now summarize the major aspects of movement and movement generation, planning and control, specially emphasizing the differences between kinematically constrained and hyper-redundant appendages and their importance for the development of future robots. I shall then concentrate on the mechanics of the octopus arm, its sophisticated nervous system and motor control.

1.1 Movement generation

Movement is the process of continuously changing position. It can be initiated by exerting force on the environment and thereby achieving acceleration in the

opposite direction. Organisms with skeletons generate movement by transforming muscle contraction into force via the interaction with their skeletons. The muscles contract against the resistance created by the skeleton, which generates force. Without resistance, muscles would simply shorten without generating force. In addition, muscles can only contract and cannot return to their resting length by themselves. Thus it is the interaction with the skeleton generated via antagonist muscle contraction that permits them to re-extend. Finally, the characteristics of the muscle-skeletal interactions (where in the skeleton the muscles are anchored and the distance between joints) can generate dynamics and kinematics amplification.

Skeletons can be external such as the cuticular exoskeletons of arthropods or internal (endoskeletons) based on bones or cartilage as in the phylum Chordata. Because of their rigidity, both endo- and exoskeletons limit animal movement to specific points (the joints). However, skeletons do not necessarily need to be rigid. Hydrostatic skeletons, for example, enable muscles to exert force against a connective tissue cavity filled with incompressible fluid (e.g. polyps). Muscular hydrostats (tongues, trunks and tentacles) constructed of only muscular tissue, have a unique muscle arrangement, where supporting elements are dynamically created by muscular co-activation (stiffening). In contrast to hard skeletons, such flexible ones do not provide protection but allow organisms to move with a larger number of DOFs.

1.2 Movement planning

Planning motor processes refers to the determination of a movement's goal, such as recognizing an object's position and shape and planning a coordination strategy to reach towards that position and move the object to another point. Planning can be performed at three different levels: *end-point coordinates*, *joint-angle coordinates* or *muscle coordinates* (Hollerbach, 1990).

End-point coordinates: This level of planning consists of programming the movement in external coordinates (extra-corporeal Cartesian coordinates), allowing very accurate control of the end-point throughout the movement (e.g. positioning the human hand in relation to the 3D space during a reaching movement). At this level of planning, the nervous system has to overcome both the inverse kinematics (e.g. adjusting joint angles to obtain a desired hand position)

and the inverse dynamics transformations (defining the necessary muscle torques to generate a desired joint rotation).

Joint-angle coordinates: Planning in joint space avoids the inverse kinematics transformations (except for the initial and final position), leaving only direct kinematics (prediction of the end-point position from known data about the joint angles) and inverse dynamics to be computed. Since both joint angles and torques are intrinsic coordinates, the necessary calculations are simpler. However, this computational simplification diminishes the degree of the end-point control, affecting movement accuracy.

Muscle coordinates: No inverse transformations are needed at this level, only direct ones are utilized. This maximally simplifies motor control but gives only minimal ability to accurately control the movement end-point.

Recording neural activity during movement may help determine at which level animals plan movements. Alternatively, looking for regularities in the motor behavior may also indicate how a particular behavior is represented or coded by the nervous system (Bernstein, 1967). This latter method has been largely used to study vertebrate motor control, especially in humans, by searching for invariants at the kinematic and dynamic levels during movement execution (e.g. arm reaching movements). Movements are performed under a variety of different experimental conditions (different velocities, weights on the arm, directions, etc.). If, despite these changes, some kinematic or dynamic variables remain unmodified, one can infer that the nervous system utilizes these variables internally to plan the movement.

For example, when humans reach towards a target, the path described by the hand (the end-effector) is a straight line and remains invariant despite the movement's speed, direction or load (the last two affecting the movement's dynamics). In addition, the hand’s normalized tangential velocity is also invariant, showing a bell-shaped profile. Thus, since subjects were not constrained to perform movements at a certain speed or path, these results imply that the nervous system utilizes mainly kinematic variables in movement planning (Morasso, 1981; Atkeson and Hollerbach, 1985; Hollerbach and Atkeson, 1987). However, controversial results suggesting that the nervous system uses dynamic

variables to plan movements will be discussed in the next section (Movement coordination).

Since these kinematic variables are only invariant for the end-effector path and its tangential velocity profile (extrinsic coordinates), but not for the joints (intrinsic coordinates), it was thought that the brain mainly deals with end-effector position in extra-personal space (Morasso, 1981). Electrophysiological experiments in behaving monkeys showed that some cortical neurons increased their activity only when the hand moved in a specific direction (directional neurons) and were unaffected by initial hand position or load (Georgopoulos et al., 1982; Camitini et al., 1991; Schwartz et al., 1988). In contrast, load-sensitive neurons were found exclusively in subcortical areas (Kalaska et al., 1990), thus reinforcing the end-point space planning hypothesis.

An alternative approach, named joint staggered interpolation, was suggested by Hollerbach and Atkeson (1987). They claimed that movements are planned in joint space and the observed end-point kinematic invariances in extrinsic coordinates derive from a non-continuum coordination scheme. This approach, in which joints are rotated with different onsets, not only gave a better fit to data from previous studies, but was also able to explain some of the discrepancies or controversies in the field.

1.3 Movement coordination

A location can be fixed in 3D space by six variables; 3 for position (X, Y, Z) and 3 for orientation (pitch, yaw and roll). Thus, it is necessary to generate movement with at least 6 DOFs to accurately reach towards and grasp an object. The human arm has 7 DOFs. This extra DOF or kinematic redundancy gives the arm the advantage of being able to accurately reach to and grasp a target using several possible paths. This attribute may be significant in avoiding obstacles and joint limits. Yet, it adds further computational complexity to the inverse kinematics transformation, since now many combinations of joint angles can determine the same end-point position in extrinsic coordinates. The inverse dynamics transformations are similarly affected, since a variety of different muscles can be contracted to achieve similar rotations by the same joint.

Optimization-based models have been developed to overcome this "ill-posed" problem. These models reduce all the possible coordination solutions to the one,

which maximizes a certain movement characteristic, usually of important evolutionary significance (e.g. smoothness, accuracy, energy, etc.). Among the first models was that of Flash and Hogan (1985) in which they calculated the extrinsic coordinates and tangential velocity profile of the end-point, when the jerk (the time derivative of acceleration) of the end-point was minimized. The model was successful in predicting both the end-point tangential velocity profiles and paths observed in experimental data from planar movements with two joints, (Morasso 1981; Atkeson and Hollerbach 1985). These results thus supported the hypothesis that the nervous system plans motion in extrinsic coordinates.

In addition, this approach has a behavioral significance, since maximizing smoothness during movement can be important, especially when handling delicate objects (e.g. avoiding spilling when bringing a glass of water to the mouth). The minimum-jerk model was also found to be the derivative or the base for the 2/3 power law (Schaal and Sternad, 2001; Richardson and Flash, 2002). This is the nonlinear relationship between tangential velocity and radius of curvature of the end-point trajectory, a constant invariant during the generation of rhythmic end-point trajectories (e.g. parabolic drawings, Viviani and Terzuolo, 1980).

Electrophysiological recordings from monkey motor cortex showed population vectors obeying the 2/3 power law (Schwartz, 1994). These population vectors always predictively preceded the movements, implying that the nervous system encodes movements in kinematic variables, as was suggested by psychophysical studies. Further, Viviano and Stucchi (1992) showed that human subjects perceive the movement of a dot in an elliptic path on a computer screen as having a constant velocity only when the 2/3 power law constraint is applied. This finding implies that the brain perceives motion in the same way that it generates it, either because perceptual processes are guided or constrained by motor schemes or because motor outputs are sculpted through perceptual learning.

An alternative model, the minimum torque-change (Uno et al., 1989) and later the minimum commanded torque-change model (Nakano et al., 1999) proposed that the nervous system minimizes muscle torque-change while generating movement. This model optimizes smoothness like the minimum-jerk model, but uses dynamic variables, thus avoiding complex inverse kinematic and dynamic transformations (the latter were not addressed by the previous models). Moreover, these models were able to better reproduce the end-point paths during reaching movements,

especially for movements in which the minimum-jerk model failed to do so (movements passing from the side to the front of the body).

Rosenbaum et al. (1995) and Alexander (1996) suggested that the nervous system plans coordination by minimizing travel or energy cost. Like the previous models, they were able to generate end-point paths similar to those observed experimentally. However, this approach discarded muscular co-contraction, which is important especially during precise movements.

A totally different theory tackling the complexity of creating movement with redundant limbs is the equilibrium-point hypothesis first formulated by Feldman in 1966. This theory proposes that the nervous system exploits the elastic properties inherent in muscles and peripheral reflex loops. Since the brain can control both muscle stiffness and rest length and since muscles are arranged in an agonist-antagonist configuration, a certain limb posture can be maintained by balancing the forces exerted by agonist and antagonist muscle contraction. These stable postures are called equilibrium-points. Feldman suggested that the brain generates movement by commanding a series of shifts in the neurally specified equilibrium-points, while the elastic properties of the muscles provide instantaneous correcting forces in reaction to external perturbations that may move the limb away from the intended trajectory.

Even though this theory did receive experimental confirmation (Flash, 1987; Bizzi et al., 1991), it was finally and decisively refuted by Gomi and Kawato in 1996. Using a high-performance manipulandum, they were able to reliably measure stiffness and torque in the human arm during certain movements. Their theoretical reconstructions of the arm's movement kinematics using equilibrium-point theory differed significantly from the kinematics measured.

The muscular synergism theory (Tresch et al, 1999; d'Avella et al., 2003) proposed that the nervous system produces motion through the combination of a small number of muscle groups (synergies) in order to deal with the high dimensionality of the musculoskeletal system (which muscles should be activated in order to generate a certain movement) and to overcome the complexity of limb dynamics. These synergetic groups could then be coupled in many different ways to generate complex motor behaviors.

Recently, two innovative models have been proposed not only to unify most of the previous ones but also to extend their application to movements other than the

generally studied arm reaching movement (e.g. eye movements). The minimum variance model (Harris and Wolpert, 1998) is based on the physiological assumption that the neural control signals are corrupted by noise, whose variance increases with the size of the control signal. It suggests that in the presence of signal-dependent white noise the minimized cost function is the positional variance across movements. This model was able to predict not only arm trajectories but also eye saccades. In addition, the optimal trajectories generated by the model were inherently smooth, as predicted by the minimum-jerk model, with gently curved paths and bell-shaped velocity profiles, and also consistent with Fitt's law (the variability of motor errors increases with the magnitude of the movement). Surprisingly, the model also revealed trajectories during elliptic drawings that followed the 2/3 power law. Todorov and Jordan (2002) then developed the optimal feedback control model. Similar to the minimum variance model, it emphasizes the role of noise in movement coordination. However, it goes a step further by incorporating feedback control, so that higher accuracy is obtained by allowing variability in redundant dimensions not relevant to the task. This model uses feedback more efficiently, correcting only deviations that interfere with the task goal (the minimum intervention principle) and resolving redundancy moment-by-moment. Thus, instead of trying to reduce redundancy like the other optimization models, this model exploits it. This approach is not only applicable to a variety of much more realistic behaviors, but also subsumes the motor behavior models described previously.

Even though these models are successful in accounting for some characteristics of experimentally observed arm movements, most of them fail when applied to kinematically redundant articulated arms. Several new approaches have now been suggested to deal with this problem. Torres and Zipser (2002) suggested a geometric stage between the sensory input and motor output. This stage consists of a computational module which transforms information about the goal of a movement (location and orientation) into a postural path that brings the hand to the target in the correct configuration to achieve the goal. The transformations are based on a gradient descent algorithm which repeatedly computes the gradient of the cost function, changing a 7 DOF arm posture gradually until the target is reached with the correct orientation, thus generating a postural path from initial position to the target's position.

Soechting et al. (1995) proposed a model which minimizes the kinetic energy during unconstrained pointing arm movements in 3D space. Nishikawa et al. (1999) analyzed similar pointing arm movements executed at a large range of speeds. Since the movements' spatial properties remained invariant despite their different velocities, they suggested that it is not the total forces (dynamic and antigravity) which are optimized but rather only dynamic forces.

Medendorp et al. (2000) proposed that during pointing movements with an extended arm (thus exploiting 3 DOFs for a task requiring 2 DOFs), the 3D vectors are restricted to a 2D curved plane. This is known as Donders' Law, and it was formulated for eye movements (Simonsz and Den Tonkelaar, 1990).

1.4 Neural correlates of motion (central pattern generators)

The complexity of motor control as described above may also be overcome by hierarchical organization of the control system. Generally, the lower levels of the control system are based on central pattern generators (CPGs), which are neural circuits capable of generating the basic spatiotemporal patterns underlying a certain motor behavior (e.g. gait, swimming, defense reactions, chewing, etc.). These CPGs alleviate the need for higher centers to control the detailed actions of each element at lower levels. Higher centers just need to activate these CPGs via global commands to generate a certain motor behavior (Arshavsky et al., 1997). Furthermore, higher centers can drastically modify the generated complex spatiotemporal patterns through simple modifications of the activation commands (e.g. higher frequency). Therefore, the same neural network can be used to produce different motor outputs (e.g. different gaits in quadrupeds).

Even though CPGs were previously thought to govern only rhythmical motor behaviors such as walking (Kremer and Lev Tov, 1997), swimming (Arshavsky et al., 1993; Grillner et al., 1995), breathing (Onimaru, 1995), gastric peristaltic movements (Selverston, 1999), etc., recent studies have found CPGs that also generate non-rhythmic motor patterns, such as the defense reaction in snails (Arshavsky et al., 1994) and vocal patterns in singing birds (Konishi, 1994), further generalizing the concept of CPGs. Thus, as CPGs have been found from invertebrates to mammals and are related to a high diversity of general stereotypical motor behaviors, they may be a common feature of neuronal motor control systems (Pearson, 1993).

There were traditionally two schools of thought about how CPGs generate the stereotypical spatiotemporal patterns underlying specific behaviors. The first proposed that these patterns are regulated by chains of peripheral reflexes, such that generating a certain phase of a motor pattern triggers the generation of the next phase and so on, until the entire cycle is completed. This hypothesis was supported by studies in which the output patterns completely disappeared when sensory feedback was mechanically or chemically removed (e.g. toad locomotion, Shik and Orlovsky, 1976; initiation of locust flight, Pearson, 1993).

The second school suggested that CPGs are based only on intrinsic properties of the neurons involved (pacemakers) or their synaptic connectivity (Shik and Orlovsky, 1976; Pearson, 1993). Support for this view comes from isolated nervous systems, which can produce spatiotemporal patterns of activity resembling behavioral ones. Such “fictive behaviors” have been shown, for example, in decerebrated cats, in which stimulation of the mesencephalon evokes a motor pattern resembling walking (Shik et al., 1969). Similarly, a firing pattern with comparable spatiotemporal characteristics to crawling can be evoked in the isolated nervous system of the leech by electrical stimulation (Eisenhart et al, 2000) and rhythmic patterns of the radula in the buccal ganglia of aplysia.(Susswein, 2002).

Neural correlates of the mating call were recorded in the isolated brain stem of male frogs following electrical stimulation (Schmidt, 1992). Further support comes from experiments where the sensory feedback was eliminated either via deafferentation or by inhibition of movement (e.g. curare application), as in the case of breathing in the goldfish (Ballintijn and Roberts, 1976) and hopping in rabbits (Viala and Buser, 1969).

Even though the spatiotemporal outputs were similar to the controls, they were mostly not identical and sometimes not very stable. This suggests that in normal functioning motor pattern generation may be based on the combination of both CPGs intrinsic properties and sensory feedback components. The intrinsic pattern of the CPG may dictate the general parameters of the patterns, while sensory feedback is responsible for fine tuning and interaction with the environment.

It has recently become clear that the traditionally proposed theory of hierarchical organization of motor control is misleading. Morphological and electro-physiological studies in both invertebrates and vertebrates indicate that many

motor systems rely on interconnected distributed ensembles, suggesting that motor control is a parallel distributed process (Kien and Altman, 1992; Schaefer and Ritzmann, 2001; Canedo, 1997). This new essentially connectionist approach suggests how a motor system may self-organize in precise adjustment with the environment.

1.5 Hyper-redundancy

In the field of motor control, hyper-redundancy usually refers to appendages with a very large number of DOFs, many more than the minimal 6 needed to move in 3D space (see Movement coordination). Hyper-redundancy enables appendages to move towards a certain target via many possible paths. This ability is important when moving in constrained environments such as coral reefs or rocky terrain. On the other hand, control of hyper-redundant systems can become extremely complex.

1.5.1 Robotic manipulators

The main motivation for building and designing hyper-redundant flexible robotic manipulators is their ability, in contrast to the human arm or the currently available jointed robots, to navigate in constrained hazardous environments such as demolished buildings, atomic reactors, the rocky seabed or even inside the human body. Their structure allows whole-arm manipulation (interaction with the world along the whole length of the structure), in contrast to the individual end-effectors of traditional manipulators, mainly inspired by the human arm. In addition, hyper-redundant robots are able to maintain a high degree of functionality even when suffering localized damage or faults.

The first hyper-redundant robots were based on discrete manipulators created by increasing the number of joints of traditional robotic limbs (Paljug et al., 1995; Walker and Hannan, 1999). Recently, new design philosophies have led to the fabrication of continuum robotic manipulators. These are based on a backbone structure actuated by a set of cables or fluid filled tubes, completely lacking joints (Hannan and Walker, 2003). Since they are usually based on one continuous, highly flexible backbone, bending can occur at any point along the structure, resulting in an infinite dimensional joint space.

Controlling these continuum manipulators requires a totally different approach from that used with multi-joint manipulators, which can still be controlled by techniques deriving from motor control studies of the human arm. To date, several control mechanisms for such continuum manipulators have come from the field of computer sciences and engineering. For example, Chirikjian and Burdick (1995) used a continuum formulation of kinematics utilizing a backbone curve model to capture the robot's essential macroscopic geometric features, such as curvature (the derivative of the tangent angle with respect to arc length). This method was able to efficiently control the manipulator, so that the robot could adopt basic curvature functions dictated by its programmer. However, these curvature functions were limited and had to be pre-programmed.

A different approach by Gravagne and Walker (2000) uses a wavelet decomposition method called modal analysis to solve the inverse kinematics problems. This method allows complex manipulator shapes to be described as a simple basis (components) (some can change the whole robot configuration while others are more spatially limited to fine details). This approach results in fair control accuracy but only for planar movements. Moreover, the method cannot be generalized to any manipulator, since the calculations depend on the manipulator's mechanical characteristics.

Thus, even though these flexible manipulators are phenotypically similar to those created in nature (trunks, tongues and tentacles; see next section), their mechanics and control strategies are still not optimal. To remedy this lack, a new approach named biodynotics (biologically inspired multifunctional dynamic robotics) has begun to take advantage of the power of natural evolution in developing truly flexible continuum structures. A new class of hyper-redundant continuum robots is being built using newly developed artificial muscle-like actuators and they are controlled according to principles learned from morphological, behavioral and physiological studies of natural hyper-redundant appendages. As well as providing exciting new robotic possibilities, it is hoped that these new robots will serve as models to further understand control mechanisms of natural hyper-redundant limbs.

1.5.2 Hyper-redundancy in nature

As explained above, hyper-redundant appendages endow an organism with enormous behavioral advantages. Evolution has mechanically solved the creation of hyper-redundant creatures or appendages using discrete skeletal structures as in snakes or monkey tails or continuum structures such as elephant trunks, tongues and cephalopods arms. Although the continuum characteristics are achieved due to the absence of a rigid skeleton, some form of skeleton is necessary for motion generation (see Movement generation). Continuum structures therefore contain one of two types of non-rigid skeletons - hydrostatic skeletons and muscular hydrostats - that provide support and transmit the force generated by muscle contraction.

Hydrostatic skeletons are found in cnidarians and annelids, among others. They are closed flexible chambers filled with incompressible fluid that transmits pressure changes uniformly in all directions, generating support and interaction with the muscles and enabling muscle re-elongation upon relaxation. Even though such structures function as flexible skeletons, they do not enable localized movement such as manipulation but are more suitable for global movement patterns like locomotion (Kristan, 2000).

An alternative solution is found in a group of organs termed muscular hydrostats - tongues, elephant trunks and cephalopod arms and tentacles. Completely lacking any rigid skeletal structure, these appendages use muscular tissue to generate both support and motion, enabling localized muscular contraction (Kier and Smith, 1985). Thus, in contrast to hydrostatic skeletons, muscular hydrostat organs possess outstanding manipulative and maneuvering abilities, as described for the octopus during arm foraging (Mather, 1998) and the human tongue during vocalization (Lowe, 1980).

Muscular hydrostats consist almost exclusively of compactly packed muscular tissue, with the only fluid in the structure being the muscle cells' incompressible cytoplasm (at least at physiological pressures). Since this liquid does not flow in or out of the structure, the volume remains constant, so that any change in one dimension generates a compensatory change in at least one other dimension.

All muscular hydrostats are characterized by muscle fibers oriented in three general directions; perpendicular to the longitudinal axis, parallel to the longitudinal axis and helical around the longitudinal axis of the organ. The perpendicular fibers are transversally arranged at the center of the organ (cephalopod appendages and

most mammalian tongues). Elephant trunks and nautilus tentacles show a radial arrangement, with fibers originating at the center of the organ and radiating towards the periphery, while in lizard tongues and squid tentacles the arrangement is circular. The parallel fibers are arranged in longitudinal bundles in the periphery around the central core of the organ (elephant trunks, cephalopod arms and mammalian tongues). They are more centrally located in lizard tongues and squid tentacles. The helical muscle fibers are generally present in two superficial layers running in opposite directions and enveloping all the other muscles.

This muscular arrangement, together with the constant volume constraint, can generate 4 basic movements. Shortening is achieved by contracting the longitudinal against the perpendicular muscles, and elongation by strong activation of the perpendicular fibers working against the longitudinal ones. Bending is achieved by activating unilateral longitudinal muscles against the perpendicular ones. Finally, clockwise and anticlockwise torsion is generated by contraction of the two helical musculature layers working against each other. The serial or simultaneous combination of these 4 basic movements can produce a theoretically infinite repertoire of different movements and postures.

Even though this hypothesis for muscular hydrostat function was based on solely morphological findings, it was later confirmed by theoretical and physiological studies. For example, Chiel et al. (1992) used muscular hydrostat principles for modeling the reptilian tongue. Using only longitudinal and transverse fibers, they were able to reproduce some of the tongue's kinematical characteristics. A more descriptive and complete approach was used by Van Leewen and Kier (1997) to model the squid tentacle during prey capture. Recently, Yekutieli et al. (unpublished results) utilized a dynamically realistic computer model of the octopus arm to gain new insights on the motor control of octopus reaching movements. EMG recordings by Smith (1984) showed that elongation of the lizard tongue is achieved by a rise in muscular activity of the circular fibers and shortening is caused by increasing the activity of the longitudinal fibers. Finally, Kier et al. (1989) demonstrated that squids co-contract longitudinal and perpendicular muscles to bend their fin.

A peculiar property of constant volume cylinders is that the relation between their length and diameter is not linear, but rather hyperbolic. This characteristic enables muscular hydrostat limbs to generate mechanical amplification of muscle

displacement or force, as observed in animals with rigid skeletons. Appendages with large length/width ratios at rest require minimal reduction in diameter to generate large and fast elongations. This strategy is observed in squid tentacles, where a length/width ratio of 20:1 and a larger number of perpendicular fibers in comparison to the longitudinal ones enable the squid to extend its tentacles by 70-100% of their resting length within only 20-40 ms (Kier and Van Leeuwen, 1997). A similar strategy was observed in extra-oral tongues (protruding tongues) (Kier and Smith, 1985). In contrast, organs designed for manipulation, such as octopus arms, elephant trunks and intra-oral tongues (vocalization tongues), possess smaller length/width ratios, cross-sections with similar relative amounts of perpendicular and longitudinal fibers, and the longitudinal muscles are located at the periphery, providing better leverage for bending (Kier and Smith, 1985).

1.6 Octopus *vulgaris*

Octopuses belong to the phylum Mollusca, invertebrates characterized by the mantle (an organ enclosing the viscera, gills and the reproductive system), the radula (a structure based on the combination of circular muscles and chitin, used for mechanical digestion), lack of body segmentation, and a muscular structure ("foot") designed for locomotion and anchorage.

A unique class among mollusks is the modern cephalopods - octopus, cuttlefish and squid. They are characterized by a completely merged head and foot (hence their name, Greek *kefalos podos*, head foot), with a ring of arms and/or tentacles surrounding the head. The arms, tentacles, and funnel (an organ used both for breathing and locomotion) are all derivatives of the "foot". Modern cephalopods are the most morphologically and behaviorally complex of the mollusks. Of these the most developed is the octopus, in which, surprisingly, vision, some cognitive functions and manipulative abilities are as highly developed as in higher vertebrates and even humans. The reason for the unique development of modern cephalopods among the invertebrates may have been selection pressures arising from competition between the cephalopods and teolosts (modern fishes). As both groups appeared and evolved at the same time and within the same habitats, there must have been a strong competition for both food and territory. This competition may have pushed modern cephalopods to rapid evolution and to an evolutionary convergence with their competitors (Packard, 1972).

Octopus vision is based on two large eyes with high resolution (17 minutes of arc), whose optical arrangement and functional structures are similar to those of vertebrates. They possess a muscle-operated focusing lens, pupils for light adaptation, and visual input is processed by bipolar, amacrine and ganglion cells, which, in the octopus, lie in optic lobes rather than in the retina (Wells, 1978).

The octopus has remarkable cognitive skills, showing learning abilities such as sensitization, habituation (Mackintosh and Holgate, 1965), classical conditioning (Papini and Bitterman, 1991), visual discrimination learning, where octopuses can be trained to differentiate between bars of different orientations or different shapes, (Sutherland, 1957), tactile discrimination learning, where blind octopuses learn to distinguish between different textures using their arm suckers (Wells and Wells, 1957), motor learning shown in the a reduction in the time taken to open a jar in subsequent trials (Fiorito et al., 1990), as well as spatial learning and the ability to learn about and solve detour problems and mazes both in laboratory and in their natural habitat (Moriyama and Gunji, 1997; Mather, 1991 and Boal et al., 2000).

Moreover, octopuses demonstrate advanced social learning abilities (Fiorito and Scotto, 1992), where a naive octopus needs only four observations of a trained octopus attacking a previously positively rewarded target before the observer itself prefers attacking the same target. The "observational" memory trace remains stable for at least 5 days. Even more amazing is the octopus' ability to morphologically and behaviorally mimic various venomous animals in its habitat, such as lion-fishes and sea-snakes, even in the absence of the model. Since octopuses can mimic more than one model and mimicry is not continuously employed, this behavior has been termed "dynamic mimicry". Intriguingly, the decision of which mimicry strategy an octopus uses depends on its intentions (Norman et al., 2001).

In addition, the octopus achieves a unique communication ability by combining an enormous number of different body postures, skin textures (from smooth to cryptic) generated by a layer of crisscross subcutaneous muscles, and a complex chromatic behavior (Packard and Sanders, 1971; Moynihan, 1975). The last is generated by a neuronally regulated chromatophore system, in which pigment-filled sacs embedded in the skin can be expanded by contracting tiny muscle fibers attached to the sacs. Both subcutaneous and chromatophore musculature are directly controlled by the brain, and changes in texture and colors may occur in as

little as 30 ms. Finally, and perhaps most amazing, octopuses may even play; this learning behavior was until recently thought only to be expressed in young higher mammals (Mather, 1999; Kuba et al., 2003).

The octopus' boneless body allows it to pass through any hole larger than its brain capsule and to move its arms to any position with a virtually infinite number of DOFs. Around 300 suckers distributed along the ventral side of each arm provide a powerful grip. The extreme flexibility and grip endow the octopus with outstanding manipulative abilities; they can build shelters (Wells, 1978), open screwtop jars (Fiorito, 1990) and even untie stitches in surgical silk thread (Mather, personal communication).

In summary, there is no doubt that the octopus is an outstanding example of the power of evolution to shape unique solutions to complex problems. Therefore, octopuses have been the subjects of behavioral and neurophysiological research, especially in the search for the neurobiological basis of learning and memory. This research was basically established by J.Z. Young (1960, 1962 and 1964) and M. Wells (1959, 1961) and followed more recently by Hochner et al. (2003).

1.6.1 Nervous system morphology

The extremely complex behaviors described above, rare among invertebrates, require sophisticated sensory and motor systems, as well as a highly developed nervous system. Octopuses have a centralized brain lying around the esophagus, which is composed of 42 million neurons (Figure 1). The brain has two main sub-divisions: The supra-esophageal mass, responsible for higher brain functions, such as visual and tactile learning and memory, motor control of the arms, chromatophores and skin texture; and the sub-esophageal region, which controls the lower and essential functions, such as breathing and heart rate. Two large optic lobes (92 million cells) are connected to the ventral part of the supra-oesophageal mass. Two main tracts leave the central mass: the pedal tract, which innervates the mantle, and the brachial tract, which divides into eight cords to innervate each arm.

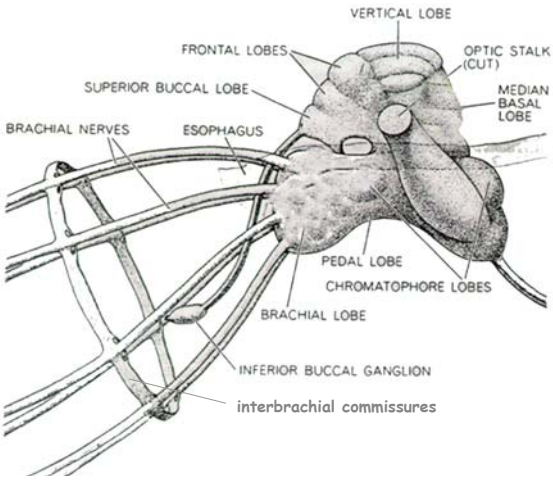

Figure 1. A diagrammatic drawing of the octopus brain and the pedal and 8 brachial tracts, view from its lateral side. The supra-oesophageal mass is the brain area above the esophagus. The sub-oesophageal mass is found bellow the esophagus (Graziadei, 1971)

On entering the arm, each brachial cord forms the axial nerve cord (Figure 2). This consists of a nerve cord of approximately 300 almost fused ganglia and, running dorsally to them, the cerebro-brachial tracts. The ganglia are positioned opposite each sucker. Each ganglion has an outer cell layer and an inner neuropil and both the outer cell layer and inner neuropil extend between the ganglia but with a reduction in size due to a decrease in cell number. The cerebro-brachial tracts, dorsal to the ganglia, consist of two large nerve trunks of around 32.000 axons (2-25μm in diameter).

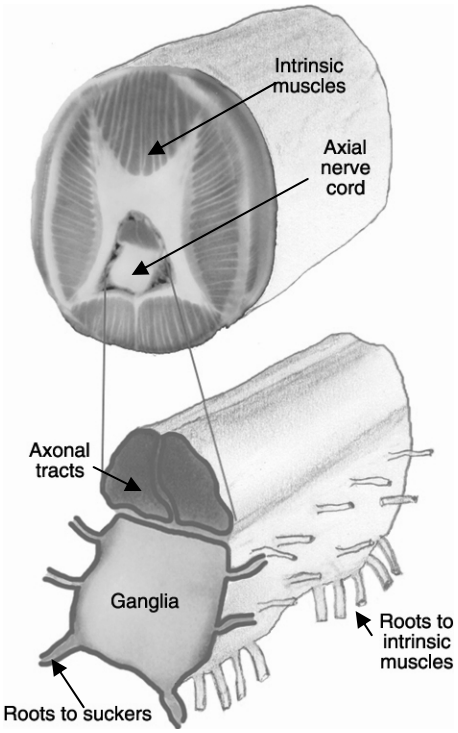

Figure 2. Top, a diagrammatic drawing of a cross section of the octopus arm, showing the arm's intrinsic musculature wrapping the axial nerve cord. Bottom, the axial nerve cord, showing the axonal tracts, the ganglia and the roots enervating the arm's musculature (Sumbre et al, 2001).

The axial nerve cords of the different arms interconnect via the interbrachial commissures at the base of each arm (Figure 1) where there are no ganglionic formations.

In addition to the axial nerve cord, each arm has five other nerve centers: four intramuscular nerve cords made up of small ganglia, lie more peripherally among the intrinsic muscles of the arm. These are connected to the axial nerve cord via segmental connectives and with each other by the anastomotic tracts. The fifth center is the ganglia of the suckers, one for each sucker, which are situated between the axial nerve cord and the sucker itself (Young, 1963).

This highly developed nervous system in the arm contains $4.75x10^7$ neurons for each arm, totaling 35 $x10^7$ for the 8 arms (cf. $15x10^7$ in the entire brain). Among the $4.75x10^7$ neurons in each arm, ~$3.8x10^5$ are motor neurons, ~$2.3x10^6$ are sensory receptors, and 32.000 nerve fibers connect the arm and the brain. Thus the bulk of the arm nervous system ($4.48x10^7$ neurons) is mainly made up of interneurons (Graziadei, 1971). This suggests a remarkable level of autonomy in the neuromuscular system, which is also indicated by the complex local motor reflexes evoked by pain, tactile or chemical stimuli to the arm (Wells, 1959, Rowell, 1963, Graziadei, 1965, Altman, 1971).

1.6.2 Neurophysiology

While many studies have examined the behavior of the octopus and the anatomy of its nervous system, the few investigations of nervous system function have been confined to analyzing behavioral changes after brain lesions (Maldonado, 1964, Wells, 1961, 1978). This lack of electrophysiological experimentation is primarily due to technical difficulties. The absence of any rigid structures in the octopus body has until now prevented stably securing recording or stimulating electrodes. In addition, the octopuses' manipulative skills enable them to remove any electrode inserted for chronic recording in awake animals, while anesthetized preparations require such high doses of anesthesia that electrophysiological recordings are not possible. *In vitro* preparations require high levels of oxygenation due to contraction of the blood vessels (since the octopus has no coagulation mechanism, blood vessels strongly contract on injury to avoid bleeding, Abbot and Miyan, 1995).

Only recently have newly developed techniques solved many of these technical obstacles and finally allowed both *in vivo* and *in vitro* electrophysiological

recordings. Bullock and Budelmann (1991) used hypodermic needles inserted through the cranial cartilage to record patterns of evoked sensory activity from the brains of unrestrained cuttlefish. Similarly, Zullo et al. (unpublished results) have used fine stainless steel microwire attached to the brain capsule to record brain activity in the various brain lobes in freely behaving octopuses. They aim to gain insights on the role of higher brain areas in sensory processing and motor control. *In vitro* recordings of brain slices were developed by Williamson and Budelmann (1991), who for the first time were able to record intracellularly from brain neurons to investigate the brain's neural connectivity. This technique was improved by Hochner et al. (2003), who demonstrated that the vertical lobe (an area related to visual learning and memory), shows similar long term synaptic potentation (LTP, a cellular phenomenon related to learning and memory) to that found in higher vertebrates.

New nerve-muscle preparations and preparations of dissociated muscle cells from the octopus arm have revealed unique physiological features. For example, muscle cells are morphologically and electrically compact and there is no electrical coupling between them (Matzner et al., 2000). They are excitable and generate fast overshooting Ca^{2+} voltage-gated action potentials (Rokni and Hochner, 2002). Each cell is innervated by three types of cholinergic synapse. Overall, these results suggest a simple, linear mechanism for transforming neural activity into muscle contraction that probably evolved to ensure a high level of localized control in the flexible arms (Matzner et al., 2000). Finally, preparations of the isolated nervous system of the arm have permitted investigation of the role of mechanosensory feedback during arm extension movements and of the connections between the intrinsic arm musculature and the axial nerve cord (Gutfreund et al., unpublished results).

1.6.3 Motor control of the arm

Previous kinematical studies of the flexible arms of the octopus (Gutfreund et al, 1996, 1998) have shown that the arm reaches towards a target in a very stereotypical manner, despite a possibly infinite number of DOFs. First, a bend is generated somewhere along the arm and then propagated to the tip of the arm. This bend is always dorsally oriented, leaving the suckers pointing forward, and the part of the arm proximal to the bend remains extended as the bend propagates.

Kinematics analyses have shown that the bend trajectory is generally slightly curved and restricted to the plane of motion. The tangential velocity has a bell-shaped profile with a maximal velocity ranging from 10-60 cm/s. A simple mathematical model (Gutfreund et al., 1998) and a dynamic model of the octopus arm (Yekutieli et al., unpublished results) have shown that this bell-shaped profile largely results from the interaction between the arm's tapering form with water forces. Normalizing bend velocity profiles to their velocity peak and distance traveled shows that the profiles are invariant, regardless of direction, speed of movement, or anatomical size of the arm, and the invariance is especially robust during the acceleration phase of the movement. These characteristics are not only restricted to reaching movements, they were also observed during non-goal directed arm extension movements while searching, walking or swimming. Taken together, these findings suggest the existence of a basic motor program that greatly simplifies the highly complex problems of the inverse kinematics and dynamics transformations involved in controlling flexible arms (Walker, 2000; Gutfreund et al., 1996, 1998).

The next step was investigating whether the wave-like propagation observed during arm extension is achieved passively or actively. A passive whip-like movement may be generated by the muscles at the base of the arm creating an initial force that propagates a bend along the arm without involving further muscle contraction. In an active mechanism, bend propagation would follow a gradual muscle contraction along the arm (Hines and Blum, 1978). EMG recordings from octopus arms have demonstrated that the arm extension movement is an active process, with maximal EMG amplitude recorded ~50 ms before the bend reaches the electrode (Gutfreund et al., 1998). The main EMG burst is sometimes followed by activity of lower intensity, presumably reflecting the tonic muscle contraction necessary to maintain the arm extension after the bend has passed. The level of activity in the burst shows a significant positive linear correlation with the global parameters of the movement right from its start (e.g. peak velocity and acceleration). These results suggest a feed-forward mechanism in the motor program controlling arm extension, in which 3 variables need to be set before onset of movement (pitch, yaw, and velocity of bend propagation). This strategy enormously simplifies the complex task of controlling hyper-redundant appendages.

1.7 Research objectives

My aim was to further explore the motor control system of the octopus arm during goal-directed movements, using both behavioral and electrophysiological methods to gather information on its organizational principles and neuronal control mechanisms. The results of the research here provide further insights on how biological systems have evolved to overcome the complex problem of controlling a highly redundant motor system. These insights are of considerable significance for the ongoing multi-disciplinary effort of developing and controlling genuine flexible robotic manipulators.

Chapter 2
Materials and methods

Experimental animals and maintenance*. Octopus vulgaris* were collected from the bay of Naples, Italy, or Israel's Mediterranean coastline. The animals were maintained in 50x50x40 cm glass tanks containing artificial seawater. The water circulated continuously in a closed system, filtered by active carbon and mechanical and biological filters. The animals were held at a temperature of 16°C in a 12 hrs. light/dark cycle.

Octopus training. A few days before experiments, octopuses were moved to a bigger aquarium (80x80x60 cm) and held at a temperature of 18°-20°C. For the experiments described in Chapter 3.2 octopuses were trained to reach with their arms towards a white disc held by a transparent fishing thread. The animals were fed with small pieces of sardine at a random frequency when they succeeded in catching the target with a reaching movement. A similar training method was used for the experiments in Chapter 3.3, but here octopuses were reinforced for reaching towards the target with only one arm and for maintaining its extension until a piece of food was placed somewhere along the arm. The experiments began once the octopuses were acclimatized and trained, typically after a one hour trial session repeated for ~3 consecutive days.

Behavioral experiments. For the experiments in Chapter 3.2, the trials began when the target was introduced into the tank and the octopus commenced reaching towards it. The target was lifted at different delays with respect to the beginning of its movement, with different velocities and amplitudes of displacement. The target was not raised during randomly chosen trials to avoid the octopus learning this movement; if the target was raised with every reaching movement, octopuses quickly learned to reach towards the final position of the target instead of reaching towards its original position, even if the target was not displaced. For the experiments in Chapter 3.3, small pieces of either sardine or anchovy (~1 cm^3), were brought close to the arm, so they could be grasped by the suckers and brought to the mouth. In all cases, the octopuses were able to move freely around the aquarium.

Denervated arm experiments. Octopuses were anaesthetized in a mixture of 2% ethanol in seawater and subdued by removing the supra-oesophageal brain mass. After a recovery period of ~24 hrs, the axial nerve cord of one of the arms was exposed and transected. The preparations were submerged in circulating aerated seawater at ~20°C. The proximal part of the denervated arm was fixed to a platform; the distal part hung freely. Electrical stimulation was applied through a Teflon coated silver bipolar electrode placed dorsally on the exposed axial nerve cord (stimulus frequency, 50 – 120 Hz; train duration, 0.1 – 1.2 s). For tactile stimulation, the skin or suckers of the arm were touched with a finger or small plastic stick. The stimulating electrical signals were recorded simultaneously with the video images in one of the two hi-fi audio channels of the video recorder.

Supra-oesophageal lesions. Octopuses were anaesthetized as described above, and the brain's supra-oesophageal mass was removed at different levels by cutting through it with fine surgical scissors. Behavioral experiments began after a recovery period of ~24 hrs in the experimental aquarium. The extent of the lesion was morphologically confirmed postmortem by observing Nissl stained brain slices (100 – 200 µm) under a light microscope.

Video recordings. Both natural and evoked movements were filmed with two super VHS PAL synchronized video cameras positioned ~90° apart (temporal resolution 20 ms, shutter speed 1/250), The images from both cameras were combined into a single image by a video mixer and recorded with a super VHS video recorder.

Kinematic analysis. Only trials in which the whole movement could be clearly seen from beginning to end were analyzed on a Silicon Graphics workstation by digitizing the coordinates of the bend or target (Chapter 3.1), bend and base of the arm (Chapter 3.2) or the object and 3 joints (Chapter 3.3) from both cameras in every frame (20 ms).

The coordinates of both 2D images were fused into 3D ones using the direct linear transformation (DLT) algorithm. This method transforms the 2D cameras'

coordinates to external XYZ ones, based on information about the coordinates of at least 12 external landmarks visible in both cameras. Thus, for calibration, a cubic structure with either 12 or 14 clear landmarks was filmed at the aquarium where the experiments were performed just before every session of experiments (Gutfreund et al., 1996; Wood and Marshall, 1986). Trials which showed small errors (less than 5%) of the transformed coordinates were chosen for analysis. The 3D trajectories of every digitized point were then smoothed using a Natural B-spline method (Craven and Wahba, 1979).

Plane of motion. The plane of motion was determined by rotating the 3D coordinates of the paths in space and subjectively determining the best plane containing the movement of the digitized points. The paths were then transformed into a coordinate system where the selected plane lay at 45° to the ZY plane. The fit to a single plane was estimated by the coefficient of determination (R^2) of the regression analysis and the relationship between the length of the path and its residual error.

Backbone curve. Additionally, for the experiments in Chapters 3.2, 3.3, the curvature of a 2D backbone curve (Chirikjian and Burdick, 1990) visually fitted along the middle of the arm was calculated for each frame of the movement, according to:

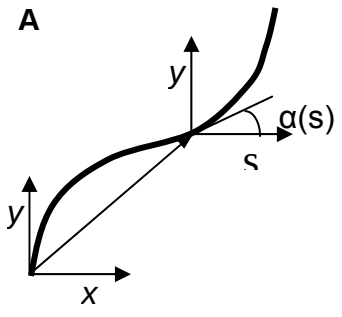

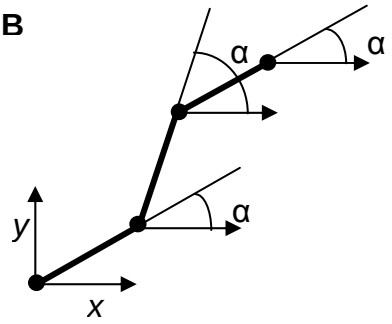

$$K(s) = \frac{d\alpha(s)}{ds(s)}$$

Continuous

$$K_i = \frac{\alpha_{i-1} - \alpha_{i+1}}{S_{i-1} - S_{i+1}}$$

Discrete

where ***s*** is the normalized backbone curve arc length and ***α*** is the local slope with respect to the Cartesian coordinates.

The curvature of the arm during a movement was calculated and then plotted against time and the normalized length of the arms.

Calculation of joint angles during fetching movements. For the experiments performed in Chapter 3.2, the joint-like angles (θ_1, θ_2 and θ_3), describing the rotations of the three segments (L_1, L_2 and L_3), see bellow (right), were trigonometrically calculated from the smoothed data points previously digitized, according to:

$$\theta_1 = ar\cos\left[\frac{\vec{L}_u}{\| L_u \|} x \frac{\vec{L}_1}{\| L_1 \|}\right]$$

$$\theta_2 = ar\cos\left[\frac{\vec{L}_1}{\| L_1 \|} x \frac{\vec{L}_2}{\| L_2 \|}\right]$$

$$\theta_3 = ar\cos\left[\frac{\vec{L}_3}{\| L_3 \|} x \frac{\vec{L}_2}{\| L_2 \|}\right]$$

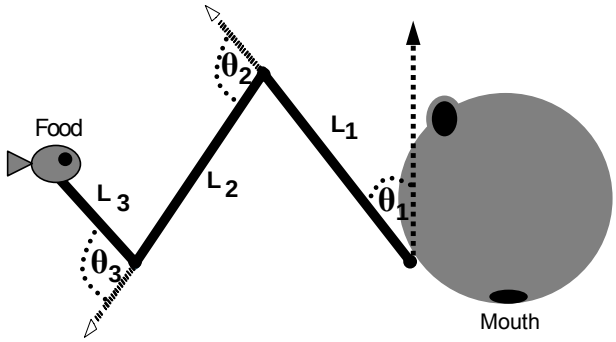

where ***L1, L2*** and ***L3*** are the vectors co-aligned with the segments of the arm, which form each of the 3 joint angles. A unit vector in the plane of motion, parallel to the gravitational force and starting at the base of the arm (***Lu***), was used to compute the angle at the base of the arm (θ_1).

The temporal order of joint generation. To calculate the time sequence of joint formation, the backbone-curve curvature function of the octopus arm during fetching movements (Chapter 3.2) was calculated as described above. The onsets of the formation of the bends were determined by defining the time at which the curvature function exceeded a specified threshold. This threshold was set as one standard deviation above the arm's average curvature previous to the formation of the joints (at this time the extended arm was relatively straight).

Tangential and angular velocities. The tangential and angular velocities of each digitized point were calculated from the time derivatives of the smoothed 3D position coordinates of the digitized points and the calculated angles.

The tangential and angular velocity [V(t)] of the bend (for reaching movements), the grasped object and joints (for fetching movements) and movement durations (t), were then normalized to the maximal velocity (V_{max}) and either the traveled distance (D) or angular amplitude (the total amount of rotation of the joints, A_{amp}) were calculated:

$$V_{norm} = \frac{V(t)}{V_{\max}}$$

$$T_{norm} = V_{\max} \times \frac{t}{A_{amp}}$$

$$T_{norm} = V_{\max} \times \frac{t}{D}$$

Since it is impossible to establish the exact initiation and termination times of the movement needed to calculate the traveled distance, we took advantage of the bell-shape velocity profiles and calculated the traveled distance from the first minimum (left arrow) to the maximum (middle arrow). The angular amplitude (A_{amp}), of the joints was calculated from the first minimum (left arrow) to the second minimum (right arrow) of the velocity profile (see below).

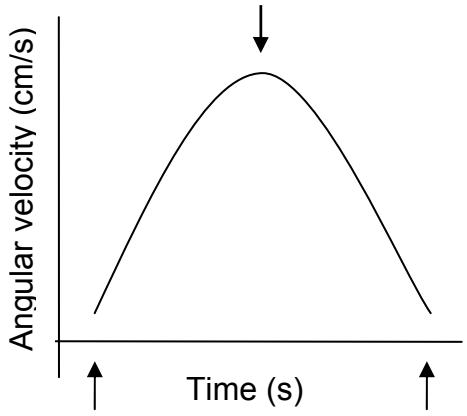

Submovement extraction. For experiments in Chapter 3.2, a 5th order polynomial was fitted to the average velocity profile calculated from the normalized and co-aligned velocity profiles of θ_2, in the least-squared sense. This polynomial was then

scaled by a constant factor to fit the highest peak of the double-peaked angular velocity profiles. The scaled polynomial was then subtracted from the original data and a second polynomial scaled to the remaining peak. The two scaled polynomials were algebraically summed (Flash and Henis, 1991; Berthier et al., 1995) and compared to the original data by minimizing the sum of squares and estimating the R^2 value.

EMG recordings and analysis. Following anesthesia (3.5% magnesium in seawater), one or two Teflon-coated stainless steel wires (0.13 mm in diameter), were implanted in the dorsal intrinsic musculature of an arm through a fine needle (26G) inserted in the arm (~1 mm of the insulation was removed from the middle of the section of the electrode inserted in the arm). The electrodes were positioned with different distances between them (~1-3 cm) and at different positions along the arm. White plastic beads (25 mm^2) marked their location along the arm. The electrodes were connected to low-level AC differential amplifiers (DP 301, Warner Instruments Inc.) and muscle activity was differentially recorded between the implanted electrodes and a second similar electrode submerged close to the implanted ones. The aquarium was grounded and connected to the amplifier, using a low resistance silver wire. The EMG signals were amplified (10.000 times), analogically band-pass filtered (0.01 – 3 KHz), and recorded separately in the two hi-fi audio channels of a Super VHS video recorder simultaneously with the video signal. The EMG signals were then digitized at 10 KHz. The sinusoidal noise components (50 Hz. and higher harmonics) were removed in the frequency domain by Fourier transforming the EMG time signal and attenuating the peaks corresponding to instrumental noise to the level of the neighboring frequency range while maintaining the Fourier phase. Then the EMG signals were rectified and smoothed (running average of 5 ms bins) using Matlab (MathWorks Inc.).

The onsets of the EMG signals at each electrode were computed using 4 independent methods: visually determined, 3 STD amplitude threshold (DiFabio 1987), 1 STD Fourier transform threshold and the Generalized Likelihood Ratio (Micera et al., 1998). For the Fourier transform threshold algorithm, the EMG signal frequency baseline between 10 – 500 Hz (the EMG frequency spectrum during fetching) was calculated from the EMG recordings previous to the onset of the

movement. We set the threshold as 1 STD of this baseline. Then, starting ~300 ms previous to initiation of the fetching movement, running bins of 25 ms in length were sequentially Fourier transformed with steps of 0.1 ms until the end of the movement. The onset of the EMG signal was set as when the threshold was constantly exceeded for a period of 1 ms (10 consecutive steps). The exact positions of the electrodes with respect to the bends during fetching were confirmed from the video recordings.

Chapter 3
Results

3.1 Control of octopus arm extension by a peripheral motor program

… Indeed, very few people are aware that in each of our fingers, located somewhere between the first phalange, the mesophalange, and the methaphalange, there is a tiny brain. The fact is that the other organ which we call the brain, the one with which we came into the world, the one which we transport around in our head and which transports us so that we can transport it, has only ever had very general, vague, diffuse and, above all, unimaginative ideas about what the hands and fingers should do. For example, if the brain-in-our-head suddenly gets an idea for a painting, a sculpture, a piece of music or literature, or a clay figurine, it simply sends a signal to that effect and then waits to see what will happen. Having sent an order to the hands and fingers, it believes, or pretends to believe, that the task will then be completed, once the extremities of the arms have done their work …

José Saramago (A caverna).

Control of Octopus Arm Extension by a Peripheral Motor Program

German Sumbre,[1] Yoram Gutfreund,[1]* Graziano Fiorito,[2] Tamar Flash,[3] Binyamin Hochner[1]†

For goal-directed arm movements, the nervous system generates a sequence of motor commands that bring the arm toward the target. Control of the octopus arm is especially complex because the arm can be moved in any direction, with a virtually infinite number of degrees of freedom. Here we show that arm extensions can be evoked mechanically or electrically in arms whose connection with the brain has been severed. These extensions show kinematic features that are almost identical to normal behavior, suggesting that the basic motor program for voluntary movement is embedded within the neural circuitry of the arm itself. Such peripheral motor programs represent considerable simplification in the motor control of this highly redundant appendage.

In directed voluntary movements, the nervous system generates a sequence of motor commands producing the forces and velocities that efficiently bring the limb to the target (*1*). In articulated appendages, the control of goal-directed movements appears to be simplified by the planning of optimal trajectories (*2*, *3*), by vectorial summation and superposition of basic movement primitives (*4*, *5*), and by the use of a flexible combination of muscle synergies (*6*). However, flexible structures introduce a further dimension of complexity.

The octopus arm can move in any direction, using a virtually infinite number of degrees of freedom. This high maneuverability results from octopus arms behaving like a muscular hydrostat, because they are almost entirely constructed of densely packed muscle fibers along their transverse, longitudinal, and oblique axes (*7*). These flexible arms are controlled by an elaborate peripheral nervous system containing $\sim 5 \times 10^7$ neurons distributed along each arm. Only $\sim 4 \times 10^5$ of these are motor neurons (*8*), which innervate the intrinsic

[1]Department of Neurobiology and Interdisciplinary Center for Neuronal Computation, Institute of Life Sciences, Hebrew University, Jerusalem 91904, Israel. [2]Laboratorio di Neurobiologia, Stazione Zoologica di Napoli "A. Dohrn," Naples 80121, Italy. [3]Department of Computer Science and Applied Mathematics, Weizmann Institute of Science, Rehovot 76100, Israel.

*Present address: Department of Neurobiology, Stanford University School of Medicine Stanford, CA 94305, USA.

†To whom correspondence should be addressed: E-mail: bennyh@lobster.ls.huji.ac.il

muscles of the arm and locally control muscle action (*9*). This peripheral nervous system is organized as an axial nerve cord composed of ~300 interconnected ganglia and two cerebrobrachial (axonal) tracts of ~30,000 nerve fibers running dorsally to the ganglia (Fig. 1B). The axons in the tracts carry sensory and motor information to and from the highly developed centralized brain (*10*).

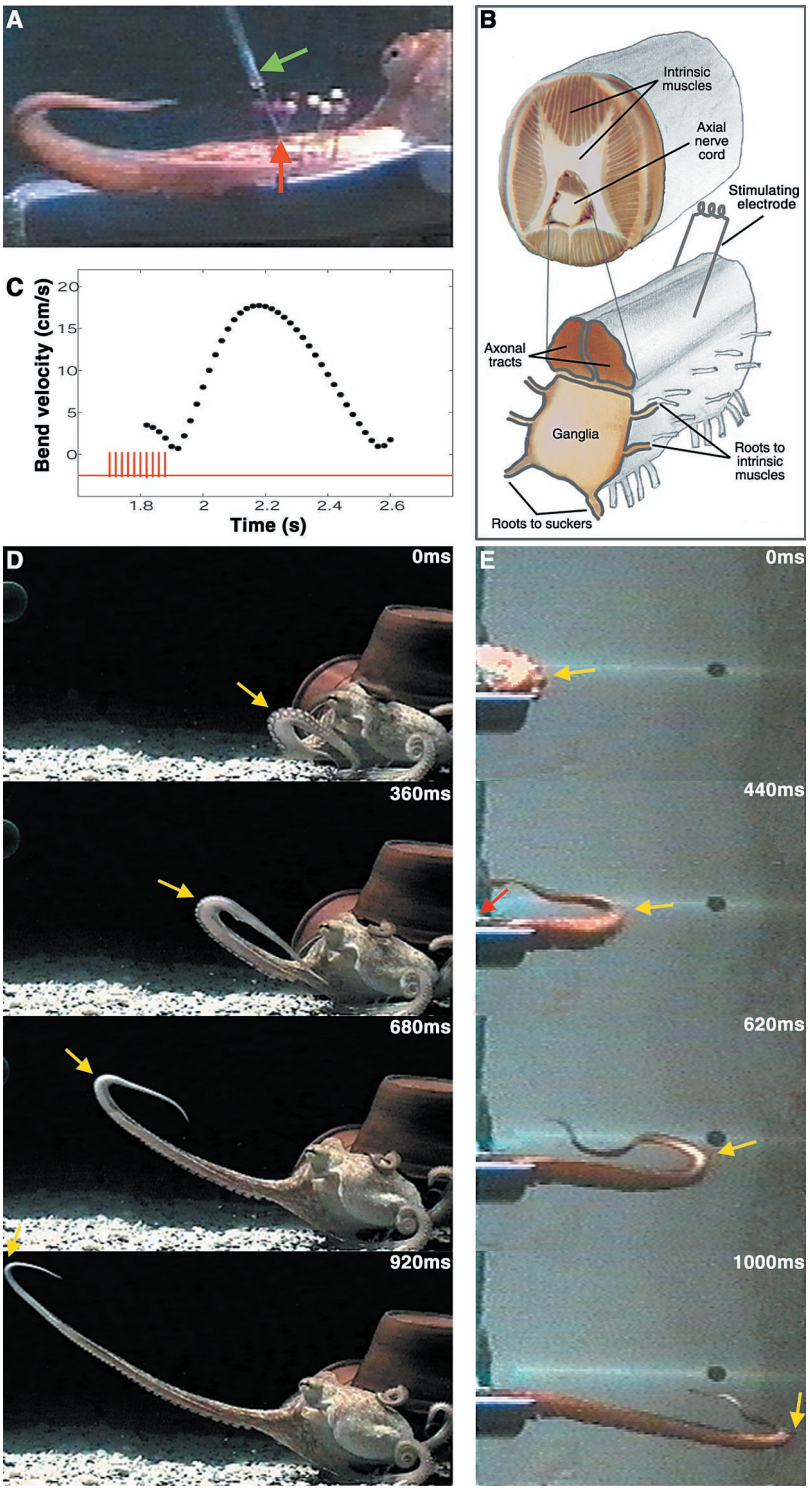

Fig. 1. Natural and evoked arm extensions are qualitatively similar. (**A**) A decerebrated preparation was fixed to the experimental platform (green arrow, stimulating electrode; red arrow, area where the axial nerve cord was transacted and stimulated). (**B**) The arrangement of the intrinsic arm muscles and an enlarged portion of the axial nerve cord showing the stimulating site. (**C**) A stimulus train (red trace) is superimposed on the velocity profile of an evoked arm extension (black dots). The acceleration phase begins after the stimulus ends. (**D**) A freely behaving octopus reaching toward a target. (**E**) Electrically evoked bend propagation in the denervated arm of a decerebrated animal (yellow arrows indicate the bend point).

The octopus reduces the complexity of controlling this flexible appendage by using highly stereotypical movements. Reaching movements consist of a bend propagating along the arm toward the tip (Fig. 1D) in a highly stereotypical and invariant way (*11*). The level of muscle activity [measured with an electromyogram (EMG)] shows a positive correlation with kinematic variables, and the EMG level measured during the initial stages of the movement predicts the bend's peak propagation velocity attained later during the movement. These predictive relations suggest that feed-forward motor commands play an important role in the motor program for arm extension (*12*).

Here we show that arm extensions can be elicited in denervated arms by electrical stimulation of the arm axial nerve cord or by tactile stimulation of the skin, suggesting that a major part of this voluntary movement is controlled by a pattern generator that is confined to the arm's neuromuscular system.

A short train of electrical stimulation to the dorsal part of the denervated nerve cord (*13*) evoked movements that involved the entire arm. Forty-six percent of these movements were characterized by a bend traveling forward along the arm (*14*). In 20 of these extensions, the movement occurred after the termination of the stimuli, indicating that the movement was indeed triggered by the stimulation and is not directly driven by the stimuli (Fig. 1C). In the remaining 30 movements, the movement started before the end of the stimulation train. The average overlap between the stimulation train and the acceleration phase of the movements was only 19%. Because kinematic analysis showed no differences between the two types of movements, both were combined for further analysis. Arm extensions were evoked by stimulation of the dorsal part of the axial nerve cord that contains the axonal tracts from the brain (Fig. 1B). In contrast, stimulation of the muscles within the same area or the ganglionic part of the cord (Fig. 1B) (*10*) evoked only local muscular contractions.

The evoked bend propagation resembled stereotypical arm extensions in freely behaving animals (*11*) (Fig. 1, D and E). As in natural behavior, a dorsally oriented bend propagated along the arm, causing the suckers to point in the direction of the movement. As the bend propagated, the part of the arm proximal to the bend remained extended. Movements resembling normal arm extensions could also be initiated in amputated

arms by electrical stimulation of the nerve cord or by tactile stimulation of the skin or suckers.

Bend propagations were more readily initiated when a bend was manually created before stimulation (n = 50 movements, 16 arms). However, such bend propagation could also be initiated in fully relaxed arms (n = 6, four arms). Here the stimuli triggered the initial phase of bend formation, followed by the arm extension. All these observations show that the nervous system of the arm does not just drive local reflexes (*15*–*17*) but controls complex movements involving the entire arm.

Kinematic analysis allowed quantitative comparison between the evoked and natural movements (*14*). In both tactile (n = 6, four arms) and electrically evoked movements (n = 50, 16 arms), the bend point (the point of maximal curvature) propagated within a single plane (*18*), generally along a lightly curved path (Fig. 2, A and B). The coefficient of determination for movement within a single plane was highly significant (average $R^2 = 0.96 \pm 0.06$); the P value was always smaller than 10^{-8} (F test). The average SE = 0.34 ± 0.39 cm, and the average distance traveled by the bend point was 12.5 ± 4.7 cm. The low SE, in comparison to the distance traveled, confirms that the bends propagate within a single plane. This result is similar to that obtained in freely behaving octopuses (*11*).

Velocity profiles were derived by calculating the tangential velocities of the bend point and plotting these against time (*19*). The velocity profiles of the evoked movements closely resembled those of arm extensions in freely behaving animals (*11*) (Fig. 2, C and D), both having bell-shaped velocity profiles and a similar maximal velocity range (7 to 60 cm/s and 9 to 61 cm/s, respectively).

Normalizing and superimposing the velocity profiles according to their maximal speed and duration and the bend propagation distance (*11*) revealed a robust invariance (Fig. 2, E and F) and showed that the evoked movements were almost kinematically identical to the movements of freely behaving octopuses (Fig. 2G). The variances of the velocity profiles of the evoked and natural movements were also similar, with lower variance during the acceleration phase of the movements (Fig. 2H).

To determine whether the evoked extension is generated passively by a whiplike moving wave or by an active propagation of muscle contraction, we analyzed the kinematics of passive bend propagations and recorded muscle activities (recorded with an EMG) during the evoked movements. Passive bend propagations were produced by dragging a dead arm behind a stick and then letting the stick collide with a solid barrier. A bend was formed and propagated along the arm (Fig. 3A), emphasizing the role of passive interactions with the water in shaping the movement (*12*). However, the velocity profiles were monotonically decelerating (Fig. 3B), unlike the bell-shaped velocity profiles of evoked or natural arm extensions (Fig. 2, C and D). Furthermore, EMGs recorded during the evoked movements (Fig. 3, C and D; n = 7, three arms) reveal an active propagation of muscle activity as in natural arm extensions (*12*).

In 23 experiments in which extensions could be repeatedly evoked, the initial posture of the arm was changed manually while the electrode location and stimulus parameters remained constant. Movements evoked from similar initial arm postures tended to have similar paths (Fig. 4). Likewise, different starting postures resulted in different final paths (15 experiments). Aiming in arm extension thus appears to involve adjusting the initial posture of the arm before, or together with, the command for arm extension.

Because the extensions evoked in denervated octopus arms were qualitatively and kinematically identical to natural arm extensions, there appears to be an underlying motor program embedded in the neuromuscular system of the arm, which does not require continuous central control. This finding is consistent with the remarkable autonomy of the arm local reflexes (*15*–*17*) and with the elaborate nervous system in each arm, which is connected to the brain by a relatively small number of nerve fibers (*8*, *10*).

The division between the central and peripheral levels of the octopus motor control system resembles the hierarchical organization of motor control systems in other invertebrates and vertebrates, even though in the octopus it uniquely serves as an important component in a goal-directed voluntary movement rather than in rhythmical or reflexive behaviors (*20*–*22*). We do not yet know whether this is a predom-

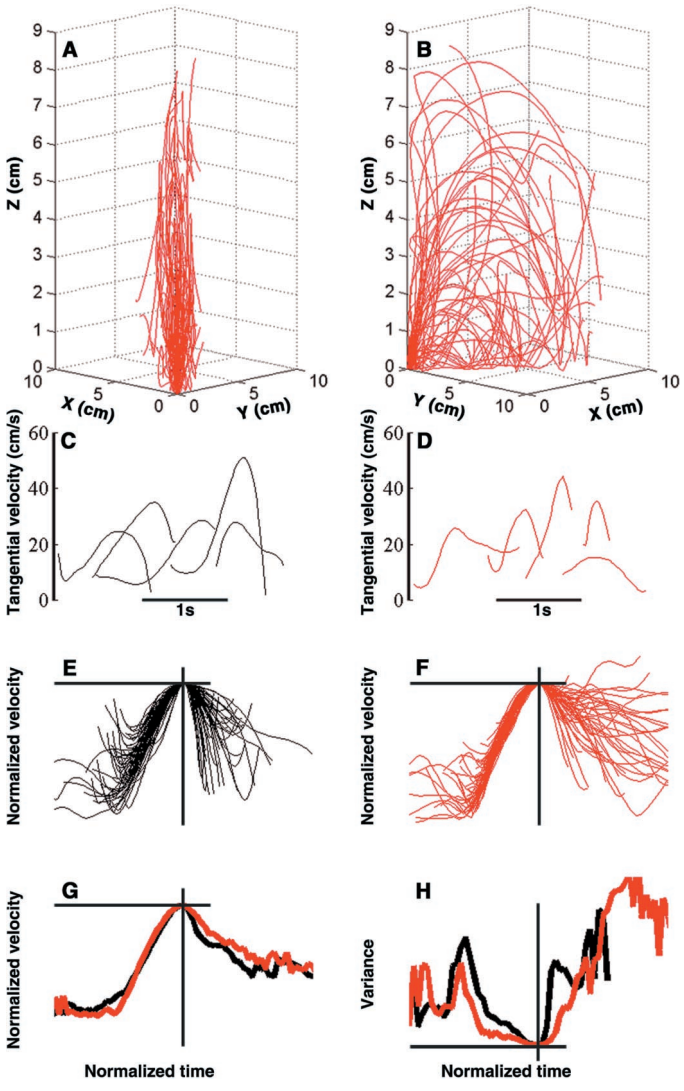

Fig. 2. Comparison between the velocity profiles of natural arm extensions (black) and evoked movements in the denervated arms (red). (**A** and **B**) The evoked arm extensions lie within a single plane. (A) The paths of 56 evoked extensions mapped into the best-fit plane. (B) The same arm extension paths rotated by 90°. Note the difference in path variability between (A) and (B). (**C** and **D**) Velocity profiles of natural and evoked movements. (**E** and **F**) Velocity profiles normalized according to their peak velocity, duration, and propagated distance and aligned at the peak (n = 56 in both cases). (**G**) The average normalized velocity profiles [calculated from (E) and (F)] of the natural and evoked movements are similar. (**H**) Superposition of the variances calculated from (E) and (F) reveals similar behavior.

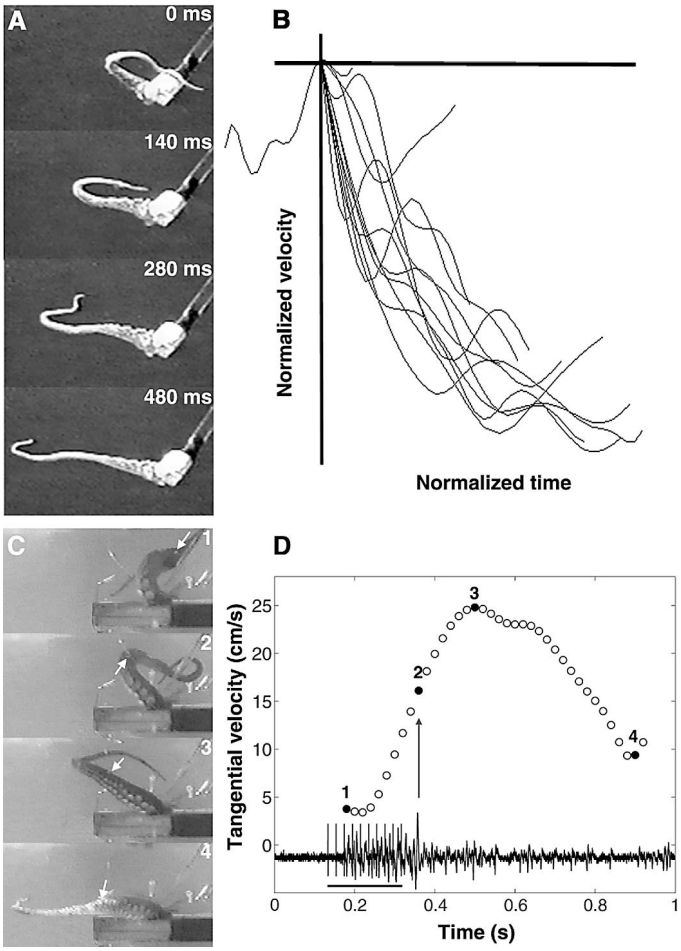

Fig. 3. Evoked movements differ from passive extensionlike movements. (**A**) A sequence showing an extensionlike movement generated by whipping a dead octopus arm. (**B**) Velocity profiles of 12 passive extensions showing decelerating velocity profiles, in marked contrast to the evoked or natural arm extensions (Fig. 2, C and D). (**C**) A sequence showing evoked extension in an amputated arm during which an EMG was recorded with a stainless steel electrode inserted though the dorsal muscles and held in place with a bead glued on each side of the arm (arrow) [see (*12*) for details]. (**D**) Velocity profile and EMG of the movement in (C). The numbers mark when the images in (C) were taken. Activity reaching the recording electrode during the stimulation train (horizontal line) probably results from fast-propagating activity along the axonal tracts. There is a burst of activity just before the bend point reaches the electrode (arrow), followed by tonic activity when the arm is extended.

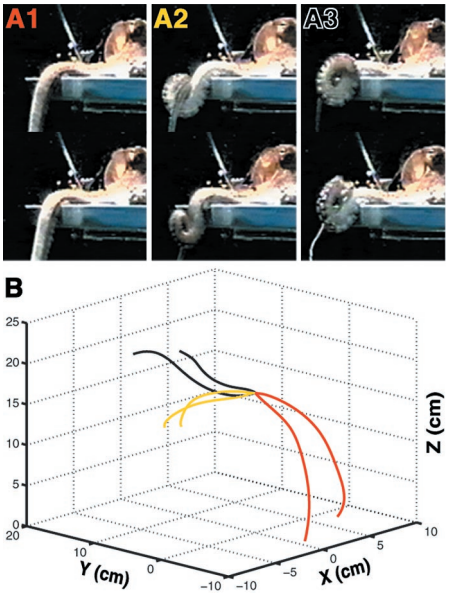

Fig. 4. Similar initial postures generate similar bend paths (when the electrode position and stimulus parameters are kept constant). (**A1** through **A3**) Three pairs of similar starting postures, just before stimulation. (**B**) The evoked paths are shown in pairs in different colors as in (A1) through (A3). The 3D paths are shifted to the same starting coordinates.

inantly feed-forward control mechanism (*12*) or involves a distributed control system based on local reflexes, as in other animals (*23*, *24*).

In this control scheme, the arm neuronal networks produce the neuronal activation patterns prescribing all of the spatiotemporal details of the basic movement patterns, suggesting that the higher central levels (that is, the brain) send global commands to the arm neuronal network to activate and scale the program variables. This division of labor between the central and peripheral nervous systems and the use of a propagating wave with a limited number of degrees of freedom greatly simplify the movement control of flexible arms.

References and Notes

1. J. M. Hollerbach, in *Visual Cognition and Action*, D. N. Osherson, S. M. Kosslyn, J. M. Hollerbach, Eds. (MIT Press, Cambridge, MA, 1990), pp. 151–182.
2. T. Flash, N. Hogan, *J. Neurosci.* **5**, 1688 (1985).
3. C. Harris, D. Wolpert, *Nature* **20**, 780 (1998).
4. T. Flash, E. Henis, *J. Cogn. Neurosci.* **3**, 220 (1991).
5. F. A. Mussa-Ivaldi, *Curr. Opin. Neurobiol.* **9**, 713 (1999).
6. E. Bizzi, M. C. Tresch, P. Saltiel, A. d'Avella, *Nature Rev. Neurosci.* **1**, 101 (2000).
7. W. Kier, K. Smith, *Zool. J. Linn. Soc.* **83**, 307 (1985).
8. J. Z. Young, *Proc. R. Soc. London Ser. B* **162**, 47 (1965).
9. H. Matzner, Y. Gutfreund, B. Hochner, *J. Neurophysiol.* **83**, 1315 (2000).
10. P. Graziadei, in *The Anatomy of the Nervous System of* Octopus vulgaris, J. Z. Young, Ed. (Clarendon, Oxford, 1971), pp. 45–59.
11. Y. Gutfreund *et al.*, *J. Neurosci.* **16**, 7297 (1996).
12. Y. Gutfreund, T. Flash, G. Fiorito, B. Hochner, *J. Neurosci.* **18**, 5976 (1998).
13. To obtain the denervated arm preparation, *Octopus vulgaris* from the Bay of Naples were anesthetized in a mixture of 2% ethanol in seawater (as was also done before each operation) and then "decerebrated" by removal of the supraesophageal brain mass [B. B. Boycott, J. Z. Young, *Symp. Soc. Exp. Biol.* **4**, 432 (1950)] to produce a subdued preparation (Fig. 1A). After a recovery period of ~24 hours, the nerve cord of one of the arms was exposed and transected. We also used acutely amputated arms. The preparations were submerged in circulating aerated seawater at ~20°C. The proximal part of the denervated arm was fixed to a platform; the distal part hung freely. Tactile stimulation was applied to the suckers or skin of the arm. Electrical stimulation (at 40 to 90 Hz for 200 to 500 ms) was applied through a Teflon-coated silver bipolar electrode placed on the dorsal part of the exposed axial nerve cord (Fig. 1B).
14. The evoked arm responses were filmed with two video cameras set ~90° apart and were recorded simultaneously with the stimulus train on a video recorder. The three-dimensional (3D) spatial position of the bend point (the point of maximum curvature) was determined with the direct linear transformation method [see (*11*)]. Out of the many evoked movements (such as local contraction, stiffening, waving, etc.), only in ~10% (n = 116) was a bend observed and its movement analyzed. Only those movements in which the bend was found to propagate were studied (n = 63). Fifty-six movements (89%) had a bell-shaped velocity profile and were compared to natural movements.
15. M. J. Wells, *J. Exp. Biol.* **36**, 590 (1959).
16. C. H. F. Rowell, *J. Exp. Biol.* **40**, 257 (1963).
17. J. S. Altman, *Nature* **229**, 204 (1971).
18. The plane of motion was determined by rotating the 3D coordinates of the paths in space and subjectively determining the best plane containing the bend point movement. The path was then transformed into a coordinate system where the selected plane lay at 45° to the zy plane. The fit to a single plane was estimated by the coefficient of determination (R^2) of the regression analysis.
19. Time derivatives of the 3D position coordinates of the bend point were calculated in order to obtain the tangential velocity in the direction of motion (*11*).
20. M. L. Shick, G. N. Orlovsky, *Physiol. Rev.* **56**, 465 (1976).
21. Y. I. Arshavsky, T. G. Deliagina, G. N. Orlovsky, *Curr. Opin. Neurobiol.* **7**, 781 (1997).
22. F. Delcomyn, *Science* **210**, 492 (1980).
23. W. B. Kristan *et al.*, in *Biomechanics and Neural Control of Posture and Movement*, J. Winters, P. E. Crago, Eds. (Springer-Verlag, New York, 2000), pp. 206–218.
24. H. J. Chiel, R. D. Beer, *Trends Neurosci.* **20**, 553 (1997).

25. Supported by the U.S. Office of Naval Research and the Israel Science Foundation. We thank E. Bizzi and Y. Yarom for advice and critical readings of this manuscript; J. Kien for suggestions and editorial assistance; and A. De Santis, A. Packard, and Y. Yekutieli for their help.

22 March 2001; accepted 11 July 2001

3.2 Insights on the motor control mechanism of the octopus reaching movement

Insights on the motor control mechanism of the octopus reaching movement.

German Sumbre,[1] Graziano Fiorito,[2] Tamar Flash,[3] Binyamin Hochner[1*]

[1]Department of Neurobiology and Interdisciplinary Center for Neuronal Computation, Institute of Life Sciences, Hebrew University, Jerusalem 91904, Israel. [2]Laboratorio di Neurobiologia, Stazione Zoologica di Napoli "A. Dohrn", Naples 80121, Italy. [3]Department of Computer Science and Applied Mathematics, Weizmann Institute of Science, Rehovot 76100, Israel.

Abstract

When reaching towards a target, octopuses simplify the complex task of controlling their flexible limbs by creating a bend somewhere along the arm and propagating it towards the tip. This reduces the number of degrees of freedom (DOFs) that need to be controlled to only 3. A further simplification is that the motor program controlling this movement lies within the neuromuscular system of the arm. Here we show that the frequency or duration of the stimulus evoking bend propagation can set the velocity with which the bend propagates along the arm. This suggests that the arm extension motor program can be modulated. We further show that the extension movement cannot be re-planned once it has been launched, based on visual information, therefore suggesting that the motor program for bend propagation is a feed-forward program. While unable to re-plan movement, octopuses can actively stop the propagation of the bend.

Introduction

In contrast to the rigid articulated limbs of vertebrates and arthropods, the octopus arm belongs to a group of appendages named muscular hydrostats (e.g. elephant trunks, tongues and tentacles). These are composed almost entirely of muscular tissue arranged so that muscles generate movement and also provide skeletal support necessary for movement generation (Kier and Smith, 1985). This neuromuscular arrangement and lack of rigid skeleton enable the octopus arm to elongate, shorten, twist and bend in any position or direction. The combination of these basic movements enable the performance of difficult and delicate tasks,

such as building shelters, searching for food in highly constrained environments, opening jars and even untying surgical threads. This extreme flexibility or 'redundancy' of degrees of freedom (DOFs), demands very complex motor control to overcome the inverse kinematics and dynamics problem (i.e., respectively calculating the appendage's shape to achieve a specific desired trajectory and the forces needed to obtain that shape, Hollerbach 1990; Kawato 1999; Wolpert and Ghahramani 2000).

In human arms, the control is simplified by planning optimal trajectories (Flash and Hogan 1985; Uno et al. 1989; Harris and Wolpert 1998), vectorial summation and superposition of basic movement primitives (Flash and Henis 1991; Bizzi et al. 1995; Mussa-Ivaldi 1999) and flexible combinations of muscle synergies (Bizzi et al. 1991; Mussa-Ivaldi et al. 1994; Bizzi 1993; Tresch et al. 1999; Mussa-Ivaldi 1999; Bizzi et al. 2000; D'avella et al. 2003).

Previous studies on the flexible arms of the octopus have shown that when swimming, crawling or reaching towards an object, octopuses generate a stereotypical movement in which a bend is formed somewhere along the arm and then propagated towards the tip. As the bend propagates, the portion of the arm proximal to the bend remains extended. This bend is always dorsally oriented so the suckers point forward in the direction of motion. This strategy reduces the number of DOFs to be controlled from literally infinite to only three: the pitch, yaw and the velocity of bend propagation (Gutfreund et al. 1996).

These flexible arms are controlled by an elaborate peripheral nervous system (4.75×10^7 neurons in each arm vs. 15×10^7 within the CNS). The peripheral nervous system consists of ~300 interconnected ganglia forming an axial nerve cord running along each arm, ventral to two cerebro-brachial tracts of ~32,000 nerve fibers carrying sensory and motor information to and from the highly developed centralized brain (Graziadei 1971). About 3.8×10^5 motor neurons within each arm innervate the intrinsic muscles of the arm allowing highly localized neural control of muscle action (Young 1963; Matzner et al. 2000).

The motor program determining the spatiotemporal features of the arm extension movement lies within this peripheral nervous system. This motor program appears to be a feed-forward program, as indicated by: the stereotypical kinematics of arm extension (Gutfreund et al. 1996); the fact that level of muscle activity (EMG) is significantly correlated with global kinematics variables (Gutfreund et al. 1998); and

the fact that arm extension movements can be triggered in denervated arms by a short train of stimuli (Sumbre et al. 2001).

Here we show that the arm extension movement does not depend on, and cannot be re-planned using visual information. However, while octopuses cannot change the movement once started, they can actively stop bend propagation. We also show that the arm extension motor program is not fixed; its output to the arm musculature can be scaled by an external input (such as efferent commands from the brain), which sets the activation parameters.

Materials and methods

Experimental animals. *Octopus vulgaris* collected from the Bay of Naples, Italy, or the Israel Mediterranean coastline were maintained in 50x50x40 cm glass tanks containing artificial seawater. The water was continuously circulated in a closed system filtered by active carbon and mechanical and biological filters. The animals were held at a temperature of 16°C in a 12 Hrs. light/dark cycle.

Behavioral task and video recording. A few days before the behavioral experiments, the octopuses were moved to a bigger aquarium (80x80x60 cm) at a temperature of ~20°C and trained to reach with their arms towards a white disc held by a transparent fishing thread. Small pieces of sardine were attached to the target as a reward in some of the successful trials.

We began with the experiments once the octopuses were acclimatized and trained. Each experiment started when the target was introduced into the tank and the octopuses commenced reaching towards it. At various delays after the octopus had started to reach, the target was raised for varying distances at different velocities. During some, randomly chosen, trials the target was not raised to prevent the octopus learning this movement; if the target was raised during every reaching movement, octopuses quickly learned to reach towards the final position of the target and no longer reached towards its original position.

The reaching movements were filmed with two super VHS PAL synchronized video cameras positioned ~90° apart (temporal resolution 20 ms, shutter speed 1/250). The images from both cameras were combined by a video mixer and the single image recorded by a super VHS video recorder. Only movements where the whole

arm and the target could be clearly seen throughout the entire movement were analyzed on a Silicon Graphics workstation by digitizing the coordinates of the target, the maximal curvature point of the bend and one of the octopus' eyes, the last being a reference for the degree of movement of the octopus' body. The coordinates of both 2D images were converted to 3D utilizing the direct linear transformation (DLT) algorithm. This method transforms the 2D camera coordinates to external XYZ coordinates from information about the coordinates of at least 12 external landmarks filmed by both cameras. For this calibration, a cubic structure with 14 clear landmarks (light diodes) was filmed by both cameras at the aquarium where the experiments were performed just before each experimental session. (Additional technical details can be found in Gutfreund 1996; Wood and Marshall 1986). Only those trials, in which the 3D transformations showed errors smaller than 5% were analyzed. The 3D trajectories of every digitized point were then smoothed using a Natural B-spline method (Craven and Wahba 1979). The tangential velocities of the bend propagations were calculated from the time derivatives of the smoothed 3D position coordinates of the bend.

Denervated arm preparations

Octopuses were anaesthetized in a mixture of 2% ethanol in seawater and subdued by removing the supraesophageal brain mass (Sumbre et al. 2001). After a recovery period of ~24 hrs, the nerve cord of one of the arms was exposed and transected. The preparations were submerged in circulating aerated seawater at ~20°C. The proximal part of the denervated arm was fixed to a platform, while the distal part hung freely. Electrical stimulation was applied through a Teflon coated silver bipolar electrode placed on the dorsal part of the exposed axial nerve cord (stimulus frequency, 50 – 120 Hz; train duration, 0.1 – 1.2 s). The evoked arm extensions were filmed and kinematically analyzed as described above. Additionally, we calculated the curvature of a 2D backbone curve (Chirikjian and Burdick 1990) visually fitted along the middle of the arm for each time frame of the movement (20 ms) according to:

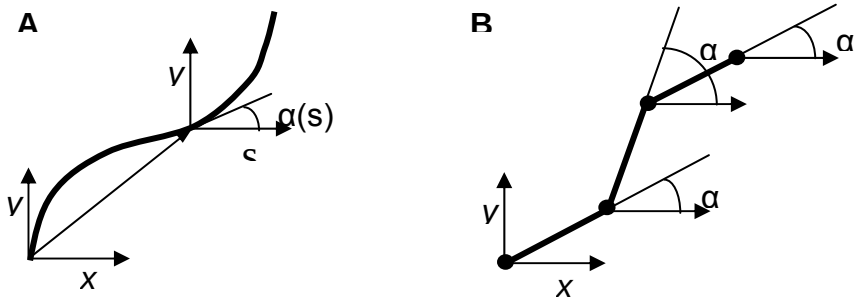

$$K(s) = \frac{d\alpha(s)}{ds(s)} \qquad K_i = \frac{\alpha_{i-1} - \alpha_{i+1}}{S_{i-1} - S_{i+1}}$$

Continuous **Discrete**

where ***s*** is the normalized backbone curve arc length and ***α*** is the local slope with respect to the Cartesian coordinates. The curvature of each movement was calculated and then plotted against time and the normalized length of the arms (see Fig. 5E, F).

Results

Involvement of visual feedback during arm extension movements

We tested the ability of the octopus to use visual information to re-plan reaching movements after the movement had already started. We thus compared the kinematics of reaching movements in trials in which the target was displaced with those where it was not displaced. Seventy-nine arm extension movements from 5 different animals were analyzed. In 63 cases the target was lifted at different speeds (16 – 80 cm/s), displaced different distances (0.7 – 14.9 cm) and with different delays between arm extension and target movement, ranging from -0.15 sec to 2 s (negative values represent trials in which the target started to move before the arm extension was initiated). The maximal velocities of arm extension ranged from 13 cm/s to 49 cm/s.

Figure 1 shows a trial in which the octopus' arm reached to the initial position of the target even though the target was lifted after the movement began (Fig. 1A, C). We observed no changes related to the onset of target movement, neither in the bend path nor in the bend's tangential velocity profile (Fig, 1B, C).

To quantitatively analyze all the 79 arm extension movements, we defined four vectors (Fig. 2I):

a) The vector connecting the position where the bend was formed and the final location of the target, the position where the target was lifted to. This vector represents the bend's pitch needed to grasp the target at its changed new position (Fig 2I (***a***, in red)).

b) The vector connecting the position where the bend was formed and the location where it stopped propagating. This vector defines the elevation of the reaching movement (Fig 2I (***b***, in blue)).

c) The vector connecting the position where the bend was formed with the location of the target before it was lifted. This vector describes the bend's elevation required to reach the target at its original position (Fig 2I (***c***, in green)).

d) The degree of the octopus' arm correction towards the shifted position of the target. This was computed as the ratio between vectors ***a*** and ***b***.

Vectors ***a*** and ***b*** were always normalized according to vector ***c***, to compensate for the inaccuracy of the movement when reaching towards a static target, thus allowing to compare between different movements for statistical analysis. During trials in which the target was displaced, we observed that the elevation of vectors ***a*** was significantly lower than the elevation of vectors ***b*** ($p = 10^{-35}$, paired t-test, n = 63; Fig. 2C, D). That is, the path of the bend was not modified towards the new location of the target. Moreover, there was no significant difference in the elevation of vector ***a*** in movements where the target was lifted and trials where it was not moved (Fig. 2A, C) ($p = 0.26$, t-test). This implies that the difference between the final position of the bend (***b***) and the initial position of the target (***c***) was not related to changes in target position but is apparently due to the inaccurate nature of the movement. In addition, non-significant correlations were found between ***d*** and amplitude of target displacement ($R^2 = 0.01$, $p = 0.42$; F-test), target velocity ($R^2 = 0.04$, $p = 0.13$; F-test), maximal velocity of target movement ($R^2 = 0.006$, $p = 0.55$; F-test), and the movement – target delay ($R^2 = 0.001$, $p = 0.79$; F-test). We then compared the velocity profiles of movements in which the target was moved and those in which the target remained still. The velocity profiles in both groups normalized with a similar small variance and similar averages (Fig. 2E - H). Similar results were obtained for movements in which the target was horizontally displaced (n = 13; data not shown). To check whether target displacement caused local rather than global changes in the arm, we divided the paths of the bends into segments of 200 ms. We then calculated the curvature of the segment prior to onset of target displacement and of the 2 consequent segments. We found no significant difference between the curvature of the segments before or after target displacement ($p = 0.22$; 0.47; 0.34 respectively, paired t-test).

When the target was lifted successively for more than ~5 times, instead of reaching towards the initial position of the target, octopuses reached towards the learned or expected final position of the target, even when the target was not shifted (data not shown). Even though octopuses were not able to re-plan their reaching movements once launched, they actively stopped the propagation of the bend in 11% of the trials in which the target was lifted. In these cases, they usually showed a faster deceleration than when the bend propagated right to the end of the arm (Fig. 3). Abortion of bend propagation could not be correlated with target velocity, tangential velocity of the bend nor delay between the movement initiation and the target displacement.

These results demonstrate that the octopus' inability to correct launched movements is not due to poor visual perception but that octopuses do not or cannot use visual information to modify bend path during reaching movements. This suggests that the motor program for reaching does not involve visual feedback during its execution.

Modulation of the motor program for arm extension

Denervated arms of subdued octopuses were electrically stimulated at the exposed axial nerve cord close to the base of the arm. In 32 cases, the train of stimuli evoked arm extension movements resembling those observed in freely behaving octopuses (Gutfreund et al. 1998; Sumbre et al. 2001). For 14 of these movements, evoked in 4 different animals from a similar initial orientation of the arm, stimulus frequency was varied between 30 -120 Hz, while train duration was kept relatively constant (~400 ms). Maximal velocity of the extension movements was significantly positively and linearly correlated to stimulus frequency from threshold (below ~35 Hz) up to ~100 Hz (R^2 = 0.52, p = 0.008; F-test. Fig. 4A, E). The plateau reached with stimulation frequencies above ~100Hz may represent the maximal firing rate of the cerebro-brachial tracts axons (intracellular recordings from these axons show that they cannot accurately follow an extracellular train of stimuli above ~100 Hz). There was no significant correlation between bend propagation distance and stimulus frequency (R^2 = 0.002, p = 0.86; F-test; Fig. 4B).

In the other 18 trials in 3 animals, we modulated the duration of the stimulus train (from 100 – 1000 ms), while keeping the stimulus frequency at 50 Hz and starting

from similar arm orientations. Again, this modulation did not affect bend propagation distance (R^2 = 0.001, p = 0.89; F-test. Fig. 4D), but there was a positive linear correlation between stimulus train durations from threshold (~200 ms) to ~700 ms) and the movement's maximal velocity (R^2 = 0.61, p = 10^{-4}; F test. Fig. 4C, F).

Above a train duration of ~700 ms, a totally different type of arm movement was evoked. We named this evoked movement “sickle-like extension” since no bend is propagated along the arm throughout the movement but the arm extends by rotating around a pivot-like area in the arm (Fig. 5A). In order to quantitatively separate reaching extensions from sickle-like extensions, we measured the curvature of the arms throughout the 32 movements as described in Methods (Fig. 5E, F). The averaged maximal curvature was plotted against the averaged velocity of the maximal point of curvature propagation and a k-means clustering algorithm used to segregate the groups (Fig. 5G).

Reaching extension movements generally showed higher curvature and velocity values (Fig. 5G, red group), while sickle-like extensions had lower curvatures and velocities (Fig. 5G, blue group). Furthermore, during reaching extensions, the portion of the arm distal to the bend (the point of maximal curvature) has higher curvature levels than the portion proximal to it (Fig. 5B, F), apparently due to the part of the arm proximal to the bend being passive (Gutfreund et al. 1998). Sickle-like extensions do not show this phenomenon, having similar levels of curvature at both sides of the curvature peak (Fig. 5A, E).

During reaching extensions, the stimulus train ended before or during the early stages of movement (Fig. 5D). In contrast, for sickle-like extension movements, the stimulus train ended at the time of the movement's maximal velocity (Fig. 5C).

To further understand the mechanisms causing sickle-like extension movements, we carried out simulations on the dynamic mathematical model of the octopus arm (Yekutieli et al. unpublished results). This model, based on a multi-segment structure, shares all the main characteristics of the octopus arm. It contains longitudinal and transverse muscles, which maintain a constant volume, and realistic forces for gravity, water drag, and buoyancy are exerted on the model. The muscles are activated by a command which dictates the spatiotemporal pattern of their contraction. When the model is activated to gradually contract the segments proximally to distally, it generates a movement with the kinematical

characteristics of octopus arm extension movements (Fig. 5B). When we commanded simultaneous activation of the segments, we observed a movement strikingly similar to the sickle-like extension (Fig. 5A). We therefore suggest that the sickle-like extensions evoked in denervated arms result from co-activation of the arm musculature, probably due to the direct and simultaneous activation of arm motoneurons via the unusually strong train of stimuli.

Discussion

When reaching, swimming or crawling, octopuses generate a stereotypical arm extension by forming a bend somewhere along the arm and then propagating it towards the tip. This movement strategy reduces the number of the arm's DOFs from virtually infinite to only 3 (yaw, pitch and propagation velocity of the bend; Gutfreund et al. 1996), thereby greatly simplifying motor control. Motor control of the arm is further simplified by having a feed-forward motor program embedded in the neuromuscular system of the arm (Sumbre et al. 2001).

Here we demonstrate that after a reaching movement is initiated, the movement cannot be re-planned using visual information, to for example, correct the arm's direction or velocity, in order to reach towards an escaping pray. This inability to correct the reaching movement does not dependent on bend velocity, target velocity, target-bend delay or amplitude of target displacement. Although octopuses could not generate on-line corrections, they learned to reach towards the target's final position or, in some cases, to actively abort arm extension movements. Thus, they were aware of the target's displacement. Visual information is apparently used only in setting the posture of the arm (pitch and yaw) before the movement's onset, and these define the final trajectory of the bend (Sumbre et al. 2001).

The strategy of aborting a movement avoids wasting energy and allows faster generation of a new extension movement with the same arm.

Arm extension movements can be evoked in denervated arms by a train of electrical pulses (Sumbre et al 2001). Here we showed that, within certain ranges of frequency and duration, the trains of stimuli positively correlate with the maximal velocity of arm extension (Fig. 4A, C). In contrast, the propagation distance of the bend is independent of the stimulus parameters, the bend always reaching the tip of the arm. The bend's propagation distance thus appears to be a property

embedded in the neural circuit controlling the extension motor output, while the parameters of spike trains in the cerebro-brachial connectives may be the control input that scales the arm motor program output (velocity probably via muscle strength as suggested by Gutfreund, 1998).

We therefore suggest that central brain areas trigger arm extension movements via a neural command, carrying information about the bend's orientation and its maximal propagating velocity. These triggering commands activate a feed-forward motor program embedded in the neuromuscular system of the arm which drives a feed-forward movement. We further suggest that the octopus arm extension motor program is a unique example of a biological time integrator in a feed-forward neural network, which is capable of reliably transmitting the input rate (the triggering stimulus) to generate a behavioral output (bend's maximal velocity) whose kinematic characteristics are highly correlated with the input. Up till now, such behavior was thought unlikely in a feed-forward neural network (Litvak et al. 2003), but possible in models with appropriate lateral feedback (van Vreeswijk and Sompolinsky 1996).

References

Bizzi E, Giszter SF, Loeb E, Mussa-Ivaldi FA and Saltiel P. (1995) Modular organization of motor behavior in the frog's spinal cord. ***Trends Neurosci.*** 18:442-446.

Bizzi E, Mussa-Ivaldi FA and Giszter S. (1991). Computations underlying the execution of movement: a biological perspective. ***Science*** 253:287-291.

Bizzi E, Tresch MC, Saltiel P and d'Avella A. (2000) New perspectives on spinal motor systems. ***Nat. Rev. Neurosci.*** 1:101-108.

Bizzi E. (1993) Intermediate representations in the formation of arm trajectories. ***Curr. Opin. Neurobiol***. 3:925-931.

Chirikjian GS and Burdick JW. (1990) Kinematics of Hyper-Redundant Manipulators. in Proceedings of the 2nd International Workshop on Advances in Robot Kinematics, pp. 392-399.

Craven P and Wahba G. (1979) Smoothing noisy data with spline functions. ***Numerische Mathematik,*** 31:377-403.

d'Avella A, Saltiel P and Bizzi E. (2003) Combinations of muscle synergies in the construction of a natural motor behavior. ***Nat Neurosci***. 6:300-308.

Flash T and Henis E (1991) Arm trajectory modifications during reaching towards visual targets. ***J. Cogn. Neurosci****.* 3:220-230.

Flash T and Hogan N. (1985). The coordination of arm movements: An experimentally confirmed mathematical model. ***J. Neurosci.*** 5:1688-1703.

Graziadei P. (1971). The nervous system of the arms. In The anatomy of the nervous system of Octopus vulgaris (ed. J. Z. Young), pp. 45-59. Oxford: Clarendon press.

Gutfreund Y, Flash T, Fiorito G and Hochner B. (1998) Patterns of arm muscle activation involved in octopus reaching movements. ***J. Neurosci***. 18:5976-5987.

Gutfreund Y, Flash T, Yarom Y, Fiorito G, Segev I and Hochner B. (1996) Organization of octopus arm movements: a model system for studying the control of flexible arms. ***J. Neurosci.*** 16:7297-7307.

Harris CM and Wolpert DM. (1998) Signal-dependent noise determines motor planning. ***Nature***. 394:780-784.

Harris CM and Wolpert DM. (1998) Signal-dependent noise determines motor planning. ***Nature***. 394:780-784.

Hollerbach JM. (1990). Planning of arm movements. In Visual cognition and action, vol. 2 (ed. D. N. Osherson, S. M. Kosslyn and J. M. Hollerbach), pp. 183-212. Cambridge, Mass: MIT Press.

Kawato M. (1999) Internal models for motor control and trajectory planning. ***Curr Opin Neurobiol***. 9:718-727.

Kier WM. and Smith KK. (1985). Tongues, tentacles and trunks: the biomechanics of movement in muscular-hydrostats. ***Zool. J. Linn. Soc****.* 83:307-324.

Litvak V, Sompolinsky H, Segev I and Abeles M. (2003) On the transmission of rate code in long feedforward networks with excitatory-inhibitory balance. ***J. Neurosci***.23:3006-3015.

Matzner H, Gutfreund Y and Hochner B (2000) Neuromuscular system of the flexible arm of the octopus: physiological characterization. ***J. Neurophysiol.***. 83:1315-1328.

Mussa-Ivaldi FA, Giszter SF and Bizzi E. (1994) Linear combinations of primitives in vertebrate motor control.***Proc. Natl. Acad. Sci. USA.*** 91:7534-7538.

Mussa-Ivaldi FA. (1999) Modular features of motor control and learning. ***Curr Opin Neurobiol.*** 6:713-717

Sumbre G, Gutfreund Y, Fiorito G, Flash T, Hochner B. (2001) Control of octopus arm extension by a peripheral motor program. ***Science.*** 293:1845-1848.

Tresch MC, Saltiel P and Bizzi E. (1999) The construction of movement by the spinal cord. ***Nat. Neurosci***. 2:162-167.

Uno Y, Kawato M, Suzuki R. (1989) Formation and control of optimal trajectory in human multijoint arm movement. Minimum torque-change model. ***Biol. Cybern***. 61:89-101.

van Vreeswijk C and Sompolinsky H. (1996) Chaos in neuronal networks with balanced excitatory and inhibitory activity. ***Science***. 274:1724-1726.

Wolpert DM and Ghahramani Z. (2000) Computational principles of movement neuroscience. ***Nat. Neurosci.*** **Suppl**. 1212-1217.

Wood GA and Marshall RN (1986) The accuracy of DLT extrapolation in three-dimensional film analysis. ***J. Biomech.*** 19:781-785.

Young JZ. (1963). The number and size of nerve cells in Octopus. ***Proc. Zool. Soc. London.*** 140:229-253.

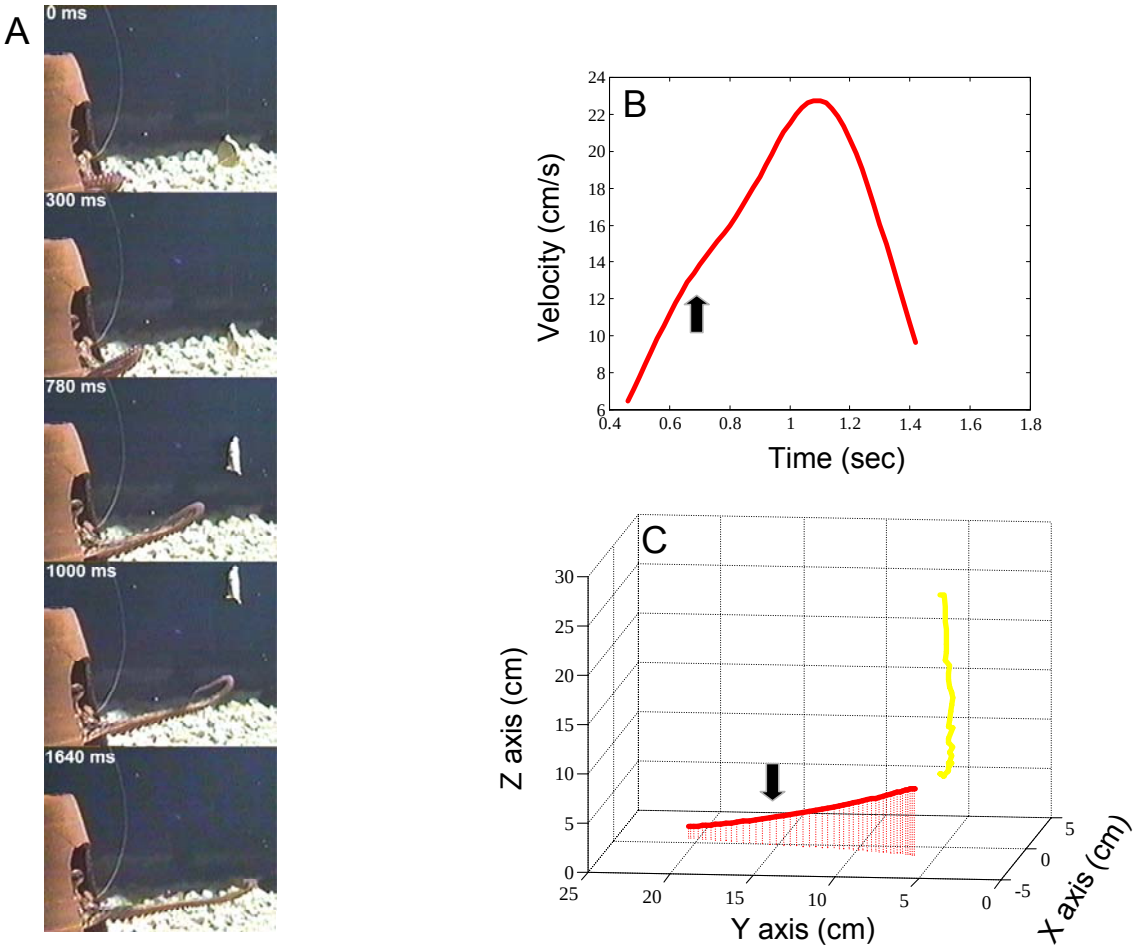

Figure 1. The arm extension movement does not involve visual feedback after its onset. (A) A sequence of 5 video images taken during an arm extension in which the target was displaced., starting to move at 700 ms. (B) The tangential velocity profile of the bend. (C) The 3D bend and target paths. Arrow in (B),and (C) represents the onset of target movement. Note that both bend path and velocity remain unchanged after target displacement starts, and that the bend reached the initial position of the target (A, and C).

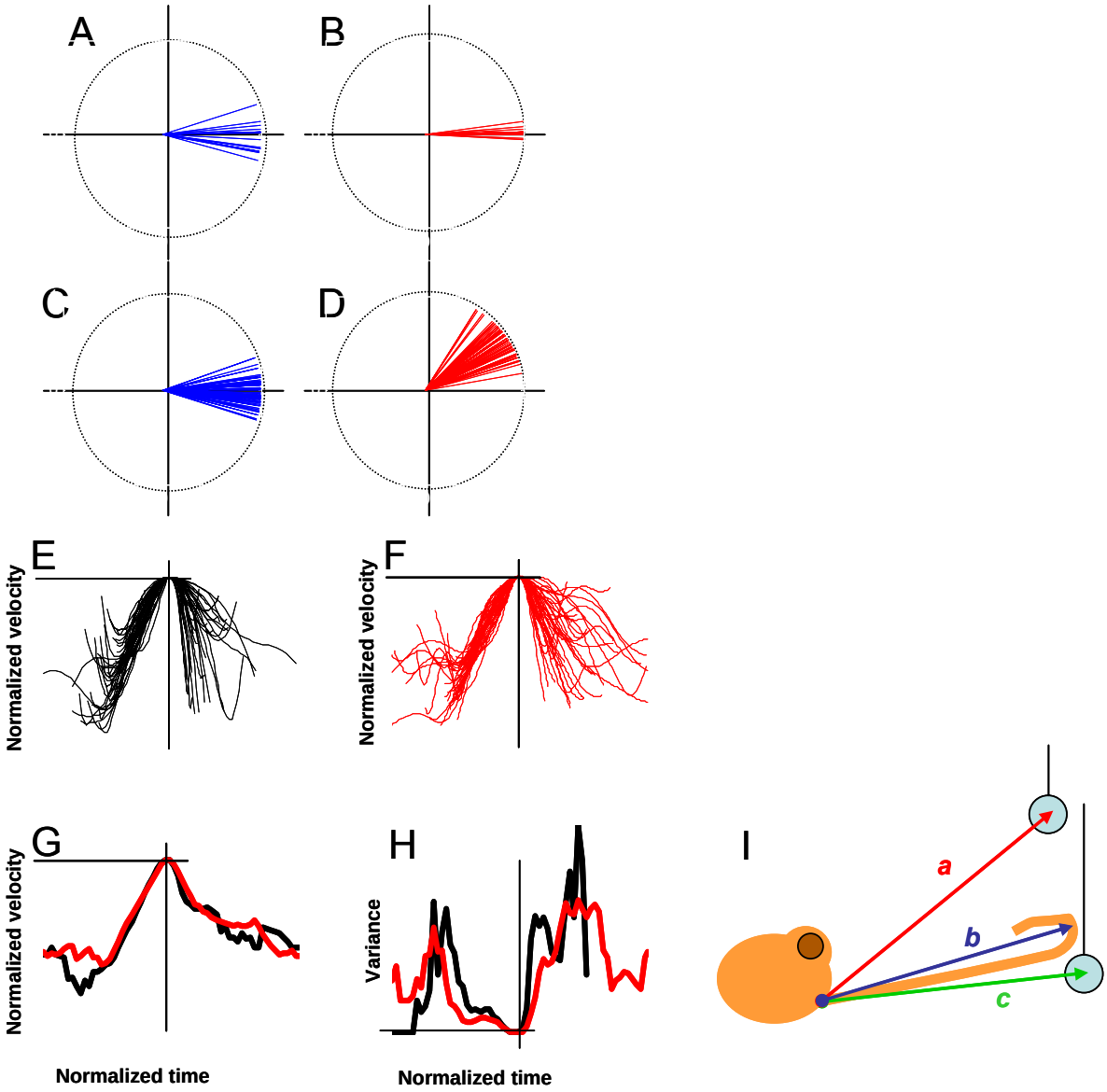

Figure 2. (A,B) The elevation of ***b*** (blue) and ***a*** (red) vectors (n = 16) in which the target was not displaced. (C, D) The elevation of ***b*** (blue) and ***a*** (red) vectors (n = 63) during trials in which the target was lifted. Elevation of vectors ***b*** and ***a*** always normalized to the ***c*** vector. (E) Superposition of the normalized tangential velocity profiles of movements in which the target was not displaced (black) and (F) of trials in which the target was moved (red). (G, H) show their average and their variance respectively. (I) A schematic drawing explaining how we calculated the vectors used for the data analysis.

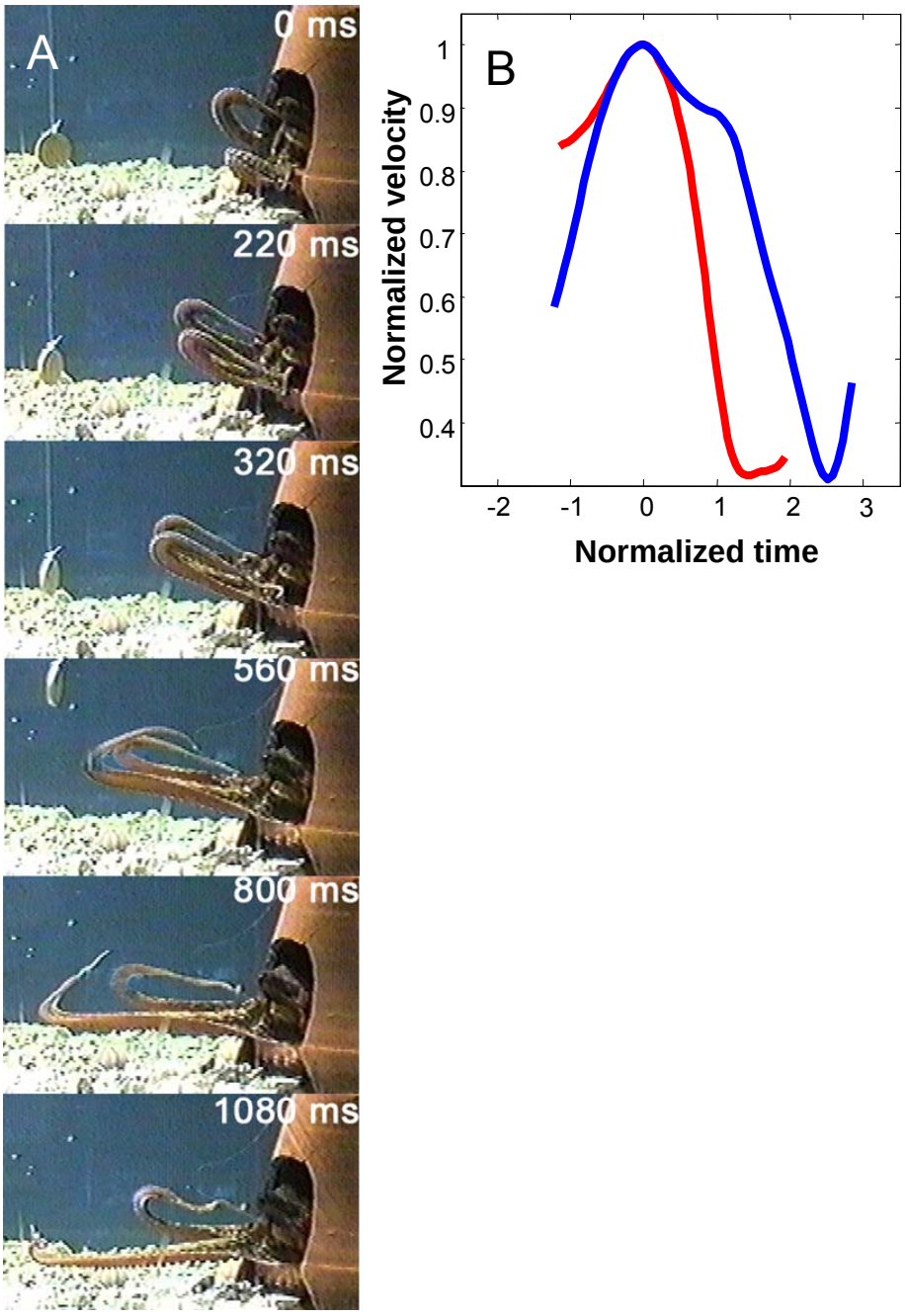

Figure 3. The bend propagation can be actively stopped. (A) A series of six video images taken during a reaching movement in which the target was lifted (at 320 ms). Note how the arm in the back suddenly stops moving in contrast to the front arm which keeps extending towards the initial position of the target. (B) The velocity profile of both arms. The velocity of the arm in the back (red) drops abruptly in comparison to that of the front arm (blue).

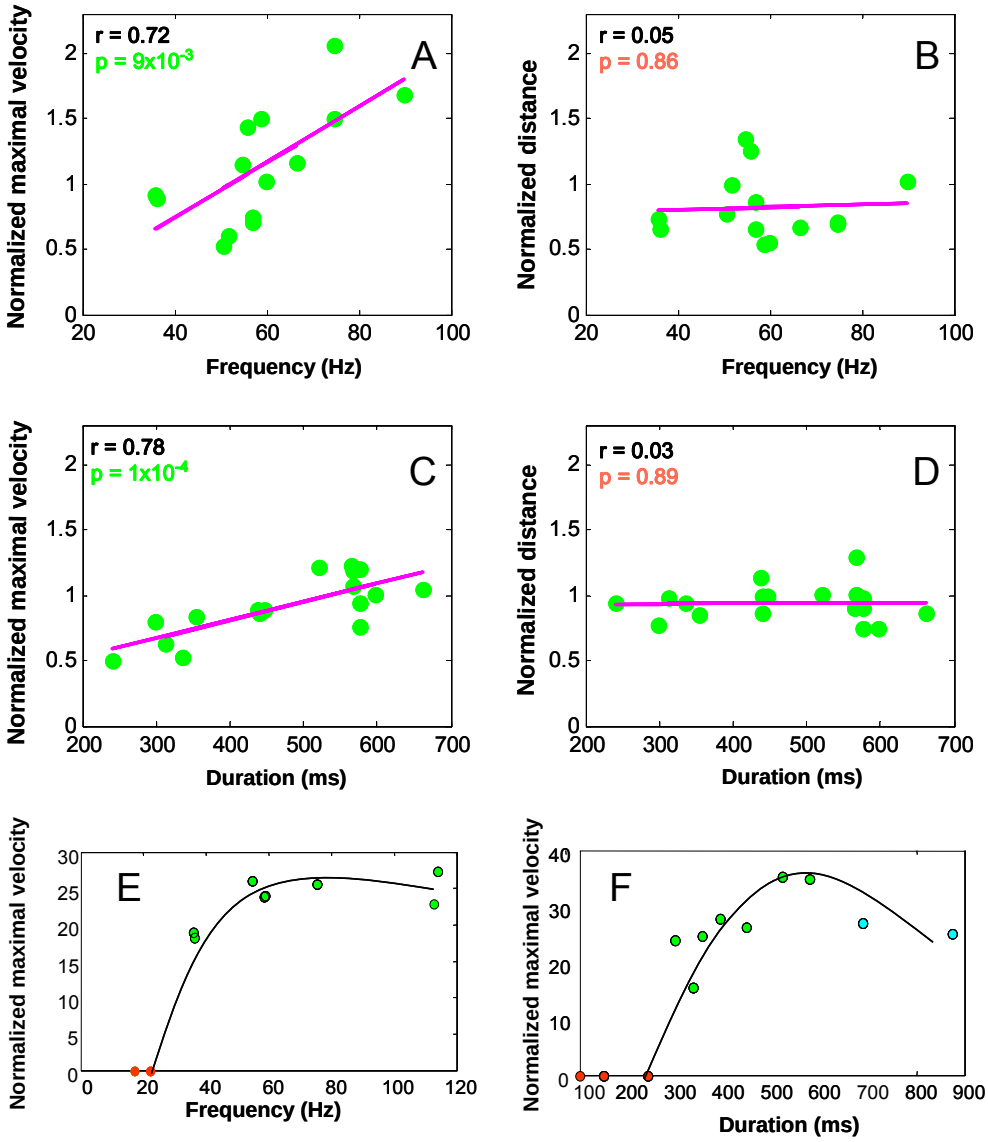

Figure 4. The arm extension motor program can be modulated to scale bend propagation velocity. (A) The relationship between the frequency of the stimulus train and the normalized maximal velocity of the evoked arm extensions (velocity was normalized to the maximal velocity obtained at 50 Hz.). (B) The relationship between the propagation distance of the bend (normalized according to the length of the arm) and the stimulus frequency. (C) The relationship between the maximal velocity (normalized to train duration of 400 ms) and the duration of the stimulus train. (D) The relationship between the normalized propagation distance (normalized to the length of the arm) and the duration of the stimulus train. The coefficient of correlation (R^2) and the p values of the F-test appear at the top left corner in (A-D). (E) The relationship between the maximal velocity of the movement and the stimulus frequency and (F) between the maximal velocity and train duration in a single experiment. Red dots represent unsuccessful stimuli, green dots represent evoked arm extensions and blue dots represent evoked sickle-like extensions.

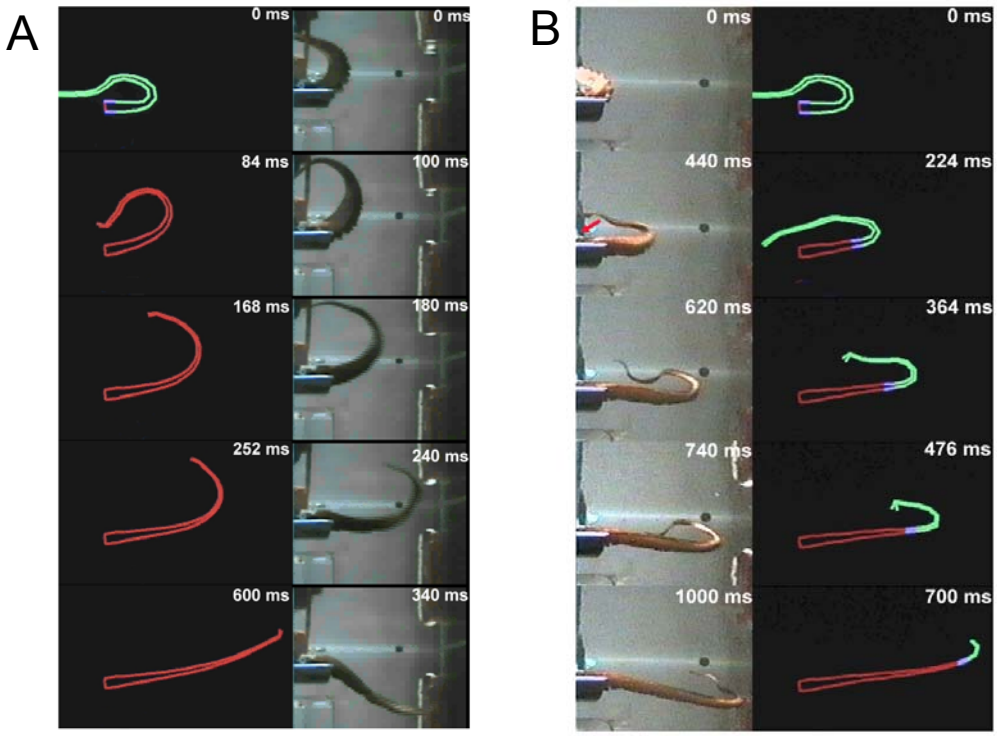
A
0 ms
0 ms
84 ms
100 ms
168 ms
180 ms
252 ms
240 ms
600 ms
340 ms
B
0 ms
0 ms
440 ms
224 ms
620 ms
364 ms
740 ms
476 ms
1000 ms
700 ms

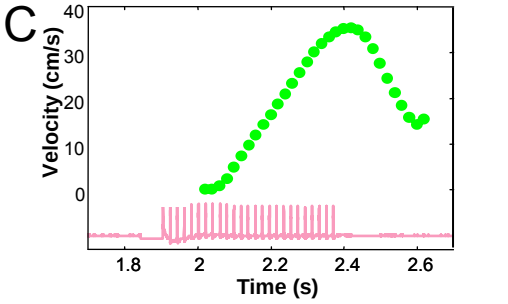
C
Velocity (cm/s)
Time (s)

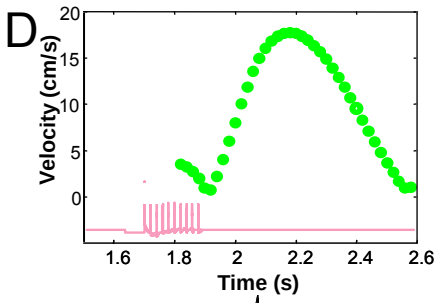
D
Velocity (cm/s)
Time (s)

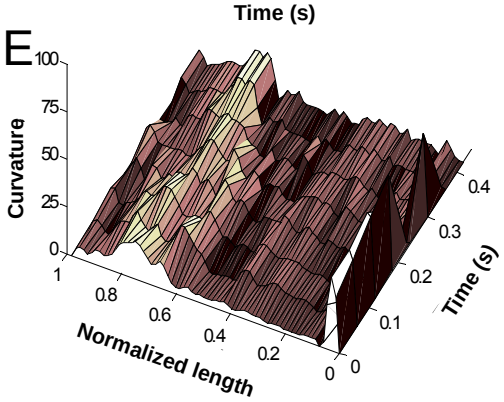
E
Curvature
Normalized length
Time (s)

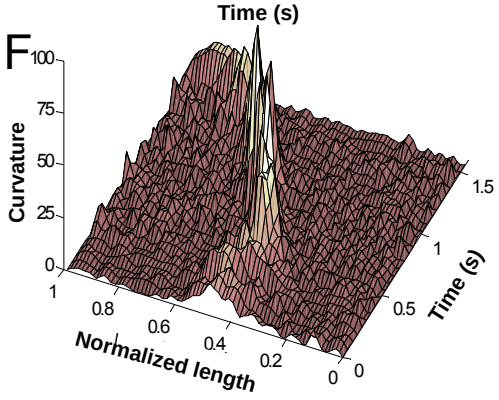
F
Curvature
Normalized length
Time (s)

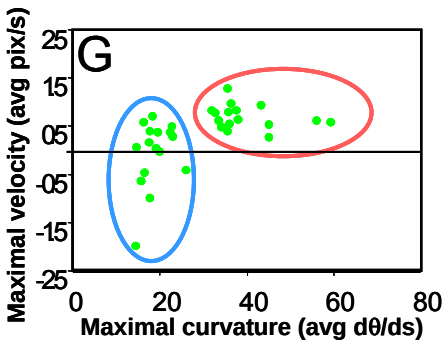
G
Maximal velocity (avg pix/s)
Maximal curvature (avg dθ/ds)

Figure 5. Long stimulus trains evoke a sickle-like movement, probably by simultaneous contraction of the whole intrinsic musculature of the arm. (A) A series of video images taken during a sickle-like arm extension (right) and the simultaneous activation of all the muscles in a dynamic mathematical model of the octopus arm (left). (B) A series of video images taken during an evoked arm extension (left) and the gradual activation of the muscles in the dynamic mathematical model (right). (C, D) The tangential velocity profiles superimposed on the stimulus trains for the sickle-like extension (C) and the evoked arm extension (D). Notice that in (C) the end of the stimulus train coincides with the time when maximal velocity is reached but that in (D) the stimulus train ends before the movement starts. (E, F) Examples of the arm's curvature plotted against the normalized length of the arm and the time during the movement for an evoked sickle-like extension (E) and evoked arm extension (F). (G) Plotting the degree of curvature of the peaks vs. the degree of bend propagation (represented by the velocity of propagation of the maximal curvature peaks) gives two significant clusters, one belonging to sickle-like extensions (blue), with low or even negative velocities and small curvature levels, and a second belonging to the arm extension movements (red), with higher curvature and propagation velocities.

3.3 Vertebrate-like strategy in octopus point-to-point arm movements suggests convergence toward an optimal control solution

Vertebrate-like strategy in octopus point-to-point arm movements suggests convergence toward an optimal control solution

German Sumbre,[1] Graziano Fiorito,[2] Tamar Flash,[3] Binyamin Hochner[1*]

[1]Department of Neurobiology and Interdisciplinary Center for Neuronal Computation, Institute of Life Sciences, Hebrew University, Jerusalem 91904, Israel. [2]Laboratorio di Neurobiologia, Stazione Zoologica di Napoli "A. Dohrn", Naples 80121, Italy. [3]Department of Computer Science and Applied Mathematics, Weizmann Institute of Science, Rehovot 76100, Israel.

Using a flexible arm for point-to-point movements is an especially complex task due to the large number of degrees of freedom (DOFs) that need to be controlled. When fetching a piece of food to the mouth, octopuses solve this problem by creating a *quasi*-articulated structure consisting of three rotary joints, thus reducing the DOFs to only 3. For each movement, joint location is dynamically adjusted according to where the object is grasped along the arm. Although these dynamically adjustable joints differ dramatically from those of vertebrates, the arm kinematics and geometrical characteristics are strikingly similar. This evolutionary functional convergence suggests that a kinematically constrained articulated limb may be the nature's optimal solution for achieving precise point-to-point movements.

Arthropods and vertebrates have evolved joints allowing them to move their rigid skeleton in 3D space, but with a limited number of degrees of freedom (DOFs). In contrast, the octopus arm belongs to a group of organs termed muscular hydrostats (e.g. elephant trunks, tongues and tentacles), which are almost entirely composed of incompressible muscular tissue, anatomically organized so that they can produce both force and the skeletal support necessary for movement generation (*1*). These characteristics enable the

octopus arm to move with an almost infinite number of DOFs. Such extreme kinematic ‘redundancy' requires a very complex control scheme to overcome the inverse kinematics and dynamics problems (i.e., calculating respectively the appendage's shape in order to achieve a specific desired trajectory and the forces needed to obtain that shape).

Several strategies have been suggested for simplifying these inverse problems in humans; minimum jerk (*2*), minimum variance strategies (*3*), the equilibrium-point hypothesis (*4*, *5*), muscular synergism (*6*, *7*) and minimum kinetic energy (*8*) are but only a few suggestions (see *9-11* for reviews). In the flexible arm of the octopus we have previously shown that the control complexities of reaching movements are simplified by generating a stereotypical movement in which a bend is propagated forward along the arm reducing the number of DOFs need to be controlled to only 3 (*12*). Further simplification is achieved in that the feed-forward motor program for this stereotypical movement (*13*) is embedded within the neuromuscular system of the arm itself (*14*).

Since octopus arms are equipped with suckers distributed along their entire length, they can reach towards a target and grasp it anywhere along the arm. In contrast, when fetching the grasped target to the mouth, a point-to-point task has to be generated; the end-effector (the site on the arm grasping the object) has to reach a specific and precise target (the mouth).

These fetching movements are stereotypical and could be easily recognized in all filmed trials (n = ~100). They can be initiated by placing a piece of food anywhere along the octopus' arm. The food is rapidly grasped by the suckers as soon as it contacts the extended arm. Then a bend begins to appear proximal to the object (distal bend, Fig. 1A, 0.8 sec), after which a second bend (medial bend) forms near the mid-point between the distal bend and the base of the arm (Fig. 1A, 1.04 sec). A third bend (proximal bend) is formed at the base of the arm. The location of the object and these three bends define a *quasi*-articulated structure, which then moved mainly by rotating the medial segment around the medial bend to bring the distal bend to the base of the arm (Fig. 1A, 1.16 - 1.64 sec). Finally, rotating the distal bend brings the object to the beak at the center of the brachial crown.

Our kinematic analysis searched for geometrical and kinematic invariants of these fetching movements to better understand the strategies underlying their generation and control (*15, 12*). Movements in which the location of the food and the 3 bends (Fig. 1C) were clearly visible through the entire movement, were kinematically analyzed (n=24). The 2D coordinates of these four points were digitized and transformed to 3D coordinates using the Direct Linear Transformation (DLT) algorithm (*16)*. Fig. 1B shows that the sequence of events occurring during fetching movements is highly conserved, with all fetching movements, except one, following the same sequence of events. After the food was grasped by the arm (red diamonds), the distal bend was formed (green), followed by the generation of the medial bend (yellow). The time delay between their formation was significantly larger than zero (- 0.1 ± 0.11 sec, $p = 2x10^{-4}$ (paired t-test)). Rotating the bends brought the distal bend to the base of the arm (blue) and then rotation around the distal bend moved the food to the mouth (black).

This sequence of events (Fig. 1B) divides the fetching movement into 4 phases. There were no significant correlations between the durations of each phase (in multiple linear regression analysis, $R^2 = 0.04$, $p = 0.84$ (F-test)), suggesting that all the different phases of the fetching movement are independently controlled.

The location of the object and the two bends divides the *quasi*-articulated structure into three segments (proximal (L_1), medial (L_2) and distal (L_3) (Fig. 1C). To test whether the bends remain at the same locations along the arm, we measured segment length throughout the movements. L_1 and L_2 remained nearly constant (Fig. 2, A and B). Slopes of L_1 and L_2 lengths over time did not differ significantly from zero (–0.05 ± 0.14, $p = 0.1$ (t-test) and 0.04 ± 0.20, $p = 0.07$ (t-test), respectively). On the other hand, L_3 showed a tendency to shorten with time (Fig. 2C, slope of L_3 vs. time differed significantly from zero; – 0.35 ± 0.26, $p = 0.03$ (t-test)). Overall, these results suggest that the bends behave like skeletal joints.

The *quasi*-articulated structure displayed a strikingly invariant geometry in all the movements (Fig. 2D). L_1 and L_2 lengths were positively correlated ($R^2 = 0.78$, $p = 1.6x10^{-12}$ (F-test)) with a slope of 0.8 ± 0.15 (mean ± confidence

interval) (n=36). That is, during each fetching movement not only is there a constant ratio between the lengths of the proximal (L_1) and the medial (L_2) segments, but they are also almost equal in length. This geometry resembles the general structure of vertebrate limbs.

Since the food was deliberately proffered at different locations along the arm, we were able to investigate the relationship between the position where the food was grasped and the length of the *quasi*-articulated structure segments. Segment lengths are positively and linearly correlated with the site where the arm grasps the food (Fig. 2, E - G; L_1 ($R^2 = 0.82$, $p = 3.8 \times 10^{-14}$ (F-test)), L_2 ($R^2 = 0.84$, $p = 2.7 \times 10^{-15}$ (F-test)) and L_3 ($R^2 = 0.7$, $p = 3.6 \times 10^{-10}$ (F-test))), implying that the joints are not created at fixed locations along the arm, but according to where the arm grasps the object. Moreover, the slopes described by the correlation of the segments and the position of the food (0.3 ± 0.05 for L_1, 0.34 ± 0.05 for L_2, and 0.35 ± 0.08 for L_3) did not significantly differ from each other ($p = 0.57$ (ANCOVA)). These results show that the *quasi*-articulated structure adjusts to the position of the object by similar changes in the length of each segment.

Plotting the paths of the object and the three joints in space (Fig. 3, A and B) reveals that all four designated points move roughly within the same linear plane. While the object and the distal joint move toward the base of the arm, the medial joint moves upwards (Fig. 3A, yellow). The paths of the object and the distal joint revealed large averaged distances traveled in the plane of motion, compared with small averaged residual errors (SE) orthogonal to this plane, as well as highly significant coefficients of correlation (Table S1). This further confirms that the fetching movements are performed mostly within a single linear plane, which generally corresponds to the sagittal plane of the arm, the suckers defining the ventral side. In contrast to the object and the distal joint, the path of the medial joint was shorter and tended to be perpendicular to the paths of the object and the distal bend (Table S1). Performing the movement in a single linear plane reduces the number of DOFs of each joint to only one, giving a total of 3 DOFs for the entire arm throughout the movement.

The creation of joints constrains the fetching movement to rotations around these joints (Fig. 3, C - E). The medial joint (θ_2) shows the most robust behavior, manifested in a large rotation (Fig. 3D) with relatively low variance among different movements (Fig. 3F, yellow). The proximal joint (θ_1) performs smaller rotations (Fig. 3C, ~10° on average) with the angle first decreasing and then increasing, with a relatively low variance (Fig. 3F, blue). θ_2 therefore appears to account for most of the movement, while θ_1 may determine the degree of linearity of the distal joint path (supporting online text). In contrast to these two joints, the angle of the distal joint (θ_3) (Fig. 3E) is highly variable (Fig 3F, green), suggesting that this angle only plays a significant role during the last phase of the fetching movement, when the joint rotates to bring the food from the base of the arm to the mouth.

Both θ_1 and θ_2 show bell-shaped velocity profiles (Fig. 3H). The angular rotations of the proximal and medial joints (θ_1 and θ_2) are linearly correlated (Fig. 3G, Fig. S1, A and B and supporting online text). In contrast, plotting the movement in terms of external Cartesian coordinates (Fig. S1G) results in more variable relationships between the locations of the food and joints. This suggests that the fetching movement is planned in joint space, therefore avoiding inverse kinematics transformations (*17*).

To study the neural control mechanisms of fetching, electromyograms (EMG) were recorded at different positions along the arm. Muscles were active throughout the whole fetching movement (Fig. 4D), but only in the part of the arm involved in the *quasi*-articulated structure, i.e., from the base of the arm to the location of the object (n=88). Arm sections not involved in this structure showed no muscle activity (n=6). These EMG recordings demonstrate that the *quasi*-articulated structure is actively contracted or stiffened.

Integrated EMG signals from electrodes positioned at the medial joint positively correlated with the total length of segments L_1 and L_2 (Fig. 4E; $R^2 = 0.76$, $p = 10^{-8}$ (F-test), n=11). Additionally, the integrated EMG signals recorded anywhere along the medial segment (L_2) or at the distal joint correlated positively with the length of the distal segment (L_3) (Fig. 4F; $R^2 = 0.69$, $p = 10^{-8}$ (F-test), n=7). These correlations were significant only during the main movement (second and

third phases of the fetching movements). No significant correlations were observed between the levels of integrated EMG activity and different kinematic variables, such as maximal tangential and angular velocities and accelerations of the object or joints, unlike the findings for extension movements (*13*). These results suggest that the level of muscle activity reflects the underlying control strategy for stabilizing the articulated structure against the water drag forces. During fetching, these forces are expected to be large since the long axis of the *quasi*-articulated structure moves perpendicularly to the direction of motion (*18*).

To gain insight into how the location of the food determines the configuration of the *qua*si-articulated structure, we analyzed the spatio-temporal patterns of muscular activity during fetching movements. Two electrodes were inserted at different positions along the arm. The sign of the delay between the EMG signal onsets at the two electrodes depended on which segment the electrodes were recording from. In the histogram in Fig. 4A, for which the two electrodes were situated within the proximal segment (L_1), the delay in EMG onset was distributed around a positive mean (0.08 ± 0.08 sec), indicating that the EMG signal propagated from the proximal to the distal electrode. In Fig. 4C the electrodes recorded from the medial segment (L_2), and the onset delays were distributed around a negative value (-0.05 ± 0.05 sec) (significantly smaller than the mean in (A), $p = 10^{-7}$ (two-tailed t-test)). Here the muscle activity propagated in distal to proximal direction along the medial segment. In Fig. 4B, the electrodes were located on either side of the medial joint; the histogram was distributed around a mean of 0 ± 0.08 sec (significantly smaller than the mean in (A) and significantly larger than in (C), $p = 0.004$ and $p = 0.005$ (two-tailed t-test), respectively). Similar onset delay tendencies were obtained when different algorithms were used to calculate the onset of the EMG signals (Table S2 and (*16*)).

These results suggest that the formation of the *quasi*-articulated structure involves two waves of muscular contraction which propagate in opposite directions toward each other. One presumably starts at the base of the arm, while the second begins at the distal joint or distally to it. The medial joint

appears to be formed at the collision point between these two propagating waves of muscle activity.

In contrast to the arm extension movement (*14*), the generation of fetching movements requires central brain areas. Of 10 animals in which the supra-esophageal mass (the brain area responsible for higher brain functions, (*19*)) was lesioned, 5 were able to generate fetching movements when a piece of food was placed somewhere along the arm. The other 5 were unable to do so, but instead succeeded in bringing the food to the mouth by transporting it along the arm with the suckers, as described by Altman *(20*). Postmortem observations revealed that, in the 5 octopuses that could perform the fetching movements, the anterior basal lobe (or the major ventral part of it) had remained intact, while this lobe was significantly damaged or eliminated in the 5 animals which had not been able to generate fetching movements. The anterior basal lobe, identified as a higher motor center in cephalopods (*21*); it is most likely essential for coordinating the sequence of movements during fetching.

Humans and monkeys with their rigid skeletons plan their movements either in hand or joint space (*2*, *15*). Here we show that when fetching, the octopus plans the movements of its flexible arms in a novel space, namely limb segment space, where the length of the segments of a *quasi*-articulated structure are dynamically adjusted according to where an object is grasped. While still preserving considerable flexibility, this strategy immensely reduces the number of DOFs to be controlled (one for each joint, 3 in total).

Besides planning movements of the *quasi*-articulated structure in limb segment space, octopuses seem to plan the rest of the fetching movement in joint space (Fig. 3, G and H, Fig. S1 and supporting online text). Thus, a unique control scheme allows an octopus to bring an object to its mouth without requiring any information about the position of the arm in space and avoiding the complexities involved in the inverse kinematics transformation in hyper-redundant structures (*22*).

Further simplification is probably achieved by a singular neural control mechanism, in which the combination of a stimulus produced by the grasped object and a central command may activate two waves of muscle contraction

that propagate in opposite directions, and create or initiate the formation of the medial joint at the collision point. Such a mechanism implies that the neuromuscular system of the octopus arm can process information about the position of the object along the arm and accordingly reconfigure the *quasi*-articulated structure. These results therefore suggest an efficient mechanism for the formation of an object position-dependent articulated structure without requiring a central representation of the arms.

It is especially surprising that of all possible ways in which a flexible arm can bring an object to the mouth, the octopus chooses to generate a *quasi*-articulated structure that, both morphologically and kinematically, strikingly resemble the multi-joint articulated limbs of vertebrates (such as the human arm). Fetching therefore appears to be a unique example where evolution has selected similar solutions through two totally different mechanisms; through morphology in arthropod and vertebrate limbs, and through a stereotypical motor control program in the octopus. This evolutionary functional convergence suggests that a kinematically constrained articulated limb, with two similar length segments, could be nature's optimal solution for achieving highly accurate point-to-point movements.

References

1. W. Kier, K. Smith, *Zool. J. Linn. Soc.* **83**, 307 (1985).
2. T. Flash, N. Hogan, *J. Neurosci*. **5**, 1688 (1985).
3. C. M. Harris, D. M. Wolpert, *Nature*. **394**, 780 (1998).
4. G. Feldman, *Biophysics.* **11**, 766 (1966).
5. E. Bizzi, N. Hogan, F. A. Mussa-Ivaldi, S. Giszter, *Behav. Brain. Sci*. **15**. 603 (1992).
6. d'Avella, P. Saltiel, E. Bizzi, *Nat Neurosci*. **6**. 300 (2003).
7. E. Bizzi, M.C. Tresch, P. Saltiel, A. d'Avella, *Nature Rev. Neurosci*. **1**, 101 (2000).
8. J. F. Soechting, C. A. Buneo, U. Herrmann, M. Flanders, *J. Neurosci*. **15**. 6271 (1995).
9. T. Flash, T. J. Sejnowski, *Curr. Opin. Neurobiol*. **11**. 655 (2001).

10. P. N. Sabes, *Curr. Opin. Neurobiol.* **10**. 740 (2000).
11. D. M. Wolpert, Z. Ghahramani, *Nature Neurosci.* Suppl. **3**. 1212 (2000).
12. Y. Gutfreund et *al*., *J. Neurosci.* **16**, 7297 (1996).
13. Y. Gutfreund, T. Flash, G. Fiorito, B. Hochner, *J. Neurosci.* **18**, 5976 (1998).
14. G. Sumbre, Y. Gutfreund, T. Flash, G. Fiorito, B. Hochner, *Science*. **293**, 1845 (2001).
15. C. G. Atkeson, J. M. Hollerbach, *J. Neurosci*. **5**. 2318 (1985).
16. Material and methods are available as supporting material on Science Online.
17. J. M. Hollerbach, In *Visual cognition and action*. D. N. Osherson, S. M. Kosslyn, J. M. Hollerbach, (MIT Press, Cambridge, Mass, 1990), pp. 151-182.
18. Y. Yekutieli et al., in preparation.
19. J. Z. Young, The anatomy of the nervous system of Octopus vulgaris, (Oxford Univ. Press, London, 1971).
20. J. S. Altman, *Nature*. **229**, 204 (1971).
21. B. B. Boycot, *Proc. R. Soc. London Ser. B*. **153**. 503 (1960).
22. D. Walker. paper presented at the International Symposium on Adaptive Motion of Animals and Machines, Montreal, Canada, August 2000.
23. This work was supported by DARPA grant N66001-03-R-8043 and by the Israel Science Foundation grant 580/02. We thank J. Kien for critical readings and editorial assistance, T. Bdolah-Abram for statistical advice and A. deSantis, E. Brown, Y. Yekutieli and G. Jacobson for their help.

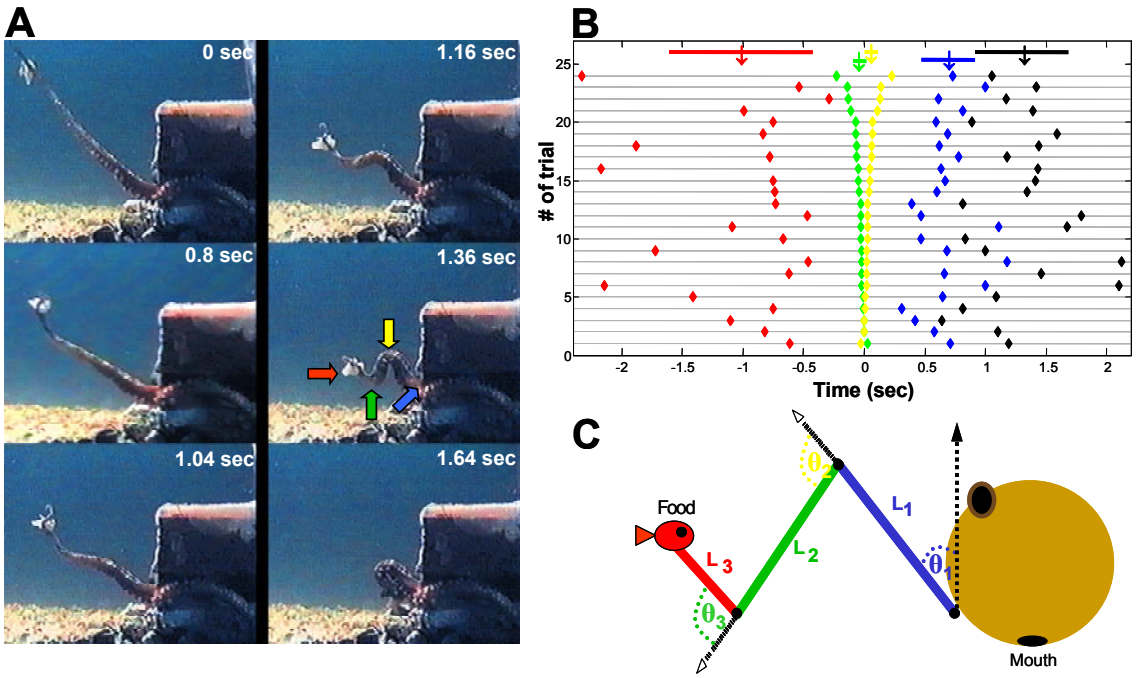

Fig. 1. Octopus fetching movements involve a *quasi*-articulated structure. (A) A sequence of six video images taken at times indicated during a fetching movement. The red arrow marks location of the food. The distal, medial and proximal bends are depicted by the green, yellow and blue arrows, respectively. (B) The typical temporal sequence of events observed during 24 kinematically analyzed fetching movements - grasping the food (red diamond), formation of the distal (green diamond) and medial (yellow diamond) bends, movement of the distal bend towards the base of the arm (blue diamond) and approach to the mouth (black diamond). The events were aligned according to the temporal mid-point between the formation of the distal and medial bends and sorted according to this delay. The arrows and error bars represent the mean and standard deviations of the movement phases, using their respective colors. (C) A schematic drawing of the *quasi*-articulated structure labeled according to the nomenclature given in the text, for the different bends and segments.

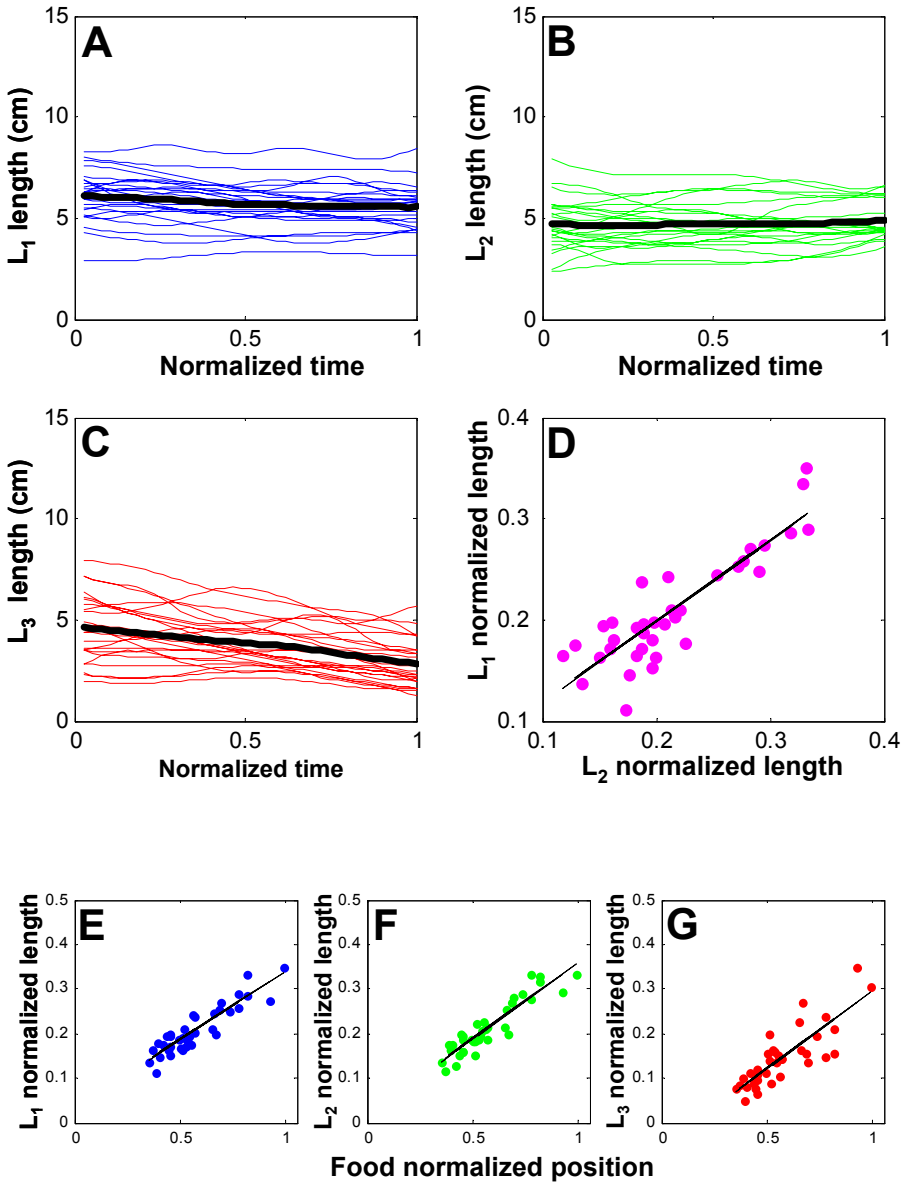

Fig. 2. During fetching movements the generated bends behave like dynamically adjustable joints and their location depends on the position of the grasped object. (A - C) The lengths of the proximal, (L_1), medial (L_2) and distal segments (L_3) as a function of movement's normalized duration (n=24). The thick black curves represent the average length as function of time. (D) There is a positive linear correlation between the lengths of the medial and proximal segments (n=36). Each point represents one trial. (E - G) There is a positive linear correlation between the position of the object along the arm and the length of the segments L_1 (blue), L_2 (green) and L_3 (red), (n=36). Segment lengths and the position of the object are given as a percentage of the total length of the arm.

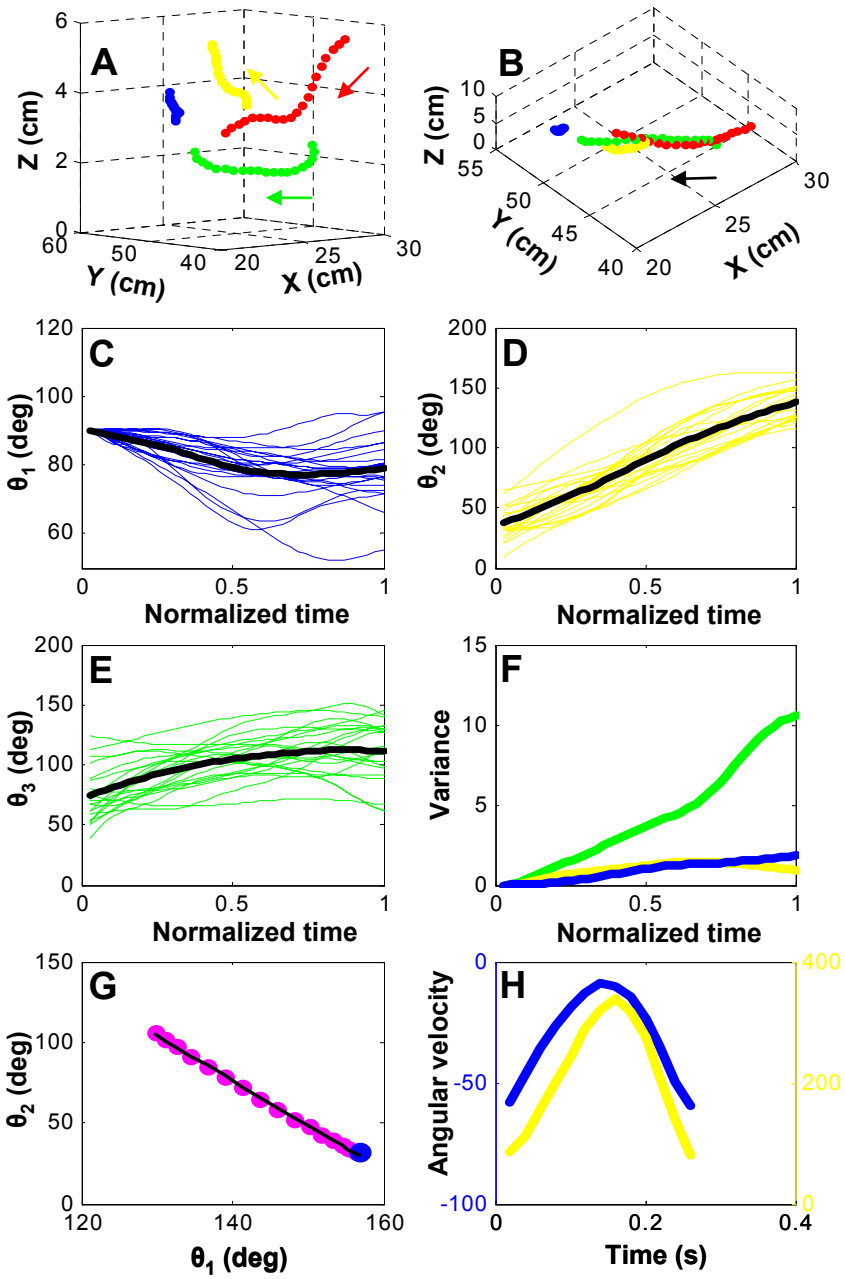

Fig. 3. The fetching movement is restricted to a single linear plane, is generated mainly by the rotation of the medial joint, and is planned in joint space. (A) The paths of the object (red), distal joint (green), medial joint (yellow) and proximal joint (blue) for one movement (arrows give direction of movement), viewed perpendicularly (A), and in parallel (B) to the plane of motion (best fitted plane). Note that all three joints and the object move within the same linear plane. (C - E) Superposition of the angular rotation of each joint, proximal (θ_1) in blue, medial (θ_2) in yellow and distal (θ_3) in green; normalized in time (n=24). In (C) the starting angles were shifted to 90°.

The thick black curves represent the averages. (F) The variances calculated from (C - E). For the variance calculation, all the movements were shifted to the same initial angle. Note the robustness of the large medial joint (θ_2) rotation, compared with the distal (θ_3) and the proximal (θ_1) joint. (G) An example of the relationship between the proximal (θ_1) and the medial (θ_2) joint rotations is nearly straight. The magenta dots represent the data, the black line is the fitted straight line and the large blue dot represents the movement's starting point. (H) The angular velocity profiles of θ_1 (blue) and θ_2 (yellow) of the movement shown in (G).

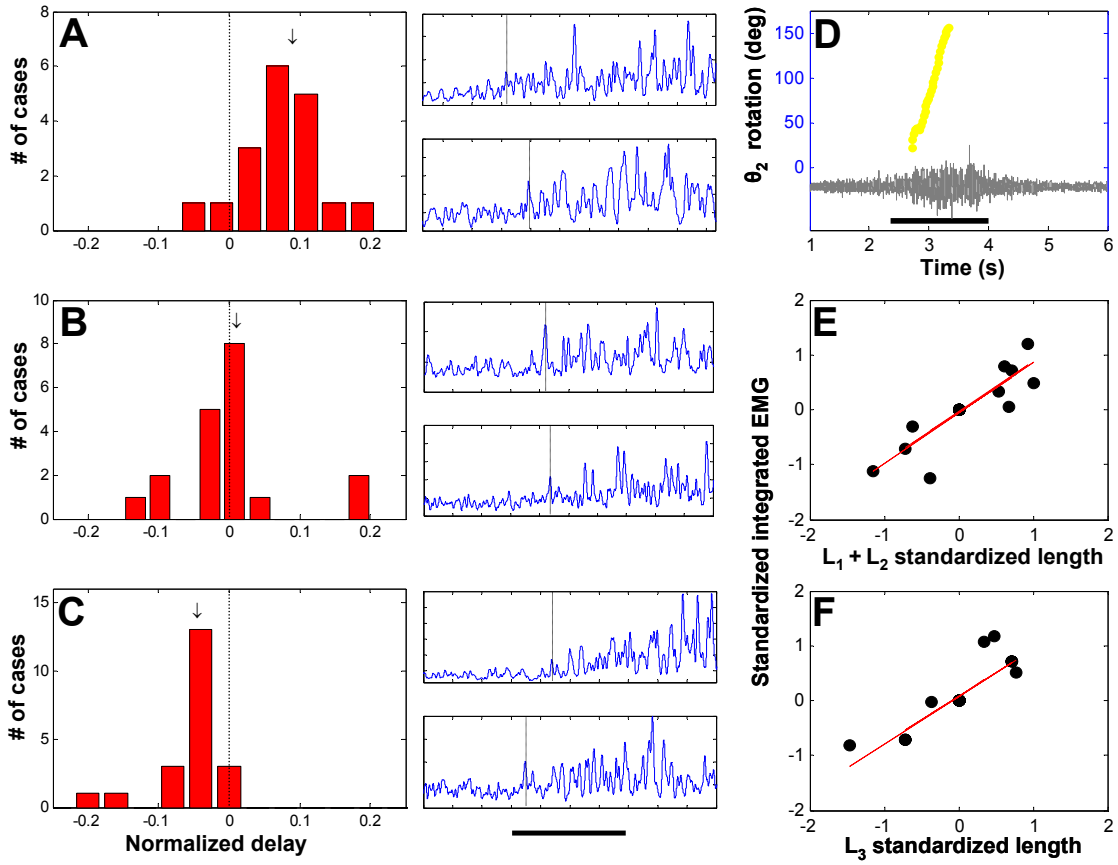

Fig. 4. The *quasi*-articulated structure involves two waves of muscle contractions which propagate towards each other. (A) Histogram of the normalized delays between the onsets of the EMG signals recorded during a fetching movement from two electrodes in the proximal segment (n = 19). (B and C) As in (A), but the electrodes were located at the medial joint (n = 19) and medial segment (n = 21), respectively. Onsets were calculated utilizing the Generalized

Likelihood Ratio algorithm and normalized according to the distance between electrodes. The black arrows represent the average delay of each histogram. On the right of each histogram are examples of the rectified and filtered EMG signals recorded at the proximal (top) and distal (bottom) electrodes; the vertical lines represent the signals' calculated onsets. The scale bar indicates 500 ms. (D) An EMG signal recorded at the medial joint during a fetching movement, superimposed on medial joint rotation (θ_2) (yellow curve). The black bar represents the duration of the movement. (E) The integrated EMG signals at the medial joint are positively and linearly correlated with the combined length of the proximal and medial segments ($L_1 + L_2$) (n=11). (F) A positive linear correlation between the integrated EMG activity recorded anywhere along the distal segment or at the distal joint and the length of the distal segment (n=7).

SUPPORTING ONLINE MATERIAL

Materials and Methods

Experimental animals. *Octopus vulgaris* collected from the Bay of Naples, Italy, were maintained in 50x50x40 cm glass tanks containing artificial sea-water. The water was circulated continuously in a closed system and filtered by active carbon and mechanical and biological filters. The animals were held at a temperature of 16°C in a 12 hr. light/dark cycle. A few days before an experiment, an octopus was moved to a bigger aquarium (80x80x60 cm) at a temperature of 18°-20°C.

Behavioral task and video recording. Octopuses were trained to extend their arms towards a target (a white disc) and wait with an extended arm, for a piece of food (a ~1 cm^3 portion of either sardine or anchovy), which was placed by the experimenter at different locations along arm. The food was rapidly grasped by the suckers at that position and brought to the mouth. The experiments began once the octopuses were acclimatized and trained (typically after a one hour trial session repeated for ~3 consecutive days). The fetching movements were filmed with two super VHS PAL synchronized video cameras positioned ~90° apart (temporal resolution 20 ms, shutter speed 1/250). The coordinates of the food, distal bend, proximal bend and the base of the arm (see Fig 1, A and C)

were digitized and transformed from 2D to 3D using the Direct Linear Transformation (DLT) algorithm (this method is able to transform the cameras' 2D coordinates to external XYZ coordinates from information about the coordinates of at least 12 external landmarks viewed by both cameras (*S1*-*S3*)). The 3D coordinates were smoothed with a Natural B-spline method (*S4*, *S5*) and then kinematically analyzed. The kinematical analysis began from the time frame in which the medial bend was first distinguishable (~30°) until the food reached the base of the arm. Twenty four of ~100 movements filmed, in which the position of the food and the three bends were clearly visible in both cameras throughout the entire movement, were kinematically analyzed. The final phase of the fetching movement (bringing the food from the base of the arm to the mouth) could not be kinematically analyzed since this phase of the movement was obscured by the octopus' body.

Kinematic analysis. The bend angles (θ_1, θ_2 and θ_3), describing the rotations of the three segments (L_1, L_2 and L_3, Fig. 1C), were trigonometrically calculated from the digitized and smoothed data points, according to:

$$\theta_1 = ar\cos\left[\frac{\vec{L}_u}{\| L_u \|} x \frac{\vec{L}_1}{\| L_1 \|}\right]$$

$$\theta_2 = ar\cos\left[\frac{\vec{L}_1}{\| L_1 \|} x \frac{\vec{L}_2}{\| L_2 \|}\right]$$

$$\theta_3 = ar\cos\left[\frac{\vec{L}_3}{\| L_3 \|} x \frac{\vec{L}_2}{\| L_2 \|}\right]$$

Where $\boldsymbol{L_1}$, $\boldsymbol{L_2}$ and $\boldsymbol{L_3}$ are the vectors co-aligning with the segments of the arm (Fig. 1C). A unit vector originating from the base of the arm in the plane of motion and parallel to gravity ($\boldsymbol{L_u}$), was used to compute the angle at the base of the arm (θ_1) (Fig. 1C). Since the octopuses were not restrained during the movements, they were able to fetch objects from any possible orientation, causing the initial value of θ_1 to differ among trials. Therefore, in order to look for kinematic invariants, θ_1 was always shifted to a starting value of 90°.

The temporal order of joints formation. To describe the time sequence of joint formation, a 2D backbone-curve (*S6*) was visually fitted along the middle of the arm, and its curvature (the derivative of the tangent angle with respect to arc length) was calculated for each time frame (20 ms) during the movement (*S7*). Below is an example of the sequential time development of the curvature function of the arm's backbone-curve. The Y-axis and the color scale bar represent the level of curvature. The length of the arm is normalized, with 0 representing the base of the arm and 1 its tip.

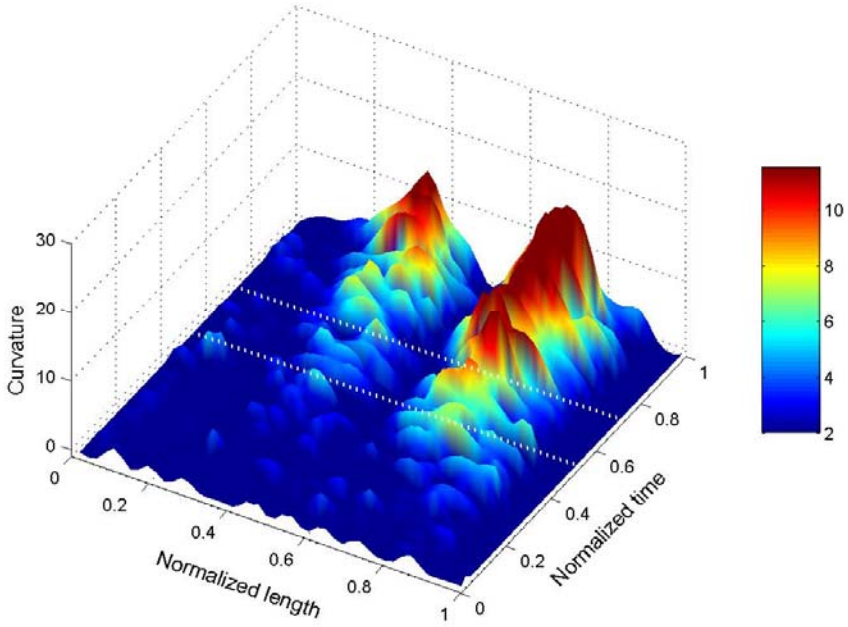

The onsets of bend formation (at the dotted white lines in the graph above) were defined as the time point when the curvature function exceeded a specified threshold. This was set at one standard deviation above the arm's average curvature prior to formation of the bends. Note that before bend formation the extended arm was relatively straight.

Normalization of velocity profiles. The calculated angular velocities [V (t)] around the medial joint (θ_2) and the movement durations (t) were normalized according to the maximal angular velocities (V_{max}) and the angular amplitudes (A_{amp}, the total amount of rotation of the joints) as follows:

$$V_{norm} = \frac{V(t)}{V_{\max}}$$

$$T_{norm} = V_{\max} \times \frac{t}{A_{amp}}$$

Since it is impossible to establish the exact time points of initiation and termination of the movement, as needed for deriving the angular amplitude (A_{amp}), we took advantage of the bell-shaped velocity profiles of the medial angular rotation (θ_2) and calculated the amplitude of the angular joint rotation starting from the first minimum until the second minimum of the bell-shaped velocity profile.

EMG recordings. Octopuses were anaesthetized in a mixture of 3.5% magnesium chloride in sea-water, and two Teflon-coated stainless steel electrodes (0.13 mm diameter) were inserted into the dorsal intrinsic arm musculature (*S2*) at different positions along the arm and with different distances between them (~1-3 cm). Approximately, 1mm of insulation was removed at the electrode's section inserted in the arm. The electrodes were connected to low-level AC differential amplifiers. Muscle activity was differentially recorded between the implanted electrodes and a similar electrode submerged in the water close to the implanted ones. The water in the aquarium was grounded using a long silver wire. EMG signals were amplified (10.000 times), analogically band-pass filtered (0.01 – 3 KHz), and recorded separately in the two high fidelity audio channels of a Super VHS video recorder, simultaneously with the video signal. The EMG signals were then digitized at 10 KHz. The sinusoidal noise components (50 Hz. and higher harmonics) were removed in the frequency domain by Fourier transforming the EMG time signal and attenuating the peaks corresponding to instrumental noise to the level of the neighboring frequency range, while maintaining the Fourier phase. Then, the EMG signals were rectified and smoothed (running average of 5 ms bins). For the EMG signal processing, we used in all cases Matlab (MathWorks Inc.).

The onsets of the EMG signals at each electrode were computed using 4 independent methods: Visually determined, 3 STD amplitude threshold (*S8*), 1

STD Fourier transform threshold and the Generalized Likelihood Ratio (*S9*). For the Fourier transform threshold algorithm, the EMG signal frequency baseline, between 10 – 500 Hz (the EMG frequency spectrum during fetching), was calculated from the EMG recordings before onset of the movement. We set the threshold as 1 STD of this baseline. Then, starting ~300 ms previous to initiation of the fetching movement, running bins of 25 ms were sequentially Fourier transformed in steps of 0.1 ms until the end of the movement. The EMG signal onset was determined when the threshold was constantly exceeded for a period of 1 ms (10 consecutive steps).

The exact positions of the electrodes with respect to the *quasi*-articulated structure were later confirmed from the video recordings.

Supra-esophageal lesions. The octopus brain was exposed under anesthesia (2% ethanol in sea-water), and different levels of the supra-esophageal mass were removed using fine surgical scissors. The behavioral experiments began after a recovery period of ~24 hrs in the experimental aquarium. The extent of the lesion was morphologically confirmed postmortem by viewing Nissl stained brain slices (100 – 200 μm) under a light microscope.

Supporting text

Results

At what level is the fetching movement planned? Studies in vertebrates suggest that motor control may involve three different levels of motion planning: trajectory planning in terms of end-point coordinates, joint coordinates and muscle coordinates (*S10*). To determine at which level the octopus plans the fetching movement, we first looked for invariant relationships between the joint angles. The 24 kinematically analyzed trials could be broadly classified into two different groups. One group showed a simple negative linear correlation between the time-dependent θ_1 and θ_2 angular rotations (n=6, averaged R^2 = 0.97 ± 0.04, in all the cases $p < 0.02$ (F-test), Fig. S1A). In the second group, the relationship between the time-dependent θ_1 and θ_2 angular rotations was described by two nearly straight lines, changing from a negative to a positive

slope, (n=18, first segment: averaged R^2 = 0.96 ± 0.05, in all cases $p < 0.027$ (F-test); second segment: averaged R^2 = 0.85 ± 0.10, in all cases $p < 0.04$ (F-test), (Fig. S1B). The abrupt change in the slope of the θ_2 vs. θ_1 curves occurred when the medial joint changed the direction of its path (i.e., at the time of joint reversal*)* (Fig. S1F, yellow dotted line). The relationships between the proximal (θ_1) or medial (θ_2) angular positions and the distal joint angular position (θ_3) were much more complex and no invariants were found.

Calculating the index of linearity (*S11*) of the paths described by the distal joint, within the best-fitted plane, showed that while in some movements the path was curved (Fig. S1G, blue), in others it was relatively linear (Fig. S1G, red). The threshold between linear and curved paths was arbitrarily set as an index of linearity value of 0.1. When these paths were classified according to their relationship between the time-dependent θ_1 and θ_2 angular rotations, movements belonging to the first group, which followed the linear joint-interpolation motion planning scheme (Fig. S1A), they showed a narrow range of index of linearity (0.092 – 0.211) (Fig. S1H), while movements in the second group had a much broader range of index of linearity (0.007 – 0.367) (Fig. S1I).

Staggered joint interpolation. The phenomenon whereby certain fetching movements show linear correlations both in joint space and in end-point space can be explained by the strategy of staggered joint interpolation motion planning (*S11*). This strategy allows the generation of straight paths both in joint space and in end-effector space by delaying onset of the movement of some of the joints with respect to others.

Velocity profiles. Of all the joint tangential and angular velocity profiles, only θ_2 generated invariant profiles. Of 24 movements, 7 showed bell-shape profiles, 13 showed double-peak profiles and 4 had either monotonically rising or decreasing profiles (Fig. S1, C and D). The tangential and angular velocities of the other joints and of the food showed complex and highly variable profiles.

Movements with θ_2 double-peak angular velocity profiles also showed a relationship between θ_1 and θ_2 corresponding to the second scheme. Moreover, the abrupt changes in slope of the θ_2 vs. θ_1 curves (Fig. S1B) coincided with the minima between peaks of θ_2 velocity profiles (Fig. S1D, dotted line), suggesting that the double-peak velocity profiles may reflect two submovements.

Decomposition into submovements. To test whether the double-peak angular velocity profiles of the medial joint (θ_2) reflect two submovements, we averaged across all normalized θ_2 single-peak velocity profiles (see methods) and fitted a 5^{th} order polynomial to the average profile (Fig. S2A). This polynomial was appropriately scaled to fit the highest velocity peak of each double-peak θ_2 velocity profile. The motion part corresponding to the scaled velocity profile was then subtracted from the original double-peak velocity profile. Next, another 5^{th} order polynomial was appropriately scaled and fitted to the remaining portion of the movement. The scaled fitted polynomials of each movement were algebraically summed (*S12-S16*) and the resulting curve was compared to the corresponding double-peak velocity profile (original data). The comparison was implemented by minimizing the sum of the squares and estimating the R^2 value. The highly significant coefficients of determination obtained in all 13 movements (averaged $R^2 = 0.97 \pm 0.03$, in all cases $p < 10x^{-4}$ (F-test), Fig. S2B) suggest that the double-peak angular velocity profiles of the medial joint result from the superposition of two submovements.

Discussion

We have found that octopuses plan their movements in joint space avoiding the complex problems associated with inverse kinematics transformations in hyper-redundant structures. By combining two submovements that are still planned in joint space, octopuses are able to generate a larger variety of distal joint paths. This may be significant for avoiding obstacles or for generating straight paths of the distal joint in Cartesian coordinates (resulting in a fetching movement that follows the shortest distance path from initial object location to the mouth).

Supporting References

S1. Y. Gutfreund et *al*., *J. Neurosci*. **16**, 7297 (1996).

S2. Y. Gutfreund, T. Flash, G. Fiorito, B. Hochner, *J Neurosci*. **18**, 5976 (1998).

S3. G. A. Wood, R. N. Marshall, *J. Biomech*. **19**. 781 (1986).

S4. P. Craven, G. Wahba, *Numerische Mathematik*. **31**, 377 (1979).

S5. G. Sumbre, Y. Gutfreund, T. Flash, G. Fiorito, B. Hochner, *Science*. **293**, 1845 (2001).

S6. G. Chirikjian, J. W. Burdick, paper presented at ASME Mechanics Conference, Chicago, IL, 1990.

S7. Y. Gutfreund, thesis, Hebrew University (1998).

S8. R. DiFabio, *Phys. Ther*. **67**, 43 (1987).

S9. S. Micera, A. M. Sabatini, P. Dario, *Med. Eng. Phys*. **20**, 211 (1998).

S10. J. M. Hollerbach, In *Visual cognition and action*. D. N. Osherson, S. M. Kosslyn, J. M. Hollerbach, (MIT Press, Cambridge, Mass, 1990), pp. 182-211.

S11. C. G. Atkeson, J. M. Hollerbach. *J. Neurosci*. **5**. 2318 (1985).

S12. T. Flash, E. Henis, *J. Cogn. Neurosci*. **3**, 220 (1991).

S13. N. Berthier, *Dev. Psychol.* **32**, 811 (1996).

S14. B. Rohrer, N. Hogan, *Biol. Cyber*. **89**, 190 (2003).

S15. B. Rohrer, et *al*., *J. Neurosci*. **22**, 8297 (2002).

S16. H. I. Krebs, M. L. Aisen, B. T. Volpe, N. Hogan, *Proc. Natl. Acad. Sci.USA*. **96**, 4645-9 (1999).

Supporting tables

Table S1

	Object	Distal joint	Medial joint	Base of arm
Distance	19.63 ± 2.13 cm	8.44 ± 1.85 cm	3.56 ± 0.98 cm	1.90 ± 1.20 cm
Residual error (SE)	0.15 ± 0.09 cm	0.15 ± 0.07 cm	0.15 ± 0.11 cm	0.04 ± 0.03 cm
R^2	0.99 ± 0.01	0.99 ± 0.01	0.71 ± 0.29	0.90 ± 0.10
p value (F-test)	$p < 1.5x10^{-10}$	$p < 1.5x10^{-10}$	$p = 0.05$	$p < 5.5x10^{-6}$

Table S1. The distance traveled in the plane of motion by the object and the 3 joints, their residual errors (SE) orthogonal to this plane and the linear correlation parameters (R^2 and p value) of the paths fitted to a single plane. To calculate the absolute movement of the arm, the movement of the base of the arm (indicating how much the octopus moved its body) was subtracted from the paths of the object, and distal and medial joints. The distances, residual errors and R^2 are given as the average ± standard deviation (n = 24).

Table S2.

Algorithm / Position	**Visually determined**	**3STD threshold**	**1STD Fourier transform threshold**	**Generalized Likelihood Ratio**
L_1	0.15 ± 0.31 s/cm	0.21 ± 0.29 s/cm	0.13 ± 0.21 s/cm	0.09 ± 0.10 s/cm
Medial joint	0.08 ± 0.14 s/cm	0.13 ± 0.45 s/cm	0.06 ± 0.22 s/cm	0 ± 0.08 s/cm
L_2	0 ± 0.08 s/cm	-0.04 ± 0.07 s/cm	-0.04 ± 0.08 s/cm	-0.04 ± 0.06 s/cm

Table S2. Delay in the onset of the EMG activity during fetching movements as measured between two electrodes located either in the proximal segment (L_1), at both sides of the medial joint (θ_2) or in the distal segment (L_2). The delay is normalized for the distance between the electrodes. The onsets were calculated using four different algorithms. The normalized delays are represented as the average ± standard deviation (n = 59).

Supporting figures

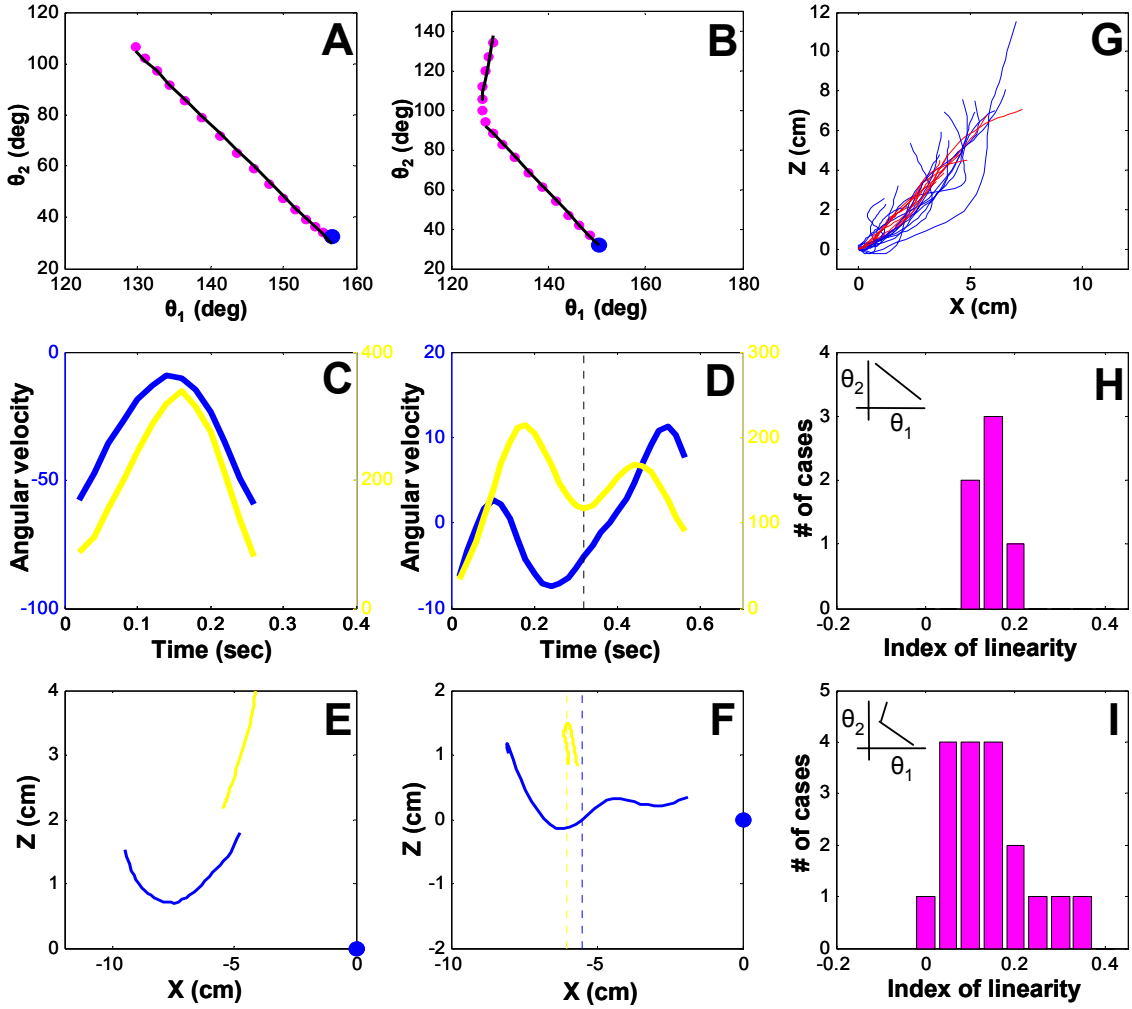

Fig. S1. Fetching movements are planned at the level of joint space and can be classified into two different groups. (A) The first group shows a single linear segment curve with a negative slope representing the relationship between the proximal (θ_1) and the medial (θ_2) joint rotations. (B) Typical for movements in the second group is a curve changing from a negative to a positive

slope. The magenta dots represent the data, the black lines represent the fitted straight lines and the large blue dots represent the movement's starting point. (C - D) the angular velocity profiles of θ_1 (blue) and θ_2 (yellow); the vertical black dotted line in (D) shows the time of the abrupt change in slope observed in (B). (E - F) The paths of the distal joint (blue) and the proximal joint (yellow) within the best-fitted plane. The dashed vertical lines represent the time point of the abrupt change in slope in (B), for the path of the distal joint (blue) and the medial joint (yellow). The blue dot represents the position of the base of the arm. (G) The paths described by the distal joint within the best-fitted plane (shifted to the same starting position and rotated to 45°). Paths with small index of linearity values are colored in red, while those with higher values are in blue. (H) The index of linearity histogram of the distal joint path for movements classified as obeying the linear joint-interpolation motion planning scheme shown in (A). (I) As in (H) for movements obeying the second motor planning scheme, which describes the time-dependent relationship between θ_1 and θ_2 by two nearly straight lines, changing from a negative to a positive slope shown in (B).

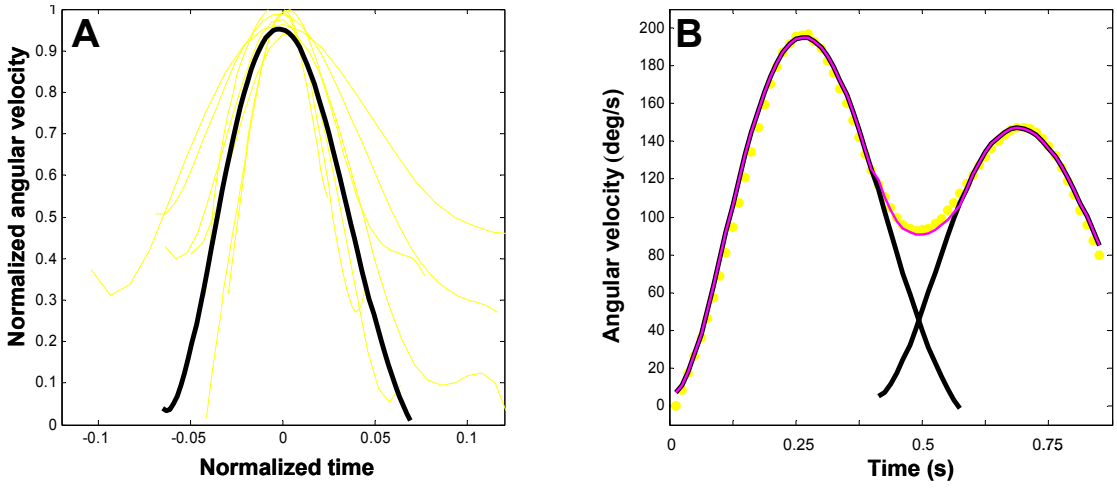

Fig. S2. Some fetching movements may be formed by the superposition of a sequence of submovements. (A) Normalized and aligned bell-shaped angular velocity profiles of the distal joint (θ_2, yellow curves) and the 5th order polynomial fitted to the average of all the single peak velocity profiles (black curve). (B) An example of the decomposition of a θ_2 double-peak velocity profile (yellow dots) into two submovements using the scaled polynomial calculated in (A). The duration and amplitude of two polynomials were adjusted to fit each of the peaks in the velocity profile (black curves) and these were subtracted from the original data. The magenta curve represents the algebraic summation of the scaled polynomials.

Chapter 4

General discussion

The question how animals generate and control movement has captured the attention of scientists and researchers since the times of Aristotle, 350 bce, who emphasized the task of the skeleton and joints in producing the movement:

> … *it is plainly impossible for movement to be initiated if there is nothing at rest, and before all else in our present subject- animal life. For if one of the parts of an animal be moved, another must be at rest, and this is the purpose of their joints…*, *as well as the mind (brain) to control it* … *Now we see that the living creature is moved by intellect, imagination, purpose, wish, and appetite. And all these are reducible to mind and desire* … (Aristotle, 350 bce).

Thus, Aristotle claimed that observing how animals move can give us clues about how their mind works.

The movement of octopuses is a unique case where the skeleton necessary for the generation of movement is not rigid but dynamic, theoretically allowing the octopus to move with an infinite number of DOFs. On the one hand, this extreme flexibility of movement may confer great evolutionary advantage, yet on the other hand, such flexibility of movement creates enormously complex problems for the motor control system. Studying octopus arm movement not only helps us understand how evolution has solved the problem of controlling hyper-redundant limbs, but may also aid us in developing new ideas on how to control hyper-redundant robotic manipulators.

Throughout this thesis, I have focused on the neuroethological aspects of the motor control of the octopus arm during goal-directed movements, concentrating particularly on strategies of movement and on the neuromuscular mechanisms involved in the control of truly flexible limbs.

4.1 Motor control of the reaching movement.

Previous studies on the octopus arm have shown that when octopuses swim, crawl or reach towards a target, they produce a very stereotypical arm movement, named a reaching movement. In reaching, a bend is formed somewhere along the arm and is then actively propagated towards the tip of the arm. This movement strategy requires control of only 3 DOFs, pitch, yaw and velocity of the bend

propagation. In addition, the movement's kinematics are also stereotypical; the bend propagates in a single plane with an invariant bell-shaped tangential velocity profile (Gutfreund et al., 1996, 1998).

In the investigations reported here, I have further explored the controlling mechanisms of this stereotypical movement. I have showed that electrical or tactile stimulation of 'denervated' octopus arms can evoke movements whose qualitative, kinematical and dynamic characteristics are extremely similar to those of freely behaving octopuses. The temporal relation between the stimulus and the evoked movement shows clearly that these movements were actually triggered by the stimulus and were not a result of direct muscular activation.

Further investigation has shown that modification of the pitch and yaw of the bend before onset of the movement determine the movement's final path. Additionally, adjusting the frequency and duration of the triggering stimulus allowed us to predictively set the maximal velocity of bend propagation. Altogether, modulation of these 3 DOFs enabled us to evoke movements with the whole range of characteristics observed in freely behaving octopuses.

These results, together with the fact that octopuses are unable to use visual information to re-plan a movement once it has already started, lead to the conclusion that the octopus's centralized brain participates only in the initiation of reaching movements, setting both the direction and velocity of bend propagation. In contrast, the spatiotemporal details of the entire movement pattern are dictated by a feed-forward motor program embedded in the neuromuscular system of the arm. This strategy, which combines a reduction in the number of DOFs to be controlled, a feed-forward hierarchically controlled peripheral motor program, and the ability to grasp objects along the entire length of the arm, drastically simplifies the complexity of overcoming the inverse kinematics and inverse dynamics transformations in hyper-redundant structures.

4.2 The fetching movement: kinematics and motor control.

A totally different type of goal-directed movement is performed when octopuses bring an object (e.g. prey) to their mouth after grasping it with the sucker on the arm. In contrast to reaching movements, where the target can be grasped anywhere along the arm, the octopus has to execute a point-to-point task, That is, the end-effector (the location along the arm where the object was grasped) has to

reach a specific and precise target (the mouth). Since objects can be grasped everywhere along the length of the arm, the end-effector's location can be different for each movement, thus introducing further difficulties to the already complex problem of controlling a flexible arm.

Here I have shown that octopuses solve these problems by creating a *quasi*-articulated structure consisting of 3 joints (each with one DOF) and three segments. The two proximal segments are of equal length, thus the structure morphologically resembles articulated vertebrates' limbs (e.g. human arm). Their lengths are determined by where along the arm the object has been grasped. Therefore, just by rotating these 3 joints the object will always accurately reach the mouth, regardless both of where along the arm it was grasped and the arm's initial position in space. The reduction of the arm's DOFs to only three, together with the fact that the movements are planned in joint space, largely simplifies the complexity of controlling a hyper-redundant structure.

Moreover, the complex task of generating a dynamic *quasi*-articulated structure is apparently simplified through a unique peripheral neuromuscular mechanism. The stimulation produced by the grasped object appears to activate, via a central command, two waves of muscle contraction propagating in opposite directions towards each other that create or initiate the formation of the medial joint at their collision point. This mechanism would allow the neuromuscular system of the octopus to process information about the position of the object along the arm and adjust the *quasi*-articulated structure accordingly, without requiring central representation of the arm.

Apparently, the fetching movement is optimized to produce an accurate movement; EMG recordings show that energy is likely to be invested in stabilizing the movement against the large drag forces generated by the structure.

The morphological and the kinematical similarity between the *quasi*-articulated structure in octopus fetching and vertebrate limbs hints at an evolutionary convergence of function. The similarity suggests that a kinematically constrained articulated limb is the optimal solution for achieving highly accurate point-to-point reaching movements. This solution has been achieved in natural evolution through two totally different mechanisms; through morphology of the rigid skeleton in

arthropod and vertebrate limbs and through a stereotypical motor control program in the octopus.

4.3 Final Conclusions.

The neuroethological experiments reported here on the motor control of the octopus arm aimed to increase our understanding of how nature overcomes the complex task of controlling flexible appendages. The experiments revealed that during goal-directed movements, either when reaching towards an object (Gutfreund et al., 1996) or when bringing an object to the mouth (fetching movement), octopuses dramatically decrease the number of DOFs of their arms from virtually an infinite number to only 3. This strategy appears to reflect a reduction in redundancy necessary to improve the degree of arm control, and 3 DOFs may be the maximum that can be centrally controlled for each arm.

Despite the redundancy limitations during goal-directed movements, the octopus' flexible arms can still generate movements with arm geometries that articulated limbs cannot possibly produce (e.g. bend propagation during reaching movement). This ability allows octopuses to generate movements which minimize the drag forces exerted by water on the arm (large drag forces are only exerted at the bend area), thus minimizing energy consumption or turbulence (important in order not to alert prey). Additionally, the arm's geometry may be adjusted to match task requirements, as in the fetching movement.

In addition to goal-directed movements, octopuses can execute a variety of unique movements, such as arm foraging and cleaning maneuvers. During these movements, it is quite clear that a large number of DOFs are exploited (personal observations). These movements may be controlled by local reflexes in the arm, as suggested by the highly developed nervous system of the arm and by the spontaneous, complex, non-stereotypical movements observed in amputated arms (personal observations). These observations imply that the arm is able to move autonomously, without supervision by the brain. This strategy may be significant when octopuses forage within their typically restricted environments, for they use their arms to search for food in crevices and small rock or coral cracks, without the possibility of any visual control. As soon as prey is encountered and grasped, the brain may take control of the arm and bring the prey accurately to the mouth. Therefore, I suggest that while arm control at lower levels can take advantage of

the arm's flexibility, the degree of control is poor. In contrast, higher levels of motor control are able to combine global sensory and motor information to more precisely control the arm, while transiently sacrificing redundancy. Future research on non-goal directed movements, such as arm foraging and cleaning maneuvers, may help us understand the mechanisms involved in the generation and control of movements using a large number of DOFs.

The results obtained here have provided further insight on how biological systems have evolved to overcome the complex problem of controlling a highly redundant motor system and will hopefully contribute to the ongoing multi-disciplinary effort of developing and controlling truly flexible robotic manipulators in highly constrained environments.

References

A

Abbot NJ and Miyan JA (1995). Cerebrovascular organization and dynamics in cephalopods. In cepahalopod Neurobiology (ed. N. J. Abbot, R. Williamson and L. Maddock), pp. 459-476. Oxford, New York, Tokio: Oxford University Press.

Alexander RM (1997) A minimum energy cost hypothesis for human arm trajectories. ***Biol. Cybern***. 76:97-105.

Altman JS (1971). Control of accept reject reflexes in the Octopus. ***Nature***. 229: 204-206.

Aristotle (350 bce) on the movements of animals.

Armstrong DM (1988). The supraspinal control of mammalian locomotion. ***J. Physiol***. 405:1-37.

Arshavsky YU, Orlovsky GN, Panchin YuV, Roberts A and Soffe SR (1993). Neuronal control of swimming locomotion: analysis of the pteropod mollusc Clione and embryos of the amphibian Xenopus. ***Trends Neurosci***. 16:227-233.

Arshavsky YI, Deliagina TG and Orlovsky GN. (1997) Pattern generation. ***Curr. Opin. Neurobiol.*** 7:781-789.

Arshavsky YI, Deliagina TG, Okshtein IL, Orlovsky GN, Panchin YV and Popova L B (1994). Defense reaction in the pond snail Planorbis corneus. II. Central pattern generator. ***J. Neurophysiol.*** 71:891-897.

Atkeson CG and Hollerbach JM (1985). Kinematic features of unrestrained vertical movements. ***J. Neurosci.*** 5:2318-2330.

B

Ballintijn CM and Roberts JL (1976) Neural control and proprioceptive load

matching in reflex respiratory movements of fishes. ***Fed. Proc***. 35:1983-1991.

Bernstein N. (1967). The coordination and regulation of movemnets. Oxford: Pergamon Press.

Berthier N. (1996). Learning to reach: A mathematical model. ***Dev. Psychol***. 32:811-823.

Bizzi E, Mussa-Ivaldi FA and Giszter S. (1991). Computations underlying the execution of movement: a biological perspective. ***Science*** 253:287-291.

Boal JG, Dunham AW, Williams KT and Hanlon RT (2000) Experimental evidence for spatial learning in octopuses (Octopus bimaculoides). ***Comp. Psychol.*** 114:246-252.

Bullock TH and Budelmann BU (1991) Sensory evoked potentials in unanesthetized unrestrained cuttlefish: a new preparation for brain physiology in cephalopods. ***J. Comp. Physiol. A***. 168:141-150.

C

Caminiti R, Johnson PB, Galli C, Ferraina S and Burnod Y. (1991). Making arm movements within different parts of space: the premotor and motor cortical representation of a coordinate system for reaching to visual targets. ***J. Neurosci.*** 11:1182-1197.

Canedo A. (1997) Primary motor cortex influences on the descending and ascending systems. ***Prog. Neurobiol.*** 51:287-335.

Chiel HJ, Crago P, Mansour JM and Hathi K. (1992). Biomechanics of a muscular hydrostat: a model of lapping by a reptilian tongue. ***Biol. Cybern.*** 67:403-415.

Chirikjian GS and Burdick JW. (1990) Kinematics of Hyper-Redundant Manipulators. in Proceedings of the 2nd International Workshop on Advances in Robot Kinematics, pp. 392-399.

Chirikjian GS and Burdick JW. (1995) The kinematics of hyper-redundant robot locomotion. ***IEEE Trans. Rob. Autom.*** 11, no. 6:781.

Craven P and Wahba G. (1979) Smoothing noisy data with spline functions. ***Numerische Mathematik,*** 31:377-403.

D

d'Avella A, Saltiel P and Bizzi E. (2003) Combinations of muscle synergies in the construction of a natural motor behavior. ***Nat Neurosci***. 6:300-308.

DiFabio RP (1987) Reliability of computerized surface electromyography for determining the onset of muscle activity. ***Phys. Ther.*** 67:43-48.

E

Eisenhart FJ, Cacciatore TW and Kristan WB Jr. (2000) A central pattern generator underlies crawling in the medicinal leech. ***J. Comp. Physiol. A***. 186:631-643.

F

Feldman AG. (1966). Functional tuning of the nervous system during control of movement or maintenance of a steady posture. III. Mechanographic analysis of the execution by man of the simplest motor tasks. ***Biophysics*** 11:766-775.

Fiorito G, Planta CV, Scotto P (1990) Problem solving ability of Octopus vulgaris Lamarck (Mollusca, Cephalopoda). ***Behav. Neural. Biol***. 53:217-230.

Fiorito G. and Scotto P. (1992). Observational learning in Octopus vulgaris. ***Science***. 256:545-547.

Flash T and Henis E (1991) Arm trajectory modifications during reaching towards visual targets. ***J. Cogn. Neurosci.*** 3:220-230.

Flash T. (1987). The control of hand equilibrium trajectories in multi-joint arm movements. ***Biol. Cybern.*** 57:257-274.

Flash T and Hogan N. (1985). The coordination of arm movements: An experimentally confirmed mathematical model. ***J. Neurosci.*** 5:1688-1703.

G

Georgopoulos AP, Kalaska JF, Caminiti R and Massey JT. (1982). On the relations between the direction of two-dimensional arm movements and cell discharge in primate motor cortex. ***J. Neurosci.*** 2:1527-1537.

Gomi H and Kawato. (1996). Equilibrium-point control hypothesis examined by measured arm stiffness during multijoint movement. ***Science***. 272:117-120.

Gravagne I and Walker ID (2000) Kinematics for Constrained Continuum Robots Using Wavelet Decomposition, Robotics 2000, proceedings of the 4th International Conference and Exposition/Demonstration on Robotics for Challenging Situations and Environments, pp. 292-298.

Graziadei P. (1965). Muscle receptors in cephalopods. ***Proc. R. Soc. London Ser. B***. 161:392-402.

Graziadei P. (1971). The nervous system of the arms. In The anatomy of the nervous system of Octopus vulgaris (ed. J. Z. Young), pp. 45-59. Oxford: Clarendon press.

Grillner S. (1985). Neurobiological bases of rhythmic motor acts in vertebrates. ***Science.*** 228:143-149.

Gutfreund Y, Matzner H and Hochner B (in preparation)

Hannan MW and Walker ID. (2003) Kinematics and the implementation of an elephant's trunk manipulator and other continuum style robots. ***J. Robot. Syst***. 20:45-63.

Gutfreund Y, Flash T, Yarom Y, Fiorito G, Segev I and Hochner B. (1996) Organization of octopus arm movements: a model system for studying the control

of flexible arms. ***J. Neurosci.*** 16:7297-7307.

Gutfreund Y, Flash T, Fiorito G and Hochner B. (1998) Patterns of arm muscle activation involved in octopus reaching movements. ***J. Neurosci***. 18:5976-5987.

H

Harris CM and Wolpert DM. (1998) Signal-dependent noise determines motor planning. ***Nature***. 394:780-784.

Hines M. and Blum JJ. (1978). Bend propagation in flagella I. Derivation of equations of motion. ***Biophys. J.*** 23: 41-57.

Hochner B, Brown ER, Langella M, Shomrat T and Fiorito G. (2003) A learning and memory area in the octopus brain manifests a vertebrate-like long-term potentiation. ***J Neurophysiol.*** 90(5):3547-3554.

Hollerbach JM. (1990). Planning of arm movements. In Visual cognition and action, vol. 2 (ed. D. N. Osherson, S. M. Kosslyn and J. M. Hollerbach), pp. 183-212. Cambridge, Mass: MIT Press.

Hollerbach JM. and Atkeson CG. (1987). Deducing planning variables from experimental arm trajectories: pitfalls and possibilities. ***Biol. Cybern.*** 56:279-92.

K

Kalaska JF, Cohen DA, Prud'homme M, Hyde ML. (1990) Parietal area 5 neuronal activity encodes movement kinematics, not movement dynamics. ***Exp. Brain Res.*** 80:351-64.

Kien J. and Altman JS. (1992). Preperation and execution of movement: parallels between insect and mammalian motor systems. ***Comp. Biochem. Physiol. A***. 103:5-24.

Kier WM. and Smith KK. (1985). Tongues, tentacles and trunks: the biomechanics of movement in muscular-hydrostats. ***Zool. J. Linn. Soc***. 83:307-324.

Kier WM and Van Leeuwen JLV. (1997). A kinematic analysis of tentacle extension in the squid Loligo pealei. ***J. Exp. Biol.*** 200:41-53.

Kier WM. Smith KK and Miyan JA. (1989). Electromyography of the fin musculature of the cuttlefish Sepia officinalis. ***J. Exp. Biol.*** 143:17-31.

Konishi M. (1994). Pattern generation in birdsong. ***Curr. Opin. Neurobiol.*** 4:827-831.

Kremer E and Lev-Tov A. (1997) Localization of the spinal network associated with generation of hindlimb locomotion in the neonatal rat and organization of its transverse coupling system. ***J Neurophysiol.*** 77:1155-1170.

Kristan WB, Skalak R, Wilson RJA, Skierczynski BA, Murray JA, Eisenhart FJ and Cacciatore TW. (2000). Biomechanics of hydroskeletons: Lessons learned from studies of crawling in the medicinal leech. In Winters, J. and Crago, P., editors, Biomechanics and Neural Control of Posture and Movement, pp. 206-218. Springer-Verlag, New York.

Kuba M, Meisel DV, Byrne RA, Griebel U and Mather JA. (2003) Looking at play in Octopus vulgaris. ***Pflugers Arch.*** 3:163-169.

Lowe AA. (1980). The neural regulation of tongue movements. ***Prog. Neurobiol.*** 15:295-344.

M

Mackintosh NJ and Holgate V. (1965) Overtraining and the extinction of a discrimination in Octopus. ***J. Comp. Physiol. Psychol***. 60:260-262.

Maldonado H. (1964). The control of attack by Octopus. ***Zeitschrift für vergleichende Physiologie*** 47:656-674.

Mather JA (1991) Navigation By Spatial Memory And Use Of Visual Landmarks In Octopuses. ***J. Comp. Physiol. A***. 168:491-497.

Mather JA and Anderson RC (1999) Exploration, play, and habituation in octopuses (Octopus dofleini). ***J. Comp. Psychol.*** 113:333-338.

Mather JA. (1998). How do octopuses use their arms? ***J. Comp. Psychol.*** 112:306-316.

Matzner H, Gutfreund Y and Hochner B (2000) Neuromuscular system of the flexible arm of the octopus: physiological characterization. ***J. Neurophysiol.*** 83:1315-1328.

Medendorp W P, Crawford J D, Henriques, D Y, Van_Gisbergen, J A and Gielen, C C (2000). Kinematic strategies for upper arm-forearm coordination in three dimensions. ***J. Neurophysiol.*** 84:2302-2316.

Micera S, Sabatini AM and Dario P. (1998) An algorithm for detecting the onset of muscle contraction by EMG signal processing. ***Med. Eng. Phys***. 20:211-215.

Morasso P. (1981). Spatial Control of Arm Movements. ***Exp. Brain Res.*** 42:223-227.

Moriyama T and Gunji Y (1997) Autonomous learning in maze solution by octopus. ***Ethology***. 103:499-513.

Moynihan M (1975) Conservatism of displays and comparable stereotyped patterns among cephalopods. In "Function and evolution in behavior" (G. Baerends, C. Beer and A. Manning. Eds.). pp. 276-292. Clarendon. Oxford.

N

Nakano E, Imamizu H, Osu R, Uno Y, Gomi H, Yoshioka T and Kawato M.(1999) Quantitative Examinations of Internal Representations for Arm Trajectory Planning: Minimum Commanded Torque Change Model. ***J. Neurophysiol***. 81:2140-2155.

Nishikawa KC, Murray ST and Flanders M (1999) Do arm postures vary with the speed of reaching? ***J. Neurophysiol***. 81:2582-2586.

Norman MD, Finn J and Tregenza T (2001) Dynamic mimicry in an Indo-Malayan octopus. ***P. Roy. Soc. Lond. B.*** 268:1755-1758.

O

Onimaru H. (1995). Studies of the respiratory center using isolated brainstem-spinal cord preparations. ***Neurosci. Res.*** 21:183-90.

P

Packard A. (1972). Cephalopods and fish: the limits of convergence. ***Biol. Rev.*** 47:241-307.

Packard A and Sanders GD. (1971). Body patterns of Octopus vulgaris and maturation of the response to disturbance. ***Anim. Behav.*** 19:780-790.

Paljug E, Ohm T and Hayati S. (1995) Serpentine robot: a 12 DOF system for inspection. IEEE Conference on robotics and automation, 3143-3148.

Papini MR and Bitterman ME. (1991) Appetitive conditioning in Octopus cyanea. ***J. Comp. Psychol***. 105:107-114.

Pearson KG. (1993). Common principles of motor control in vertebrates and invertebrates. ***Annu. Rev. Neurosci.*** 16:265-97.

R

Richardson MJE and Flash T. (2002) Comparing smooth arm movements with the two-thirds power law and the related segmented-control hypothesis. ***J. Neurosci.*** 15:8201-8211.

Rokni D and Hochner B (2002) Ionic currents underlying fast action potentials in the obliquely striated muscle cells of the octopus arm. ***J. Neurophysiol.*** 88:3386-3397.

Rosenbaum DA, Loukopoulos LD, Meulenbroek RG, Vaughan J, Engelbrecht SE.(1995) Planning reaches by evaluating stored postures. ***Psychol. Rev***. 102:28-67

Rowell CHF. (1963). Excitatory and inhibitory pathways in the arm of Octopus. ***J. Exp. Biol***. 40:257-270.

S

Schaal S, Sternad D. (2001) Origins and violations of the 2/3 power law in rhythmic three-dimensional arm movements. ***Exp. Brain Res***. 136:60-72.

Schaefer PL and Ritzmann RE (2001) Descending influences on escape behavior and motor pattern in the cockroach. ***J. Neurobiol***. 49:9-28.

Schmidt RS (1992) Neural correlates of frog calling: production by two semi-independent generators. ***Behav. Brain Res***.50:7-30.

Schwartz AB (1988) Direct cortical representation of drawing. ***Science***. 265:540-542.

Selverston A (1999) General principles of rhythmic motor pattern generation derived from invertebrate CPGs. ***Prog. Brain Res***.123:247-257.

Shik ML, Severin FV and Orlovsky GN. (1969) Control of walking and running by means of electrical stimulation of the mesencephalon. ***Electroencephalogr. Clin. Neurophysiol***. 26:549.

Shik, M. L. and Orlovsky, G. N. (1976). Neurophysiology of locomotor automatism. ***Physiol. Rev.*** 56:465-501.

Simonsz HJ and Den Tonkelaar I. (1990) 19th century mechanical models of eye movement: Donders' law, Listing's law, and Helmholtz's direction circles. ***Doc. Ophthalmol***. 74:95–112.

Smith KK. (1984). The use of the tongue and hyoid apparatus during feeding in lizards (Ctenosaura similis and Tupinambis nigropunctatus). ***J. Zool. London.*** 202, 115-143.

Soechting JF, Buneo CA, Herrmann U and Flanders M (1995) Moving effortlessly in three dimensions: does Donders' law apply to arm movement? ***J. Neurosci***. 15:6271-6280.

Susswein AJ, Hurwitz I, Thorne R, Byrne JH and Baxter DA.(2002) . Mechanisms underlying fictive feeding in aplysia: coupling between a large neuron with plateau potentials activity and a spiking neuron. ***J. Neurophysiol.*** 87:2307-2323.

Sutherland NS. (1957). Visual discrimination of orientation and shape by the octopus. ***Nature***. 179:11-13.

T

Terzuolo CA and Viviani P. (1980) Determinants and characteristics of motor patterns used for typing. ***Neuroscience***.5:1085-1103.

Todorov E and Jordan MI. (2002) Optimal feedback control as a theory of motor coordination. ***Nat. Neurosci***. 11:1226-1235.

Tresch MC, Saltiel P and Bizzi E. (1999) The construction of movement by the spinal cord. ***Nat. Neurosci***. 2:162-167.

Torres EB, Zipser D (2002) Reaching to grasp with a multi-jointed arm. I. Computational model. ***J. Neurophysiol***. 88:2355-2367

U

Uno Y, Kawato M, Suzuki R. (1989) Formation and control of optimal trajectory in human multijoint arm movement. Minimum torque-change model. ***Biol. Cybern***. 61:89-101.

V

Van Leeuwen JL and Kier WM. (1997). Functional design of tentacles in squid: Linking sarcomere ultrastructure to gross morphological dynamics. ***Philos. Trans. R. Soc. London Ser. B***. 352:551-571.

Viala G and Buser P (1969) Stereotyped rhythmic motor activities in the rabbit. A study of their general characteristics. ***Exp. Brain Res***. 8:346-363.

Viviani P and Stucchi N. (1992) Biological movements look uniform: evidence of motor-perceptual interactions. ***J. Exp. Psychol. Hum. Percept. Perform.*** 18:603-623.

W

Walker ID and Hannan MW (1999), A Novel 'Elephant's Trunk' Robot, IEEE/ASME International Conference on Advanced Intelligent Mechatronics.

Wells MJ. (1959). A touch learning centre in Octopus. ***J. Exp. Biol.*** 590-612.

Wells MJ. (1961). Weight discrimination by Octopus. ***J. Exp. Biol.*** 38:127-133.

Wells,MJ. (1978). Octopus. London: Chapman and Hall.

Wells MJ. and Wells J. (1957). The function of the brain of Octopus in tactile discrimination. ***J. Exp. Biol.*** 34:131-142.

Williamson R and Budelmann BU. (1991). Convergent inputs to Octopus oculomotor neurons demonstraed in a brain slice preparation. ***Neurosci. Lett.*** 121:215-218.

Wood GA and Marshall RN (1986) The accuracy of DLT extrapolation in three-dimensional film analysis. ***J. Biomech.*** 19:781-785.

Y

Yekutieli Y et al. (unpublished results)

Young JZ. (1960). The visual system of octopus. (I) Regularities in the retina and optic lobes of Octopus in relation to form discrimination. ***Nature.*** 186:836-839.

Young JZ. (1962). The optic lobes of Octopus vulgaris. ***Philos. Trans. R. Soc.***

London Ser. B. 245:19-58.

Young JZ. (1963). The number and size of nerve cells in Octopus. ***Proc. Zool. Soc. London.*** 140:229-253.

Young JZ. (1964). Paired centers for the control of attack in by octopus. ***Proc. R. Soc. London Ser. B***. 159:565-588.

Z

Zulo L et al (unpublished results).

תוכן העניינים

פרק 1

מבוא כללי.....1

1.1 ביצוע תנועה.....1

1.2 תכנון תנועה.....2

1.3 תאום תנועה.....4

1.4 הבסיס העצבי של תנועה (מחוללי תנועה מרכזית).....8

1.5 רב עודפות.....10

1.5.1 זרועות רובוטיות.....10

1.5.2 יתר-יתירה בטבע.....12

1.6 התמנון המצוי.....14

1.6.1 מורפולוגיה של המערכת העצבית.....16

1.6.2 נוירופיסיולוגיה.....18

1.6.3 בקרת תנועה של הזרועות.....19

1.7 מטרות המחקר.....21

פרק 2

שיטות וחומרים.....22

פרק 3

תוצאות

3.1 בקרה של זרועות התמנון ע״י תוכנית תנועה מרכזית.....35

3.2 תובנות על מנגנוניים של בקרת תנועה של תנועות הושטה של התמנון.....39

3.3 אסטרטגיה דמוי-בעלי חוליות בתנועות מנקודה לנקודה בזרועות התמנון מציעה התכנסות אבולוציונית לפתרון בקרה אופטימאלי.....58

פרק 4

דיון כללי.....82

4.1 בקרת התנועה של תנועת ההושטה.....82

4.2 תנועת ההבאה: קינמאטיקה ובקרת התנועה.....83

4.3 מסכנות סופיות.....85

רשימת ספרות.....87

הנדרשות לבקרה לשלוש בלבד (אחת לכל פרק), ולכן מפשטת את בקרת התנועה בלי לפגוע בדיוקה.

רישומי אלקטרומיוגרמיים הראו שתכנית הזמן והמרחב של פעילות השרירים ביצירת הפרקים מעידה על שני גלים של כיווץ שרירים שמתקדמים בכיוונים נגדיים לאורך הזרוע. אופן פעילות שרירים זו יחד עם הנחיצות של אזורים מוחים לתזמון יצירת הפרקים בזמן תנועת ההבאה, מתאים לתרחיש בו שילוב של פקודה מרכזית והגירוי הנוצר כתוצאה מאחיזת העצם יכול לאתחל שני גלים של פעילות שרירית אשר קובעים במקום התנגשותם את נקודת היצירה של הפרק האמצעי. שיטה זו מציעה מנגנון יעיל ופשוט על-מנת ליצור מבנה מפרקי שאורכו תלוי במיקום העצם הנאחז לאורך הזרוע, ללא צורך בייצוג מרכזי של הזרוע, ולכן מפשט עוד יותר את בקרת תנועת ההבאה.

מעניין לציין שבין כל סוגי תנועה האפשריים לזרוע גמישה על מנת להביא עצם לפה, התמנון מציג תנועה דומה מאוד מבחינה מורפולוגית וקינמטית לזו של בעלי חוליות (כגון בני אדם). התכנסות אבולוציונית תפקודית זו מציעה שעל-מנת להשיג תנועת מדויקת 'מנקודה לנקודה', זרוע מפרקית, מוגבלת דרגות-חופש, עם שני מקטעים שווי-אורך היא הפתרון הטוב ביותר. תנועת ההבאה היא דוגמא יחידה במינה לפתרון אבולוציוני דומה במנגנונים בלתי-תלויים: מחד, קיבוע מורפולוגי בבעלי חוליות ופרוקי רגליים, ומאידך, תוכנית בקרת-תנועה סטראוטיפית בתמנונים.

לפיכך, על מנת לבקר ביעילות את הזרוע הגמישה בזמן תנועות מכוונות, התמנון משתמש בתוכניות בקרת-תנועה סטראוטיפיות המורידות בצורה משמעותית את מספר דרגות החופש; מאין-סוף לשלוש בלבד, ובכך לפשט בעיות הקשורות לבקרה מוטורית של זרועות רב-יתירותיים.

למרות המגבלה באפשרויות תנועה בזמן תנועות מכוונות, הזרוע הגמישה של התמנון מאפשרת יצירת מבנים גיאומטריים בלתי אפשריים לזרוע מפרקית. לדוגמא, התקדמות הכיפוף במהלך ההושטה מורידה את כוח החיכוך עם המים, או מבנה דינאמי דמוי-מפרקי, בתנועת ההבאה, מאפשר הבאת אוכל לפה בצורה מדויקת. בנוסף לתנועות מכוונות, תמנונים יכולים לבצע תנועות מקומיות, לא מכוונות, כמו חיפוש אחר טרף או תנועות ניקיון בהן מנוצל מספר דרגות חופש גדול במיוחד. תנועות אלה כנראה מבוקרות ע"י מעגלים עצביים מקומיים בזרוע.

התוצאות שהתקבלו בעבודה זו מספקות תובנה באשר להתפתחות מערכות ביולוגיות אל מול בעיית הבקרה המורכבת על איברים רב-יתירותיים ידע זה עשוי להיות משמעותי מאוד לפיתוח רובוטים עתידיים גמישים במיוחד.

תקציר

השילוב בין זרועות גמישות מאוד וכשלוש מאות כפתורי הצמדה לאורך הזרוע, מעניקים לתמנון יכולות מניפולציה יוצאות מן הכלל, אשר מאפשרות לו להזיז את זרועותיו עם דרגות חופש רבות ולאחוז עצמים בחזקה יוצאת-דופן. לפיכך, התמנון הוא חיית ניסוי אידיאלית על-מנת לחקור בקרת תנועה באיברים רב-יתרותיים (hyper-redundant) כצעד ראשון לקראת בנייה ובקרה של רובוטים עתידיים גמישים ורציפים.

חקרתי את עקרונות הבקרה בתנועת ההושטה בעקבות ניסוים קודמים (Gutfreund Y. et al. 1996, 1998). תנועה זו מבוצעת כאשר תמנונים מנסים לתפוס עצם מסוים או כתנועה המשולבת בשחייה זחילה או הליכה. תנועה זו מבוססת על התפשטות של כיפוף לאורך הזרוע, ובכך מושגת הורדה של מספר דרגות החופש של הזרוע לשלוש בלבד (עלרוד, וסיבסוב ומהירות ההתקדמות של הכיפוף) וכתוצאה מכך מושג פישוט דרסטי של בקרת התנועה בזרועות גמישות

במהלך המחקר, הוכחתי שפישוט נוסף בבקרת תנועת ההושטה נובע מהעובדה שתוכנית מוטורית בדגם מעגל פתוח (feed-forward) היקפי מוטבעת במערכת עצב-שריר בזרוע עצמה. בזרועות שהקשר העצבי בין המח לזרוע נותק, עירור תנועות הושטה התאפשר בעזרת גירויים חשמליים או מכנים. ההיבט הקינמטי והדינאמי של תנועות אלו היה זהה לזה המתקבל בחיה מתנהגת.

תוכנית מוטורית זו ניתנת לויסות כך שאפשר לעורר תנועות שכיוונן ומהירותן שונים. לדוגמא שינוי התנוחה ההתחלתית של הזרוע קובע את מסלולה הסופית בעוד שמהירותה נקבעת ע״י שינוי תדר או משך הגירוי. לעומת זאת, את מרחק התקדמות הכיפוף לא ניתן להכתיב כך שתמיד יתקדם עד קצה הזרוע, בדומה למתרחש בתמנונים מתנהגים.

למרות אופייה הבליסטי של תנועת ההושטה, אשר לא מאפשרת תיקון לאחר תחילת התנועה, תמנונים מסוגלים לעצור את התקדמות הכיפוף באופן פעיל.

מאחר וכפתורי ההצמדה ממוקמים לכל אורך הזרוע, התמנון יכול לתפוס את המטרה בכל מקום לאורך הזרוע . אולם, כאשר תמנונים מביאים לפיהם את המטרה שנתפסה, הם חייבים לבצע תנועת ׳מנקודה לנקודה בה המיקום הסופי צריך להיות מסוים ומדויק (הפה). מצאתי שתמנונים מבצעים משימה זו בעזרת יצירת תנועה סטריאוטיפית המכונה תנועת הבאה (fetching). תנועה זו מבוססת על יצירת שלושה פרקים לאורך הזרוע, כך שנוצר מבנה דמוי-מפרקי. ע״י סיבוב של פרקים אלה במישור אחד, העצם מובא בדיוק רב לפה. סדר יצירת הפרקים הוא סטריאוטיפי: ראשית נוצר הפרק הדיסטאלי (פרוקסימאלי למיקום האוכל) ולאחר מכן הפרק האמצעי (באמצע המרחק בין הפרק הדיסטאלי ובסיס הזרוע). בנוסף, יש מתאם חיובי וליניארי בין מיקום האוכל לבין מיקום הפרקים, כך שעצם שנתפס קרוב לקצה הזרועה יצור מבנה דמוי-מפרקי ארוך יותר. יוצא מכך שמבנה זה מאפשר להביא עצם לפה בדיוק רב, ללא תלות במיקום הזרוע במרחב. אסטרטגיה זו מצמצמת את מספר דרגות החופש

עבודה זו נעשתה בהדרכתם של

ד״ר בנימין הוכנר
פרופ׳ יוסף ירום

מעורבות מנגנונים מרכזיים והיקפיים בבקרת התנועה של זרוע התמנון

חיבור לשם קבלת תואר דוקטור לפילוסופיה

מאת
גרמן סומברה

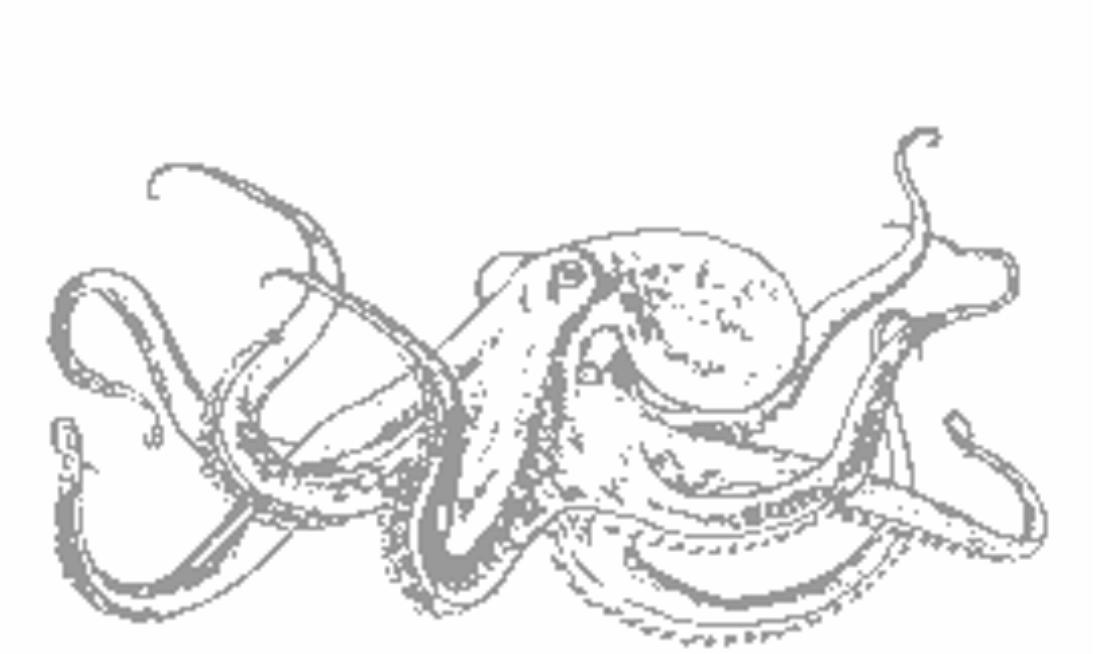

הוגש לסינט האוניברסיטה העברית בירושלים
תשס״ד